The Study of Fork Processing and DSB Repair in Bacteriophage T4: Roles of the MR Complex and Endonuclease VII

by

Joshua Richard Almond

Department of Biochemistry
Duke University

Date:_____

Approved:

_____
Kenneth N. Kreuzer, Supervisor

_____
Arno L. Greenleaf

_____
Margarethe Kuehn

_____
Michael D. Been

_____
Sue J. Robertson

Dissertation submitted in partial fulfillment of
the requirements for the degree of Doctor
of Philosophy in the Department of
Biochemistry in the Graduate School
of Duke University

2013

ABSTRACT

The Study of Fork Processing and DSB Repair in Bacteriophage T4: Roles of the MR Complex and Endonuclease VII

by

Joshua Richard Almond

Department of Biochemistry
Duke University

Date:_____

Approved:

_____
Kenneth N. Kreuzer, Supervisor

_____
Arno L. Greenleaf

_____
Margarethe Kuehn

_____
Michael D. Been

_____
Sue J. Robertson

An abstract of a dissertation submitted in partial fulfillment of the requirements for the degree of Doctor of Philosophy in the Department of Biochemistry in the Graduate School of Duke University

2013

Abstract

During DNA replication, organisms often encounter different types of DNA damage or lesions that lead to the stalling or breakage of replication forks. Cells must repair this damage or it can lead to genome instability and the loss of cell viability. It is now accepted that recombination plays a vital role in the rescue and restart of replication forks. The study of replication fork processing by recombination is important for understanding how cells avoid DNA damage which, if unrepaired, can lead to cancer or cell death.

One of the most detrimental forms of DNA damage experienced by the cell is a double-stranded DNA break (DSB). DSBs can be repaired in an error-free manner by homologous recombination through many different proposed mechanisms. Homologous recombination is of particular interest as defects in the recombination proteins often lead to deadly human syndromes characterized by a predisposition to cancer. For example, mutations in the BRCA2 protein, which is involved in homologous recombination for the repair of DSBs, have been linked to an increased incidence of breast cancer. Therefore, our lab is interested in studying the mechanism of homologous recombination and in particular how it relates to stalled fork processing and DSB repair.

We studied the different characteristics of DNA recombination using bacteriophage T4 as a model system. Phage T4 is a well-characterized virus that infects

Escherichia coli. Phage T4 has a simple genome that encodes for almost all of the proteins involved in its own replication, recombination, and repair. At late times of infection, phage T4 predominantly uses recombination-dependent replication (RDR) to replicate its DNA. This recombination-dependent replication system is very similar to homologous recombination used by higher organisms. One major advantage of using phage T4 as a model system is that unlike other model systems, "lethal" mutations can be examined in T4 using strains that suppress specific mutations. Using this system, we investigated a few of the phage T4 proteins (homologous with higher organism proteins) that are thought to be involved in DSB repair and replication fork processing and whose roles are not yet fully defined.

One such protein that we studied was gene product 47 (gp47). The gp47 protein is a member of the bacteriophage T4 Mre11/Rad50 complex and is homologous to the human Mre11 protein (gp47 will be referred to as T4 Mre11). We investigated the *in vivo* functions of T4 Mre11 in double-strand end processing, double-strand break repair, and recombination-dependent replication. Specifically, we tested the importance of the conserved histidine residue in nuclease Motif I (catalytic active site) of the T4 Mre11 protein. Substitution with multiple different amino acids (including serine) failed to support phage growth, completely blocked plasmid recombination-dependent replication, and led to the stabilization of double-strand ends. Our collaborator, Dr. Scott Nelson, also constructed and expressed a T4 Mre11 mutant protein with the same

conserved histidine changed to serine. The mutant protein was found to be completely defective for nuclease activities, but retained the ability to bind T4 Rad50 and double-stranded DNA. These results indicate that the nuclease activity of T4 Mre11 is critical for phage growth and recombination-dependent replication during T4 infections.

Another such protein that we studied was gene product 46 (gp46). The gp46 protein is the other member of the bacteriophage T4 Mre11/Rad50 complex and is homologous to the human Rad50 protein (gp46 will be referred to as T4 Rad50). We investigated the *in vivo* functions of T4 Rad50 in double-strand end processing, double-strand break repair, and recombination-dependent replication. Specifically, we tested different aspects of the protein such as the Signature motif, which is part of the nucleotide binding domain (ATPase active site). Substitution with different ATPase-deficient mutations completely blocked plasmid recombination-dependent replication and led to the stabilization of double-strand ends. These results indicate that the ATPase activity of T4 Rad50 is critical for recombination-dependent replication during T4 infections.

Finally, we investigated Endonuclease VII (gp49), which is encoded by gene *49*. EndoVII was the first endonuclease shown to cleave Holliday junctions *in vivo* and was shown to cleave stalled replication forks *in vitro*. We were interested in investigating the proposed regulation of EndoVII expression along with EndoVII's role in replication fork processing. Specifically, we used the gene *49* hairpin mutation to address the

proposed regulation of EndoVII expression. In the presence of wild-type gene *49* we observed only the full-length EndoVII protein, whereas in the presence of the gene *49* hairpin mutant, we observed no EndoVII protein. This result indicates that EndoVII is not regulated to express different length proteins at different times of infection.

We also used the gene *49* hairpin mutation to investigate EndoVII's role in replication fork processing. We generated phage strains to monitor EndoVII's effect on recombination using a plasmid x phage recombination assay. Taken with the above conclusions, we propose that the gene *49* hairpin mutation disrupts the late promoter and reduces the amount of active EndoVII available. In turn, this would affect the phage's ability to package its DNA due to unresolved recombination junctions and its ability to survive.

Contents

List of Tables

List of Figures

Acknowledgements

I would like to acknowledge my advisor and mentor, Dr. Kenneth N. Kreuzer. I am honored to have had the opportunity to work in his lab, as his guidance and support these past several years have been instrumental in my growth and success.

I would also like to acknowledge my family for their continued love and encouragement; in particular, my father, who originally sparked my interest in science. His invaluable advice has guided me throughout the years.

Lastly, I would like to acknowledge my wife and best friend, Jennifer. She has been a source of love and support during my time at Duke. I would not be where I am today without her. Thank you for taking this journey with me. I am also thankful for our newest addition, Mae Lillian. I am so blessed to be her father and to experience the joy that she brings us every day.

This research was supported by NIH grant GM 066934 and NCI grant T32CA009111.

1. Introduction

1.1 DNA Replication – Overview

Deoxyribonucleic acid (DNA) is a molecule that encodes the genetic information necessary for growth and development of all living organisms and many viruses. DNA consists of two long polynucleotide chains that run anti-parallel to each other in a double helix. The nucleotides in the chain are covalently linked to each other by a sugar-phosphate backbone that is attached to one of the following bases: adenine (A), cytosine (C), guanine (G), or thymine (T). The two polynucleotide chains in the DNA double helix are held together through hydrogen-bonding between the bases on the different chains. In order for a cell to pass on its genetic information, the cell must accurately duplicate its DNA in a process known as DNA replication.

DNA replication is characterized by the unwinding and duplication of both parental DNA polynucleotide chains. The process of DNA replication begins with initiator proteins that bind the DNA and pull the two chains apart. The specific DNA positions where this unwinding occurs are referred to as replication origins. Once an initiator protein binds the DNA at the replication origin and unwinds the DNA, it attracts a group of proteins that form an active replication complex (replisome) to proceed with DNA replication. The replisome typically consists of DNA polymerase, DNA helicase, and primase (among other proteins, i.e. DNA ligase and topoisomerase). The replication fork contains an active DNA-replisome complex that performs replication. At the replication

fork, the replication machine is moving along the DNA, opening up the two polynucleotide chains of the double helix and using each chain as a template to make a new daughter polynucleotide chain.

DNA Replication - Origin-Dependent Replication (*Escherichia coli* vs. Phage T4)

As stated above, the initiation of DNA replication usually occurs at specific DNA sequences known as origins. Origins contain specific DNA elements that are essential for promoting assembly of the replisome. The replisome is known to be required for coordinated leading- and lagging-strand synthesis during DNA replication.

In *E. coli*, bi-directional DNA replication initiates form a single origin, *oriC*. DnaA activates *oriC* after DnaA binding to ATP. This ATP-bound DnaA binds to AT-rich sequence elements at the origin that are referred to as DnaA boxes to promote opening of a DNA unwinding element. DnaA next recruits the helicase loader, DnaC, and the replicative helicase, DnaB, to *oriC* to the open complex of DNA. DnaB then recruits the primase, DnaG, to initiate synthesis of RNA primers for leading- and lagging-strand synthesis on the open complex (BRAMHILL and KORNBERG 1988).

In bacteriophage T4, replication and recombination are tightly coupled. Similar to *E. coli*, phage T4 initiates DNA replication from specific origins at early times of infection (KREUZER and ALBERTS 1986). However, unlike *E. coli*, phage T4 forms an open complex where the duplex DNA strands are separated when the RNA transcript hybridizes to one parental strand of DNA. This RNA-DNA hybridization (referred to as

the R-loop) initiates DNA replication. At late times of infection, the dominant form of replication is dependent on recombination and is referred to as recombination-dependent replication which is discussed below (NOSSAL *et al.* 2001). The switch from origin-dependent to recombination-dependent replication is mediated by the helicase, UvsW.

1.2 Replication Fork Inactivation - Overview

Replication forks often stall or fail during DNA replication. It is understood that replication fork rescue and restart occurs during normal DNA replication as well as during periods of stress or in response to DNA damage (HELLER and MARIANS 2006; MCGLYNN and LLOYD 2002; PETERMANN and HELLEDAY 2010). Replication fork failure can be attributed to many different factors including but not limited to: reduced nucleotide pools, damaged replication proteins, and DNA damage such as covalently-linked DNA-bound proteins. These stalled and blocked replication forks must be repaired to not only continue regular DNA replication but also to protect genome stability and cell viability.

1.3 Replication Fork Reactivation – Overview

Numerous replication fork repair pathways exist based on the type and position of the DNA damage (reviewed in (MCGLYNN and LLOYD 2002)). If the cause of the replication fork blockage is quickly removed or repaired, then the replication fork can be directly repaired (direct restart). If the cause of the replication fork blockage cannot be

quickly repaired, it may be necessary to back up the replication fork (fork regression) and re-load the replisome in order to bypass the blockage or avoid it altogether.

Additionally, stalled and blocked replications forks can become broken or cleaved, producing broken double-stranded DNA ends. These double-stranded ends can be repaired in an error-free manner using homologous recombination. The broken DNA ends can use homologous DNA to fill in the gap where the break occurred. This DNA end repair is error free because the lost nucleotides are replaced in a 'relatively' error free manner by polymerase extension as opposed to trans-lesion polymerase extension or non-homologous end joining, which are usually error prone.

One of the most harmful forms of DNA damage experienced by the cell is double-strand DNA breaks (DSB). DSBs can be detrimental to cells and can lead to genome instability and cell death. Homologous recombination is known to play important roles in DSB repair as well as the rescue and restart of stalled replication forks (KREUZER 2000; MOSIG 1998; SONODA *et al.* 2006). It has also been shown that proteins involved in homologous recombination, such as BRCA1 and BRCA2, are frequently mutated in cancer (SUNG and KLEIN 2006). Thus, the study of replication fork repair and restart by homologous recombination is important in understanding the mechanisms of genome stability and cell viability and how these processes contribute to cancer development/formation.

1.4 Bacteriophage T4 Model System - Overview

One useful model system for the study of different characteristics of DNA replication and recombination is bacteriophage T4. Phage T4 is a well-characterized virus that infects *E. coli*. Its genome is terminally-redundant and circularly permutated, and encodes for almost all of the proteins involved in its own replication, recombination, and repair (EDGAR 2004). As discussed above, at early times of infection, phage T4 replicates from specific origins of replication through the formation of R-loops (KREUZER and ALBERTS 1985; KREUZER and ALBERTS 1986; KREUZER 1994b). At late times of infection, the dominant form of DNA replication is recombination-dependent replication (RDR) (GEORGE *et al.* 2001; MOSIG 1983) (see Figure 1-1). This RDR system is very similar to homologous recombination used by higher organisms (MCGLYNN and LLOYD 2002). Many of the proteins used by phage T4 for RDR are homologous to proteins of higher organisms (discussed below). Another advantage of using phage T4 as a model system is that replicated phage DNA is modified. Phage T4 incorporates hydroxymethyl cytosine into its DNA, which is then glycosylated (REVEL 1983). Phage T4 uses this DNA modification as a mechanism to protect phage DNA from the host restriction system. This DNA modification also serves as a useful maker for the detection of phage-replicated DNA, which is protected from restriction by certain enzymes. Phage T4 was employed as a useful model system for gaining further insights into how an organism repairs DNA damage and maintains genome stability with homologous recombination.

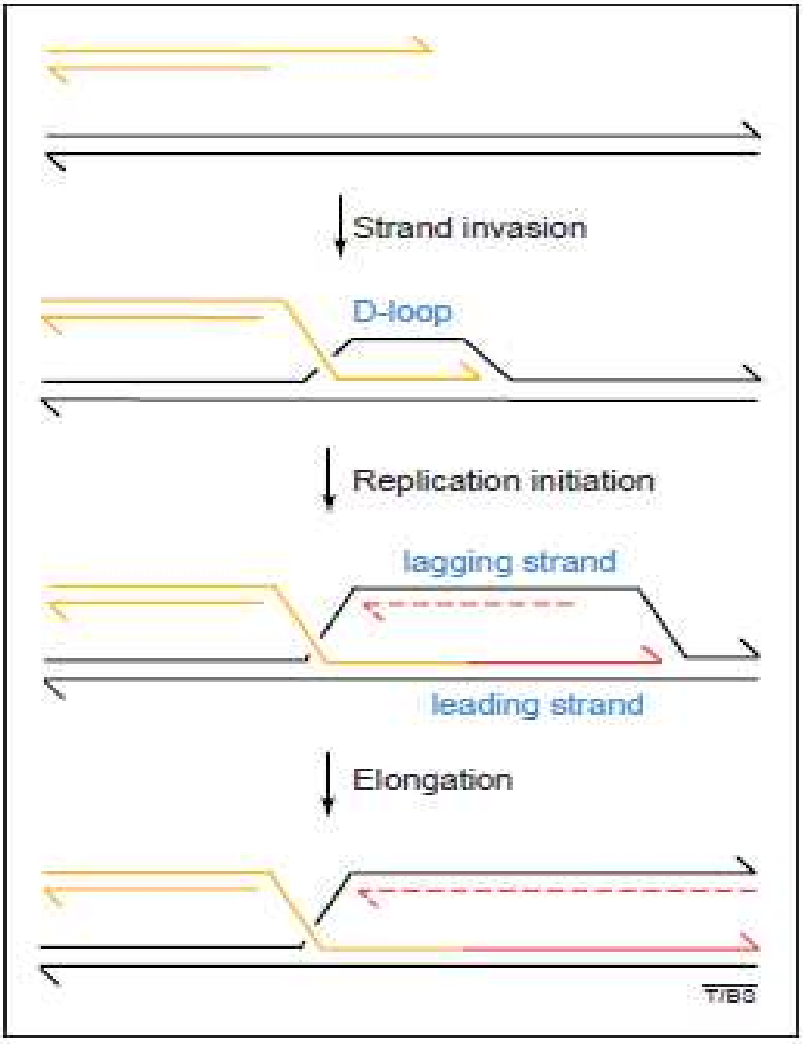

Figure 1-1: Model of T4 RDR (KREUZER 2000).

Bacteriophage T4 Model System – Large Collection of T4 Amber Mutations

Another advantage of the bacteriophage T4 model system is the large collection of available amber mutations, which we made use of throughout this study. Amber mutations that result in lethality are conditional lethal mutants and are helpful in elucidating the specific functions of different genes. These amber mutations allow one to study "lethal" mutations that are difficult to study in other systems. Amber mutations were first isolated when a group of graduate students were able to isolate phage plaques that displayed different phenotypes on different *E. coli* host strains (EDGAR *et al.* 1964; EPSTEIN *et al.* 1963). They noticed that wild-type (WT) phage could grow on both *E. coli* strains CR63 and B, whereas amber mutant phage could only grow on strain CR63. It has since been clarified that an amber mutation in a specific gene has a mutated mRNA to introduce a premature stop codon. When an amber mutant phage infects a non-suppressing *E. coli* strain such as strain B or BE-BS, the phage expresses a truncated protein that is degraded by proteases. However, when an amber mutant phage infects an amber suppressing *E. coli* strain such as CR63 (*supD*), the suppressing strain has a mutated tRNA that can read the premature stop codon of the mutant phage and insert the correct amino acid during translation to allow translation past the premature stop codon (NORMANLY *et al.* 1986). Thus, when an amber mutant infects an amber suppressing strain, the full-length protein is expressed from the mutated gene. These amber mutants are useful in providing direct means to analyze gene function (STAHL 1995).

Bacteriophage T4 Model System – T4 Genome Structure

As mentioned above, bacteriophage T4 has a linear, double-stranded DNA genome that encodes for almost all of the proteins involved in its own replication, recombination, and repair (EDGAR 2004). Each phage T4 particle contains one linear duplex of phage DNA. This packaged DNA is longer than the T4 genetic material. The DNA sequence at one end of the packaged DNA is repeated at the other end (terminally redundant). Additionally, the phage T4 genome is circularly permutated, referring to the finding that different phage DNA ends are found in different phage DNA molecules (reviewed in (KREUZER 2000)).

During the course of the phage T4 infection, linear DNA is replicated by RDR into long, branched concatamers that contain hundreds of phage genome equivalents (see Figure 1-2). The RDR D-loop is formed when the 3' single-stranded end of one phage DNA molecule invades a homologous region of DNA of another phage molecule, or the other end of the same phage DNA molecule (reviewed in (KREUZER 2000)). Every time a replication fork reaches a DNA end, you get two ends, each of which can initiate another round of RDR by invading a region of homology. Thus, DNA becomes longer and more branched than the infecting molecule as replication proceeds. The resulting phage DNA is packaged into the phage head (single concatamer) by endonucleolytic cleavage. The circular permutation of the phage genome is a direct result of the phage DNA packaging as each packaged phage head contains DNA with a different end

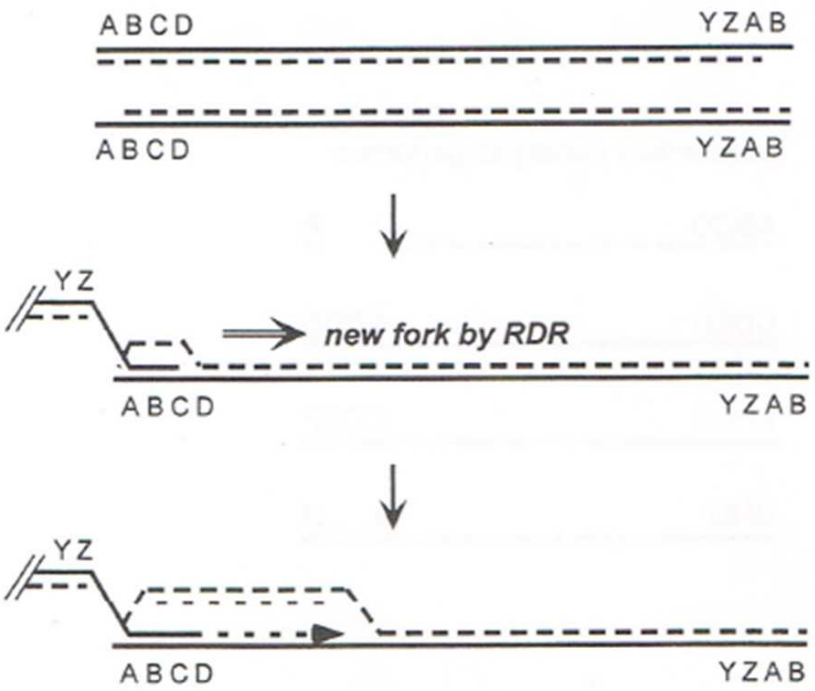

Figure 1-2: Model of T4 branched concatamer formation from replication (KREUZER 2005).

Phage T4 origin replication leads to unreplicated 3' ends (dashed lines in Step 1). The DNA ends of the replicating T4 are terminally redundant (represented by ABCD and YZAB). The RDR D-loop is formed when the 3' single-stranded end of one phage DNA molecule invades a homologous region of DNA of another phage molecule, or the other end of the same phage DNA molecule (Step 2), leading to a new replication fork (Step 3). Additionally, every time a replication fork reaches a DNA end, you get two ends, each of which can initiate another round of RDR by invading a region of homology. Thus, many rounds of this RDR reaction lead to the long, branched concatamer of DNA.

sequence since more than one genome length is packaged. It is also important to note that the recombinational branches created during RDR are often not resolved until packaging, explaining why the structure is complex and branched. The enzyme involved in cleaving these complex DNA branches (Endonuclease VII) is discussed below.

1.5 Recombination-dependent Replication (E. coli vs. Phage T4)

In *E. coli*, double-stranded DNA ends that arise from DNA damage or that are produced by the action of endonucleases can be processed by RecBCD to generate single-stranded 3' DNA ends (CONNELLY *et al.* 1999; KOWALCZYKOWSKI 2000). RecBCD then promotes the coating of the resulting 3' ssDNA region by RecA (ANDERSON and KOWALCZYKOWSKI 1997; MORIMATSU and KOWALCZYKOWSKI 2003). RecA is a strand exchange protein that promotes strand invasion by searching double-stranded DNA for regions that are homologous to the coated ssDNA (KOWALCZYKOWSKI 1991).

Once homology is found, strand invasion forms a D-loop (see Figure 1-1), which is similar to the R-loop structure mentioned above. The D-loop structure contains both a single-stranded DNA region that can function as a replisome assembly site and a free 3' DNA end that serves as a primer for leading-strand synthesis.

Although useful in *E. coli*, recombination plays a vital role in normal phage T4 replication. As mentioned above, phage T4 replication is tightly coupled to recombination. Specifically, phage T4 replication is shifted from R-loop replication from specific origins to D-loop replication by RDR at late times of infection when late gene

expression begins (LUDER and MOSIG 1982; MOSIG 1983). The late protein, UvsW, has been shown to play an important role in the regulation of replication origins. UvsW acts as a RNA-DNA helicase that unwinds the R-loops and inactivates R-loop replication (CARLES-KINCH *et al.* 1997). UvsW also promotes RDR (though not required). This T4 RDR is strikingly similar to one pathway of homologous recombination used in *E. coli* and higher organisms. Specifically, this T4 RDR system is very similar to the homologous recombination used by higher organisms in break-induced replication (BIR) (reviewed in (KRAUS *et al.* 2001; LLORENTE *et al.* 2008; MCGLYNN and LLOYD 2002; PAQUES and HABER 1999)). For example, in *Saccharomyces cerevisiae*, BIR is initiated to repair broken replication forks by first performing 5' to 3' resection of the broken DNA ends to form a 3' ssDNA overhang. This 3' ssDNA overhang in turn forms a D-loop where the replisome is re-loaded and replication is restarted. Not only is BIR important in eukaryotes for the restart of collapsed replication forks, but it has also been implicated in telomere maintenance for the repair of chromosome ends (reviewed in (LLORENTE *et al.* 2008)).

As mentioned above, many of the proteins involved in phage T4 RDR are homologous and/or functionally similar to the *E. coli* homologous recombination proteins as well as higher organism recombination proteins (see Table 1-1). For instance, UvsX catalyzes strand invasion of the 3' DNA ends into homologous DNA similar to RecA in *E. coli* (D-loop formation). UvsY is an accessory protein that assists in the loading of UvsX onto ssDNA that is coated with gp32 (BLEUIT *et al.* 2001). UvsW is a

helicase involved in Holliday Junction (HJ) branch migration and has recently been shown to catalyze the replication fork regression for replication fork restart in vivo (LONG and KREUZER 2008; LONG and KREUZER 2009; WEBB *et al.* 2007). UvsW is structurally similar to Rad54 in yeast while many functional similarities exist between UvsW and Sgs1 helicase in budding yeast (BERNSTEIN *et al.* 2009). Since the phage recombination proteins are strikingly similar to the eukaryotic recombination proteins we used phage T4 as our model system to study the various proteins involved in RDR.

1.6 Bacteriophage T4 MR Complex

As mentioned before, DSB repair with homologous recombination in *E. coli* initiates when the DSB is resected by RecBCD to produce 3' ssDNA overhangs that can initiate D-loop formation and homologous recombination (see Figure 1-1). It has been proposed that the highly conserved eukaryotic Mre11/Rad50/Nbs1 (MRN) complex, which has sequence similarities to *E. coli* SbcCD, is a functional homolog of RecBCD (although no sequence homology) (SHIN *et al.* 2004). The MRN complex has also been proposed to be vital in coordinating the repair of two broken DNA ends (CONNELLY and LEACH 2002; CROMIE and LEACH 2001; WILLIAMS *et al.* 2008).

Table 1-1: Proteins involved in recombination-dependent replication and repair

Summary table. Proteins involved in recombination-dependent replication and repair			
General function	Bacteria (*E. coli*)	Bacteriophage (T4)	Eukarya (*S. cerevisiae*)
Initiating protein(s)	RecBCD, RecQ, RecJ	gp46, gp47	Mre11, Rad50, Xrs2
DNA strand exchange	RecA	UvsX	Rad51
ssDNA-binding protein	SSB	gp32	RPA
Accessory protein(s)	RecF, RecO, RecR	UvsY	Rad52, Rad54, Rad55/57, Rad59
Branch migration	RecG RuvAB	UvsW, Dda gp41	Rad54
Holliday junction cleavage	RuvC	gp49	**Yen1**
Priming proteins	PriA, PriB, PriC DnaC, DnaG, DnaT	gp59 (?), gp61	DNA polymerase α
Replicative polymerase	DNA polymerase III	gp43	DNA polymerase α, δ/ε
Replicative helicases	DnaB, Rep	gp41	Mcm proteins (?)
Processivity factor	β	gp45	PCNA
Processivity (clamp) loader	γ complex	gp44/62	RFC
Lesion bypass polymerases	UmuD′$_2$C (Pol V) DinB (Pol IV)		Rad30 (Pol η) Rev3/7 (Pol ζ)

Adapted from *Trends in Biochemical Sciences,* **25:** 206.

It has been suggested that the 5' resection activity to create 3' ssDNA is contained in the eukaryotic MRN complex (SHIN *et al.* 2004). This 5' resection activity remained controversial as *in vitro* studies of the eukaryotic MR complex showed an opposing 3' to 5' exonuclease activity (KROGH *et al.* 2005; LEWIS *et al.* 2004; LLORENTE and SYMINGTON 2004; TRUJILLO *et al.* 1998). However, more recent studies clarified that the eukaryotic MR complex along with other recruited proteins acts to resect the DSB and expose a 3' single-strand end. Specifically, the MR complex (in *Saccharomyces cerevisiae*), along with Xrs2 and Sae2 clips 50-100 nucleotides from the 5' end of a DSB (MIMITOU and SYMINGTON 2008). Next, ExoI and RPA or Sgs1/Top3/RmiI, Dna2, and RPA bind to the processed DSB and proceed with a more extensive resection of the DSB (NIU *et al.* 2010; ZHU *et al.* 2008).

The MR protein complex has been highly conserved throughout evolution, with homologs in *Saccharomyces cerevisiae*, *Pyrococcus furiosus*, *Escherichia coli* (SbcCD), and bacteriophage T4 (gp46/47) (see Figures 1-3 and 1-4) (CONNELLY and LEACH 2002; SHARPLES and LEACH 1995). The basic structure of the protein complex was elucidated in humans, *S. cerevisiae*, and *E. coli* (ANDERSON *et al.* 2001; CONNELLY *et al.* 1998; DE JAGER *et al.* 2001b; HOPFNER *et al.* 2002). The core MR complex consists of an Mre11 dimer, with each Mre11 subunit bound to a single Rad50 subunit (see Figure 1-5) (see Chapter 2 Introduction for further details). The eukaryotic Mre11 protein has several conserved phosphoesterase motifs, and in addition binds to double-stranded, single-stranded, and

forked DNA structures (see Figure 1-3) (CONNELLY and LEACH 2002; DE JAGER *et al.* 2001a; TRENZ *et al.* 2006). Additionally, the eukaryotic Rad50 protein has several conserved motifs, six of which form the nucleotide binding domain for the binding of ATP (discussed below) (see Figure 1-4).

To our advantage, the T4 MR complex is both functionally and structurally homologous to the MRN complex (see Figures 1-3 and 1-4). Therefore, we investigated gp47 (Mre11 homolog) and gp46 (Rad50), which form the T4 MR complex gp46/47 (Rad50/Mre11 homolog) (CONNELLY and LEACH 2002; SHARPLES and LEACH 1995). Both Mre11 and Rad50 are essential proteins in DSB repair. For instance, mutations in the Mre11 protein lead to an ataxia-telangiectasia-like disorder that is characterized by a predisposition to cancer (STEWART *et al.* 1999).

Prior work in T4 has demonstrated that the MR complex is required for RDR, DSB repair, and phage growth (reviewed in (KREUZER 1994a; KREUZER 1994b)). For example, knockouts of the T4 MR complex are essentially lethal (CUNNINGHAM and BERGER 1977; WIBERG 1966). Additionally, previous members of our lab as well as other labs have observed that the T4 MR complex plays a key role in processing the two broken ends of DNA during DSB repair (like the eukaryotic MR complex) (ALBRIGHT and GEIDUSCHEK 1983; KREUZER *et al.* 1995; MICKELSON and WIBERG 1981; MOSIG and BOCK 1976; STOHR and KREUZER 2002; TOMSO and KREUZER 2000). For example, Tomso *et al.* showed that a mutation in T4 Rad50 leads to the accumulation of DSB-DNA.

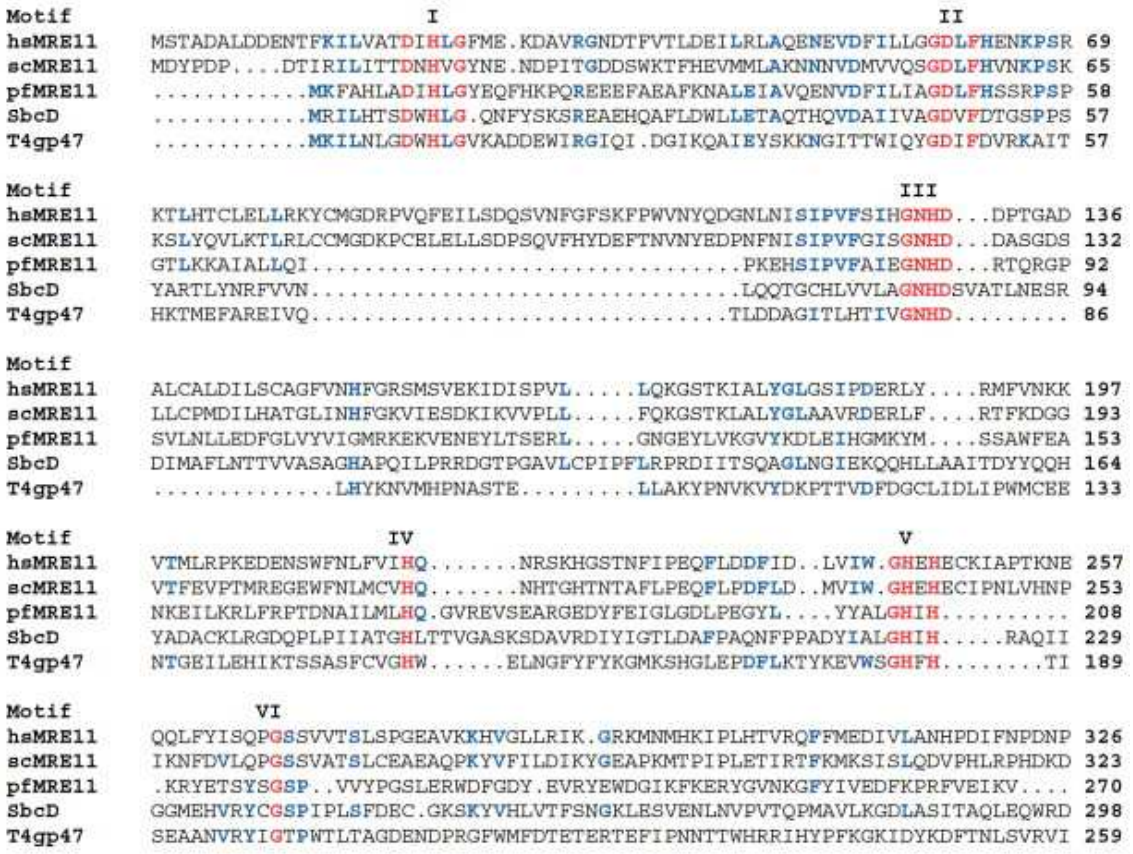

Figure 1-3: Conserved Mre11 N-terminal region sequence alignment (CONNELLY and LEACH 2002).

The conserved Mre11 phosphodiesterase motifs are indicated by I-VI.

Conserved residues are highlighted in red whereas residues conserved in three or four of the five sequences are highlighted in blue. Abbreviations: hs = *Homo sapiens,* pf = *Pyrococcus furiosus*, and sc = *Saccharomyces cerevisiae*.

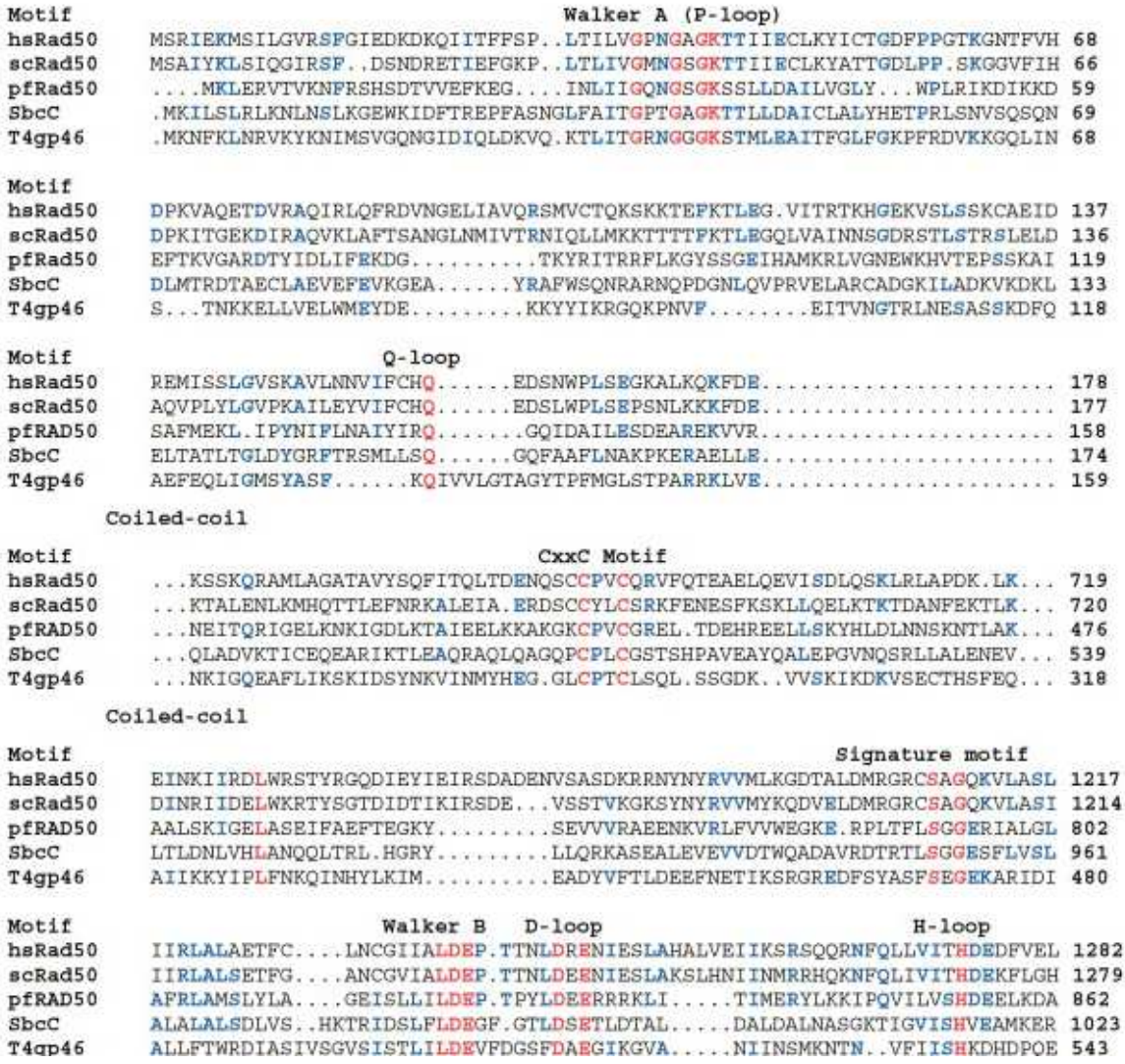

Figure 1-4: Conserved Rad50 sequence alignment (CONNELLY and LEACH 2002).

The conserved Rad50 regions are indicated above the sequences. Conserved residues are highlighted in red whereas residues conserved in three or four of the five sequences are highlighted in blue. Abbreviations: hs = *Homo sapiens,* pf = *Pyrococcus furiosus*, and sc = *Saccharomyces cerevisiae*.

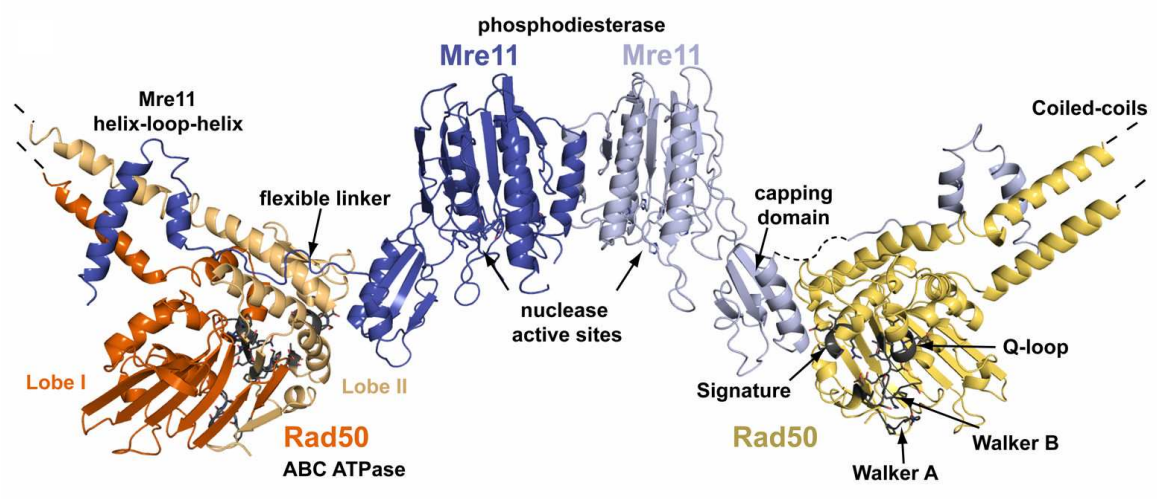

Figure 1-5: Ribbon representation of *Thermotoga maritima* MR complex catalytic head (LAMMENS *et al.* 2011).

The conserved MR complex is active as a heterotetramer and is made up of two Mre11 (nuclease) and two Rad50 (ATPase) monomers.

We were interested in investigating the role of T4 Mre11 in DNA end resection and RDR. Specifically, T4 Mre11 has many conserved phosphodiesterase motifs, which contain its nucleolytic processing function (DE JAGER *et al.* 2001a; SHARPLES and LEACH 1995). Studies in other systems have demonstrated the importance of the Mre11 phosphoesterase motifs (DXH), including the highly conserved motif I (DXH) very near the N terminus. We tested mutations of the highly conserved T4 Mre11 histidine (His-10) within motif I (ALMOND *et al.* 2013). Mutations in this motif of the *S. cerevisiae* Mre11 protein resulted in informative partial-function mutants (KROGH *et al.* 2005). For example, a mutation of the conserved aspartate (**D**XH) caused severe sensitivity to ionizing radiation (which produces double-stranded DNA breaks) and inhibited MR complex formation. Mutations in this motif of the *S. pombe* Mre11 protein also caused hypersensitivity to DNA damaging agents comparable to that of Mre11-deleted mutants (WILLIAMS *et al.* 2008). Additionally, mice either lacking Mre11 entirely or harboring a nuclease-deficient mutant Mre11 showed lethality and their cells were hypersensitive to ionizing radiation (BUIS *et al.* 2008). Finally, the crystal structure of the *Pyrococcus furiosus* Mre11 active site revealed that the His10 residue is critical for binding one of the two Mn^{2+} ions that are required for nuclease activity (see Figure 1-6)(HOPFNER *et al.* 2001). Hopfner *et al.* proposed that the two Mn^{2+} ions coordinate binding of the DNA and cleavage of the sugar-3'-O-phosphate bond of DNA.

We also investigated the role of T4 Rad50 in DNA end resection and RDR. Rad50 is an ATPase and a known member of the ATP-binding cassette (ABC) protein superfamily (reviewed in (JONES *et al.* 2009)). This ABC superfamily of proteins is one of the largest protein families and is conserved throughout many different organisms. Based on different ABC protein crystal structures, it was determined that the ATPase active site (bind/hydrolyze ATP) is formed by the nucleotide binding domain (NBD) (DAVIDSON *et al.* 2008; HOPFNER and TAINER 2003). The NBD is formed by six conserved motifs: the Walker A, Walker B, D-loop, H-loop, Q-loop, and Signature motifs. We investigated the role of the T4 Rad50 NBD to examine if T4 Rad50 plays a key role in the 5' resection of DSBs.

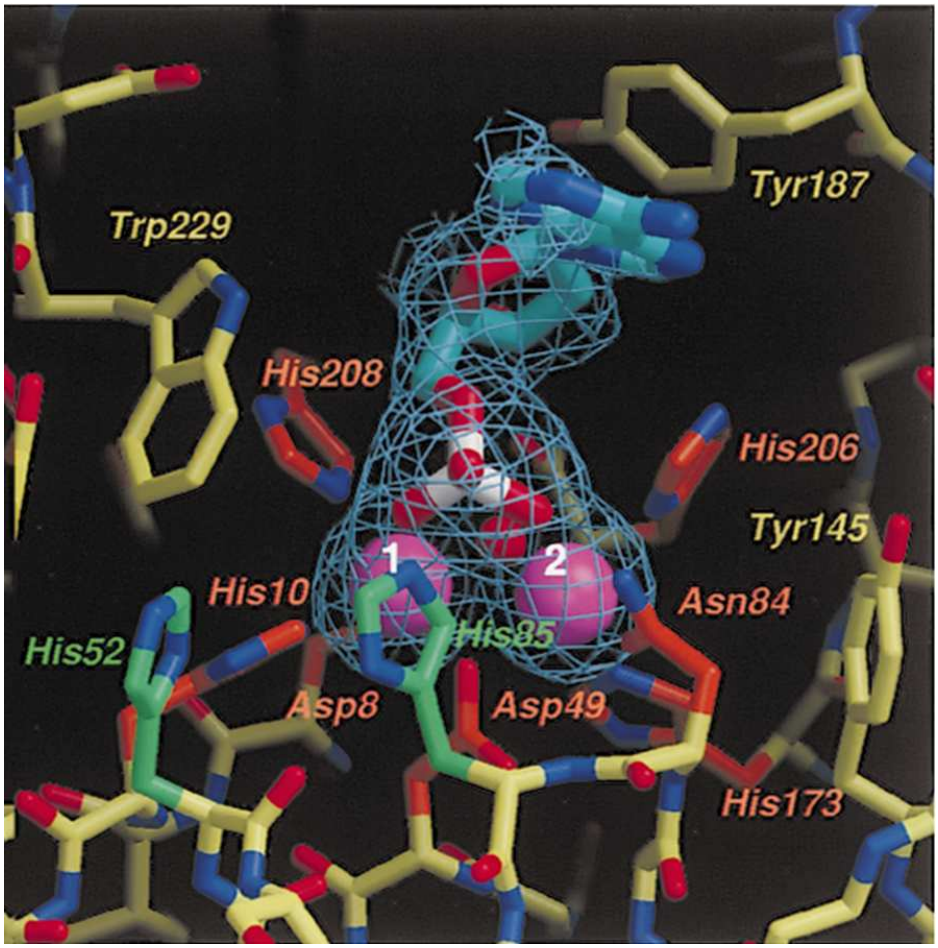

Figure 1-6: *Pyrococcus furiosus* Mre11 active site (HOPFNER *et al.* 2001).

The *Pyrococcus furiosus* Mre11 active site reveals binding of two Mn^{2+} ions (shown in magenta). The His10 residue is critical for metal binding and nuclease activity.

1.7 Phage T4 Endonuclease VII

Finally, we investigated T4 Endonuclease VII (EndoVII) which is encoded by gene *49*. EndoVII is an endonuclease and was the first enzyme shown to cleave HJs (MIZUUCHI *et al.* 1982). Many similarities exist between EndoVII and Yen1/GEN1 in yeast/humans as well as RuvC in *E. coli* (RASS *et al.* 2010; TAY and WU 2010). It is known that an EndoVII-deficient infection results in the accumulation of heavily-branched phage DNA intermediates (KEMPER and BROWN 1976; KEMPER and JANZ 1976) and the accumulation of empty or partially-filled phage heads (EPSTEIN *et al.* 1963; LUFTIG *et al.* 1971). Thus, it is accepted that a major role of EndoVII is the cleavage of highly branched intermediates produced from homologous recombination for the packaging of DNA into phage heads at late times of infection. As EndoVII's major known functions occurs at late times of infection, it is of interest how the protein is regulated to coincide with the timing of RDR during an infection.

As stated above, the regulation of EndoVII expression is of great interest. It was proposed that wild-type gene *49* has two different transcripts that are transcribed from two different promoters to produce a short, 12 kDa nuclease-inactive protein and a full-length, 18 kDa functional protein (MOSIG 1998; MOSIG *et al.* 1991) (see Figure 1-7). Based on the gene *49* sequence and plasmid protein expression the authors hypothesized that at early times of infection, the Shine-Dalgarno sequence of the first ribosome binding site located near the first AUG start codon is involved in a hairpin

loop. Thus, at early times of infection the ribosome cannot bind to the hairpin loop to translate the full-length protein. Instead, the ribosome is proposed to bind to an internal GUG start codon to translate the short form of the protein. The authors hypothesized that a possible function of the short protein could be the binding of HJs to prevent early, unwanted cleavage. At late times of infection, the authors proposed that the late transcript starts in the loop region of the proposed hairpin so that the hairpin loop is not formed. This disruption of the hairpin loop allows the ribosome to bind to the ribosome binding site to initiate translation of the full-length protein from the AUG start codon. The regulation of EndoVII is of great interest in our studies, especially due to the recent proposal that phage T4 homing endonuclease I-*Tev*I is self-regulated by a similar hairpin loop mechanism (GIBB and EDGELL 2010).

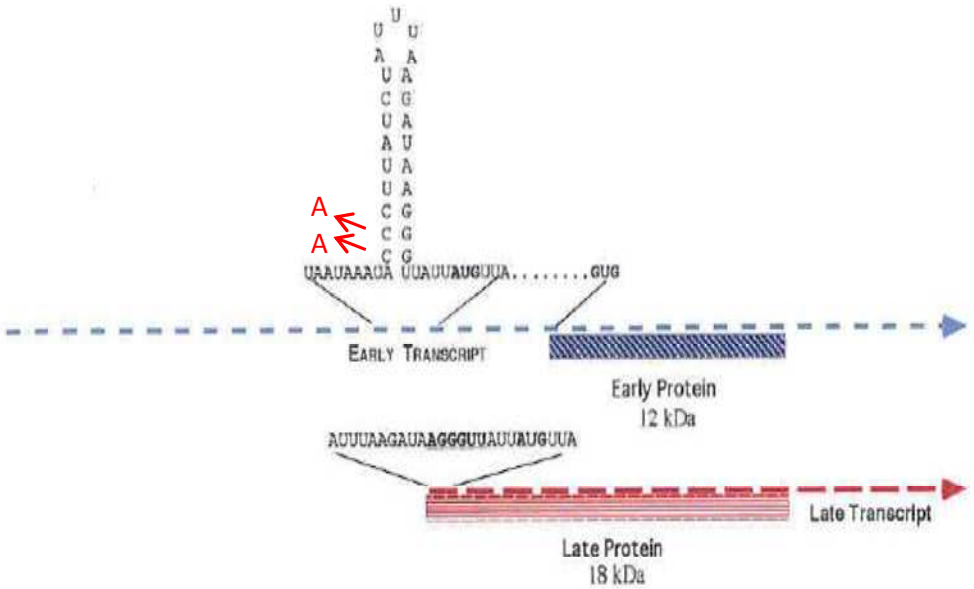

Mosig G., Annu. Rev. Genet. 1998;32:379-413

Figure 1-7: Proposed gene *49* hairpin loop and early/late transcripts (MOSIG 1998).

Also shown is the gene *49* hairpin mutation (CC→AA).

Another area of focus for our studies came from a previous discovery in our laboratory that EndoVII can cleave stalled replication forks *in vitro* (HONG and KREUZER 2003). It was noted that if stalled forks are unable to be directly restarted, they are cleaved by recombination nucleases to facilitate processing and reactivation through homologous recombination/RDR. Hong and Kreuzer were able to show that EndoVII can cleave *m*-AMSA induced stalled replication forks *in vitro* and proposed that this increases toxicity of the drug (i.e. unrepaired damage when the repair system is overwhelmed). The anti-cancer drug *m*-AMSA (4'-(9-acridinylamino)methanesulfon-*m*-anisidide) was previously shown to create a cleavage complex that stalls replication forks *in vivo* (HONG and KREUZER 2000). Specifically, *m*-AMSA stabilizes the temporary intermediate (cleavage complex) of the type II topoisomerase strand passage reaction (ROBINSON and OSHEROFF 1990). The type II topoisomerase normally binds to duplex DNA and cleaves both DNA strands. Topoisomerase becomes covalently linked to the 5' ends of both DNA strands through phosphotyrosine linkages (cleavage complex). At the end of the normal reaction, the linkages are reversed and the cleaved DNA is resealed (lose the cleavage complex). Additionally, Hong and Kreuzer (2003) were able to show that arrested forks accumulate at a higher level *in vivo* when EndoVII is not active (see Figure 1-8). These results implicate EndoVII in the cleavage of stalled replication forks *in vivo*. We proposed that the cleavage of stalled forks should produce double-stranded ends that can be funneled into RDR.

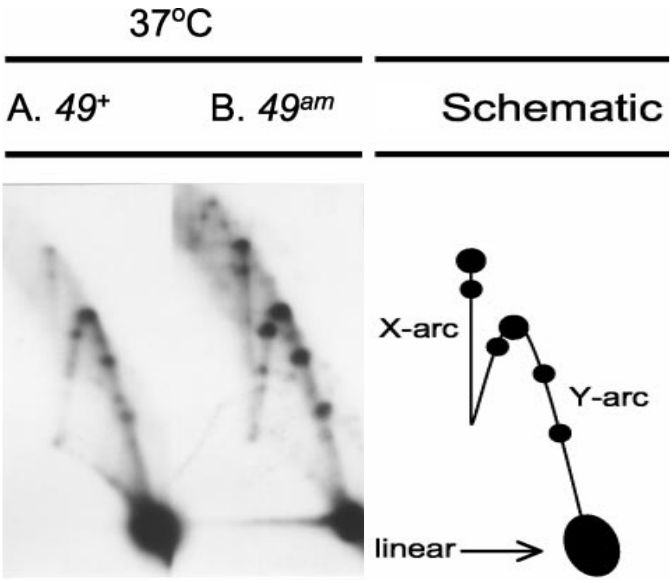

Figure 1-8: Accumulation of *m*-AMSA-induced blocked forks.

Bacterial cells with plasmid pGH2-01 were infected with WT K10 phage (49^{+}) or EndoVII-deficient phage (49^{am}) at 37°C. The cells were treated with *m*-AMSA and the DNA from the infections was extracted, purified, and digested with the enzymes *AseI* and *HaeIII*. After using 2D gel electrophoresis, the DNA was visualized using Southern blot hybridization and a pBR322 plasmid probe. As the schematic indicates, blocked forks are expected to accumulate on the Y-arc. One can see that in the absence of EndoVII, the amount of blocked forks was dramatically increased.

(HONG and KREUZER 2003).

2. The Bacteriophage T4 Mre11/Rad50 Complex

This chapter contains excerpts from Almond *et al.* 2013.

2.1 Introduction

The Mre11/Rad50 (MR) protein complex plays a central role in the response to double-strand breaks (DSBs) in eukaryotic cells (STRACKER and PETRINI 2011). The MR complex is quickly recruited to the site of DSBs, where its diverse functions include checkpoint activation mediated by the ataxia-telangiectasia mutated (ATM) kinase (LEE and PAULL 2005; MASER *et al.* 1997; NELMS *et al.* 1998). Mutations in the human *Mre11* gene cause the ataxia-telangiectasia-like disorder (ATLD), which is characterized by immunodeficiency, predisposition to certain cancers, and cellular hypersensitivity to ionizing radiation (STEWART *et al.* 1999).

The MR protein complex has been highly conserved throughout evolution, with homologs in *Saccharomyces cerevisiae*, *Pyrococcus furiosus*, *Escherichia coli* (SbcCD), and bacteriophage T4 (gp46/47) (CONNELLY and LEACH 2002; SHARPLES and LEACH 1995). The basic structure of the protein complex was elucidated in humans, *S. cerevisiae*, and *E. coli* (ANDERSON *et al.* 2001; CONNELLY *et al.* 1998; DE JAGER *et al.* 2001b; HOPFNER *et al.* 2002). The core MR complex consists of an Mre11 dimer, with each Mre11 subunit bound to a single Rad50 subunit. Each Rad50 subunit adopts a long coiled coil structure and can dimerize with a second Rad50 subunit through their so-called zinc-hooks, a conserved CXXC motif at the apex of the coiled-coil domain that forms a zinc

tetrathiolate center upon dimerization. This Rad50 dimer serves as a flexible tether connecting Mre11 proteins on each end (HOPFNER *et al.* 2002).

The eukaryotic Mre11 protein has several conserved phosphoesterase motifs, and in addition binds to double-stranded, single-stranded, and forked DNA structures (CONNELLY and LEACH 2002; DE JAGER *et al.* 2001a; TRENZ *et al.* 2006). The role of the Mre11 phosphoesterase activity in nucleolytic processing of the broken double-strand ends during repair was initially confusing, since the protein complex has an exonuclease activity with the wrong polarity for generating a 3' resected end (KROGH *et al.* 2005; LEWIS *et al.* 2004; LLORENTE and SYMINGTON 2004; TRUJILLO and SUNG 2001; TRUJILLO *et al.* 1998). However, recent research has clarified a key role of the MR complex nuclease activity. MR (with partner proteins) removes a small segment of the 5' terminal strand at a DSB and thereby licenses other exonucleases for efficient resection to generate the long 3' single-stranded ends (HOPKINS and PAULL 2008; MIMITOU and SYMINGTON 2008; ZHU *et al.* 2008).

The eukaryotic Rad50 protein is an ATPase and a known member of the ATP-binding cassette (ABC) protein superfamily (reviewed in (JONES *et al.* 2009). The ATPase active site (bind/hydrolyze ATP) is formed by the nucleotide binding domain (NBD) (DAVIDSON *et al.* 2008; HOPFNER and TAINER 2003). The NBD is dimeric and is formed by six conserved motifs: the Walker A, Walker B, D-loop, H-loop, Q-loop, and Signature motifs (reviewed in (HERDENDORF and NELSON 2011). The Walker A, Walker B, H-loop, and Q-

loop motifs from one monomer interact with the D-loop and Signature motifs of the adjacent monomer to form the active site.

The unique structure of the MR complex suggests that it could tether the ends of a DSB to facilitate proper repair (CONNELLY and LEACH 2002; CROMIE and LEACH 2001; WILLIAMS *et al.* 2008), a possibility supported by *in vitro* and *in vivo* findings. The human MR complex can link two linear DNA strands *in vitro*, with the globular Mre11 proteins binding the DNA ends and the Rad50 zinc-hooks interacting to tether the two DNA ends together (DE JAGER *et al.* 2001b). A similar role *in vivo* is supported by the work of Lobachev (LOBACHEV *et al.* 2004).

Bacteriophage T4 provides a simple model system for DSB repair via homologous recombination, which has been studied using genetic, biochemical, and structural approaches. The phage encodes the UvsX strand exchange protein (Rad51 homolog), recombination mediator protein UvsY (Rad52 paralog), a branch specific DNA helicase UvsW (most similar to eukaryotic Rad54), and the archetype single-strand binding protein gp32, all of which are involved in the strand exchange reaction (CARLES-KINCH *et al.* 1997; FORMOSA and ALBERTS 1986; GAJEWSKI *et al.* 2011; HINTON and NOSSAL 1986; KODADEK *et al.* 1989; MORRICAL and ALBERTS 1990; YONESAKI and MINAGAWA 1985; YONESAKI and MINAGAWA 1989). The mechanism of strand exchange between a single-stranded circle and homologous duplex has been studied in great detail *in vitro*, and crystallography has revealed 3-dimensional structures of all or parts of the UvsX, UvsW

and gp32 proteins (GAJEWSKI *et al.* 2011; SHAMOO *et al.* 1995b; SICKMIER *et al.* 2004). Advantages of the T4 system include the limited number of involved proteins and the absence of complex post-translational modifications and other regulatory events in response to DNA damage, allowing a simpler view of the core recombination reaction.

Phage T4 also has a well-conserved homolog of the MR complex, which is necessary for DNA end processing *in vivo* but dispensable for strand exchange *in vitro* (in reactions that are initiated with a single-stranded substrate). The T4 MR complex consists of gp47 (the Mre11 homolog) and gp46 (the Rad50 homolog), which will hereafter be referred to as T4 Mre11 and T4 Rad50, respectively. The structure of the T4 MR complex has not been determined. However, the T4 homolog shows conservation of MR functional features, including the CXXC motif, Walker A and B motifs, signature motif, D-, H- and Q-loops, and heptad repeat region (presumed extended coiled coil) of the Rad50, along with the phosphoesterase motifs of Mre11 (CONNELLY and LEACH 2002; SHARPLES and LEACH 1995).

Prior work in T4 has demonstrated that the MR complex is required for recombination-dependent replication (RDR) and DSB repair *in vivo*, and is absolutely required for phage growth (reviewed in (KREUZER 1994a; KREUZER 1994b). Interestingly, knockouts of the T4 MR complex are essentially lethal, while knockouts of other recombination proteins (UvsX, UvsY, and UvsW) reduce the burst but are not lethal (CUNNINGHAM and BERGER 1977; WIBERG 1966). This could reflect UvsXYW-independent

recombination reactions (perhaps single-strand annealing) or could reflect some essential role for the MR complex outside of the RDR reaction (see Discussion). Consistent with results mentioned above with the eukaryotic protein, genetic studies support a role for the T4 MR complex in end coordination during DSB repair (ALMOND *et al.* 2013; SHCHERBAKOV *et al.* 2006).

Until very recently, the T4 MR complex was recalcitrant to purification and biochemical characterization. Limited success at purifying the complex was reported by Bleuit *et al.*, but only small amounts of protein were obtained and the purification procedure was not reliable (BLEUIT *et al.* 2001). In a major advance, Herdendorf *et al.* recently developed a robust procedure for purifying milligram amounts of the T4 MR complex (HERDENDORF *et al.* 2011). They found that the complex has activities very similar to the eukaryotic MR complex, including DNA-stimulated ATPase, 3' to 5' DNA (Mn^{++}-dependent) exonuclease, and single stranded endonuclease activities. This advance allowed the Scott Nelson lab to characterize the kinetics of ATP hydrolysis, modulation by partner proteins UvsY and gp32, and multiple biochemical analyses of substitution mutants in various functional motifs (ALBRECHT *et al.* 2012; DE LA ROSA and NELSON 2011; HERDENDORF *et al.* 2011; HERDENDORF and NELSON 2011). Perhaps most interesting is their finding was that UvsY and gp32 activate a Mg^{++}-dependent endonuclease activity that was postulated to be involved in end resection (HERDENDORF *et al.* 2011). One of the key questions that remain in the T4 system is whether the MR

complex nuclease itself catalyzes extensive resection (in spite of the incorrect directionality of the exonuclease *in vitro*) or whether MR licenses another exonuclease(s), as in the eukaryotic system.

In this study, we used the bacteriophage T4 model system to address *in vivo* roles of the T4 MR complex. We generated infections of phage with multiple different substitutions in the conserved histidine residue in phosphoesterase motif I of T4 Mre11. Every tested substitution prevented phage growth and completely blocked RDR as measured by a DSB-dependent plasmid model system. We conclude that the T4 Mre11 nuclease activity is critical for T4 growth and for RDR.

We also generated infections of phage with substitutions of key residues in the conserved motifs that form the T4 Rad50 nucleotide binding domain. Every tested ATPase-deficient substitution completely blocked RDR as measured by a DSB-dependent plasmid model system. We conclude that the T4 Rad50 ATPase activity is critical for T4 RDR.

2.2 Materials and Methods

Materials. Restriction enzymes and T4 DNA ligase were purchased from New England Biolabs (Beverly, MA), 4-20% Mini-PROTEAN TGX gels and Precision Plus Dual Color Standards from BIO-RAD (Hercules, CA), O'GeneRuler DNA Ladder Mix from Thermo Fisher Scientific (Waltham, MA), Goat anti-Rabbit IR Dye 800CW from LI-COR Biosciences (Lincoln, NE), *E. coli* Proteins-Agarose affinity gel (for removing *E. coli*

antibodies) from Alpha Diagnostic International (San Antonio, TX), Nytran Nylon Transfer Membrane from GE Healthcare (Waukesha, WI), λDE3 Lysogenization Kit from Novagen (Madison, WI), Isopropyl-β-D-thiogalactopyranoside (IPTG) from Fermentas (Waltham, MA), Random Primed DNA Labeling Kit from Roche Diagnostics (Indianapolis, IN), and [α-^{32}P] from PerkinElmer (Boston, MA). Luria Broth (LB) was formulated as follows: Bacto-Tryptone (10 g/L), Yeast Extract (5 g/L), and NaCl (10 g/L). T4 plates were formulated as follows: Bacto-Tryptone (13 g/L), NaCl (8 g/L), Na Citrate-2$H_2$0 (2 g/L), Glucose (dextrose) (1.3 g/L), and Bactoagar (10 g/L). T4 top agar was formulated as follows: Bacto-Tryptone (13 g/L), NaCl (8 g/L), Na Citrate-2$H_2$0 (2 g/L), Glucose (dextrose) (3 g/L), and Bactoagar (6.5 g/L). Terrific Broth (TB) was formulated as follows: Bacto-Tryptone (12 g), Yeast Extract (24 g), and Glycerol (4 mL) were added to 900 mL of water and autoclaved. This TB mixture was completed after adding a separately autoclaved 100 mL solution of 0.17M KH_2PO_4 and 0.72M K_2HPO_4.

Strains. Escherichia coli strains KL16-99 (CGSC #4206) (Hfr λ^- *e14*$^-$ *recA1 spoT1 thiE1 deoB13*) and CSH108 (CGSC #8081) [F'128 *Δ(gpt-lac)5* λ^- *ara(FG) gyrA-0(Nal*^{R}*) argE(Am) rpoB0(rif*^{R}*) thiE1*] were obtained from the Yale University *E. coli* Genetic Resource Center (New Haven, CT). The *E. coli* strain CR63 (*supD*) was described previously (EDGAR *et al.* 1964). The INTERCHANGE amber suppressor strains were purchased from Promega (Madison, WI). Suppressor-containing plasmids from the plasmid INTERCHANGE strains, along with plasmid pTD101, were moved into strains

KL16-99 and CSH108 for analysis of T4 RDR. The INTERCHANGE strains with chromosomal-borne suppressors are derivatives of CSH108. The pET28-gp46 WT and mutant plasmids, along with plasmid pTD101, were moved into strains KL16-99 and KL16-99λ for analysis of T4 RDR.

The bacteriophage T4 strains used for plasmid DNA replication experiments are derivatives of strain K10, which carries the following mutations: *am*B262 (gene *38*), *am*S29 (gene *51*), *nd*28 (*denA*), and *rIIPT8* (*denB-rII*$^{\Delta}$) (SELICK *et al.* 1988).

The T4 K10 derivative with an amber mutation at the His-10 residue of gene *47* was constructed using the T4 insertion/substitution system (SELICK *et al.* 1988). Additional T4 strains were constructed by genetic crosses.

Plasmids. Plasmid pTD101 contains the I-*Tev*I recognition sequence, which suffers a double-stranded DNA break during bacteriophage T4 infection, flanked by direct repeats. It was derived from pTD001 (TOMSO and KREUZER 2000) as follows. Plasmids pACYC184 and pTD001 were both digested with AvaI and HindIII. The pACYC184 2848-bp fragment was ligated to the pTD001 2228-bp fragment to give pTD101.

The Scott Nelson lab amplified the T4 Rad50 open reading frame from gp46-pTYB1 (HERDENDORF *et al.* 2011) and subcloned into the pET28b expression plasmid (HERDENDORF and NELSON 2011). Along with WT T4 Rad50, they generated different T4

Rad50 ATPase-deficient mutations on the pET28-gp46 plasmid. All T4 Rad50 mutations were constructed using the Stratagene QuikChange™ site-directed mutagenesis kit.

Growth and titering of T4 phage stocks.

To grow phage stocks, an *E. coli* CR63 overnight culture was first added to melted T4 top agar and the mixture was allowed to solidify on a T4 plate. Next, the desired phage strain was struck out on the T4 plate using autoclaved paper strips and incubated at 37°C overnight to produce single phage plaques.

To grow a low titer lysate, CR63 was pre-grown in LB with shaking at 37°C to an OD_{560} of 0.5, and a single phage plaque from the above T4 plate was added. The culture was vigorously shaken at 37°C for 90 min. The culture was then chilled on ice for 15 min. About 500 µl of chloroform was added to the culture and the culture was lysed overnight at 4°C. The next day, the culture (not chloroform) was spun at 8500 rpm for 20 min. The supernatant (low titer lysate) was stored in a glass phage vial at 4°C with a small amount of chloroform.

To grow a high titer lysate, CR63 was pre-grown in TB with shaking at 37°C to an OD_{560} of 0.75, and 500 µl of the above low titer lysate was added to 10 mL TB/cells (or 50 µl low titer lysate/mL of culture). The culture was vigorously shaken at 37°C for 3-5 hr, monitoring for when the culture lysed. If lysed (culture turned clear) or after 5 hr, the culture was then chilled on ice for 15 min. About 1 mL of chloroform was added to

the culture and the lysis was completed overnight at 4°C. The next day, the culture (not chloroform) was spun at 8500 rpm for 30 min. The supernatant (high titer lysate) was stored in a glass phage vial at 4°C with a small amount of chloroform. T4 phage stocks used throughout this study are all high titer lysates.

Phage stocks were titered by preparing serial dilutions in LB and then mixing 100 µl of each phage dilution with 100 µl of CR63 overnight culture. This mixture was allowed to sit for 5 min to allow for phage attachment. Molten T4 top agar was then added to the mixture and plated on a T4 plate. The T4 plates were incubated at 37°C overnight to produce phage plaques. The next day, the phage plaques were counted (plaque forming units) and multiplied by the serial dilution/100 to calculate the phage titer/µl.

Analysis of plasmid DSB formation and processing in T4-infected cells (T4 Mre11). The indicated bacterial strains were pre-grown in LB containing appropriate antibiotic(s) with shaking at 37°C to an OD_{560} of 0.5, and the indicated phage strain was then added at a multiplicity (MOI) of 3 (3 phage/*E. coli* cell). The infected cultures were incubated at 37°C for 4 min without shaking to allow phage adsorption (attachment) and then 40 min with vigorous shaking. Aliquots were taken at 20 and 40 min, and total cellular DNA was purified using SDS/proteinase K treatment, phenol extraction, and dialysis as described previously (STOHR and KREUZER 2001). The purified DNA was digested with the indicated restriction enzymes and subjected to agarose gel electrophoresis and Southern blotting.

The probe for experiments with pTD101 consisted of a 1,184-bp fragment of pACYC184 that had been doubly digested with XmnI and DrdI. Blots were visualized using a Phosphorimager and quantitated using ImageQuant software (Molecular Dynamics, Sunnyvale, CA).

Analysis of T4 Mre11 expression levels after infection with 47^{am} (His-10) mutant. The same growth and infection steps described just above for analysis of plasmid DSB formation and processing were used to produce cells infected with the indicated T4 phage for 20 min. The infected cells were collected by centrifugation in a microfuge and the pellets were resuspended by vortexing in 500 µl of a wash buffer (100 mM NaCl, 50 mM Tris-HCl pH 8, 1 mM EDTA). The cells were recollected by centrifugation and the supernatant was removed. The pellets were resuspended by vortexing in 25 µl of H_20 and then 25 µl of 2X SDS Loading Buffer (2.7 M glycerol, 0.1 M Tris pH 6.8, 2% SDS, 0.29 M 2-mercaptoethanol, bromophenol blue at 10 mg/L) was added. Samples were boiled for 5 min and debris was removed by centrifugation in a microfuge for 10 min, with the cleared supernatant ready for gel electrophoresis. Total protein concentrations across samples were roughly equalized by subjecting each sample to polyacrylamide gel electrophoresis in triplicate, followed by staining with Coomassie Blue and quantitation using an Odyssey Infrared Imager (LI-COR Biosciences) and Odyssey Infrared Imaging System Application Software (LI-COR Biosciences, Version 3.0). The average intensities

(using multiple bands) were compared between samples and then the volumes adjusted for equal loading of total protein on the final gel (Western blot below).

The samples were analyzed by Western blotting using a gp46/47 rabbit primary antibody that had been twice purified by passage over a total *E. coli* protein affinity gel. Samples were run on 4-20% Mini-PROTEAN TGX gels and then transferred to a nitrocellulose membrane using an iBlot (Invitrogen). The membrane was blocked with 5% non-fat milk buffer for 1 hour at room temperature. Next, 0.1% Tween 20 and a 400-fold dilution of the primary antibody were added into the blocking buffer and incubated overnight at 4°C with shaking. The following day, the membrane was rinsed once with TBS-T (0.14M NaCl, 0.02 M Tris HCl (pH 7.6), 0.1% Tween 20) followed by three 10-min washes with TBS-T at room temperature. The membrane was next incubated with goat anti-rabbit IR Dye 800CW secondary antibody (1:20,000) in 5% non-fat milk buffer for 1 h at room temperature with shaking. The membrane was rinsed with TBS-T once followed by three 10-min washes with TBS-T at room temperature. Western blots were scanned using an Odyssey Infrared Imager (LI-COR Biosciences) and analyzed with the Odyssey Infrared Imaging System Application Software (LI-COR Biosciences, Version 3.0).

In vitro characterization of the H10S Mre11 mutant protein. The H10S mutation was generated by the Nelson lab in the Mre11 expression vector pTYB1-gp47 (HERDENDORF *et al.* 2011) using the Quickchange™ mutagenesis protocol (Stratagene).

The sequence of the forward mutagenic primer was as follows: 5'-gaaaattttaaatttaggtgattgg**agt**ttaggcgttaaagctgatgatg-3', where the mutant codon is shown in bold. The second mutagenic primer was the reverse complement of the forward. The expression, purification, and biochemical assays were performed essentially as described (HERDENDORF *et al.* 2011).

Analysis of plasmid DSB formation and processing in T4-infected cells (T4 Rad50). The *in vivo* T4 Rad50 experiments were conducted as above (see Analysis of plasmid DSB formation and processing in T4-infected cells (T4 Mre11)).

The T4 Rad50 induction experiments were conducted with a few key differences: Using the λDE3 Lysogenization Kit, λDE3 prophage was integrated into the *E. coli* KL16-99 chromosome to allow for IPTG-induced expression of the indicated pET28-gp46 mutants. The indicated λDE3 bacterial strains were pre-grown in LB containing appropriate antibiotic(s) with shaking at 37°C to an OD_{560} of 0.5. Next, the bacterial strains were added to pre-warmed LB containing appropriate antibiotic(s) and the indicated amount of IPTG and grown up to an OD_{560} of 0.5. The indicated phage strain was then added at a MOI of 3 and the procedure proceeded as described above (see Analysis of plasmid DSB formation and processing in T4-infected cells (T4 Mre11)).

2.3 Results

Substitutions in the nuclease motif of the T4 Mre11 subunit (gp47)

Studies in other systems have demonstrated the importance of the Mre11 phosphoesterase motifs (DXH), including the highly conserved motif I (DXH) very near the N terminus (see Introduction). We are particularly interested in the possible importance of the T4 Mre11 (gp47) nuclease activity, since the T4 MR complex is so important in double-strand end processing. To begin to test the importance of functional motifs and potentially uncover viable separation-of-function mutants, a previous member of our lab, Anil Panigrahi mutated the highly conserved histidine (His-10) within motif I (ALMOND *et al.* 2013). Mutations in this motif of the *S. cerevisiae* Mre11 protein resulted in informative partial-function mutants (KROGH *et al.* 2005). Since any mutation of this highly conserved residue might turn out to be lethal in the T4 system, Anil introduced an amber mutation in place of the His codon, and isolated the desired strain using a host containing a histidine-tRNA suppressor. The presence of the desired amber mutation ($47^{amHis10}$) in the resulting phage was confirmed by amplifying the region containing the mutation using the PCR and verifying the presence of an expected BfaI restriction enzyme site (see Materials and Methods).

We then took advantage of a collection of strains that each carry a different suppressor tRNA to introduce different amino acid substitutions at this position of the Mre11 (KLEINA *et al.* 1990; NORMANLY *et al.* 1990), with the histidine-tRNA suppressor

strain serving as positive control. The amber mutant phage failed to grow on multiple suppressor strains, implying that substitutions of lysine, arginine, proline, leucine, tyrosine, serine, glutamic acid and glycine all result in lethality. Both the parental K10 strain and the *47*^{amHis10} strain contain unrelated amber mutations in genes *38* and *51* (involved in tail and head assembly, respectively). Since the parental K10 strain grows in each of these suppressing hosts, the suppressor tRNA's must be functional (several other suppressing strains did not allow growth of either parental K10 or the *47*^{amHis10} mutant, presumably due to lack of suppression of the *38* and/or *51* mutation). We conclude that the conserved histidine within phosphoesterase Motif I of the T4 Mre11 is essential for T4 growth. This mutant should be useful for studies of the detailed role of the nuclease function of the Mre11, but does not provide a viable partial-function mutant of the T4 MR complex.

It is important to note that initial attempts to introduce different amino acid substitutions at the conserved His10 position of T4 Mre11 with the histidine-tRNA suppressor strain serving as positive control were compromised. The key obstacle that arose was with the positive control (histidine-tRNA suppressor strain). The histidine-tRNA suppressor strain had a low efficiency of suppression and as a result, did not produce wild-type (WT) levels of T4 Mre11 when infected with *47*^{amHis10} phage. The *47*^{amHis10} phage grew only about 20% as well as the K10 WT phage in the presence of the histidine-tRNA suppressor (The K10 WT average phage titer was 2.61 E10 phage/mL

whereas the *47*^{amHis10} average phage titer was 5.5 E9 phage/mL). We wanted to increase the efficiency of the histidine suppressor strain (along with the other suppressor strains) for *47*^{amHis10} phage growth to allow for the production of near-WT levels of T4 Mre11, so that we could compare infections of K10 WT phage and *47*^{amHis10} phage. This would enable the use of the histidine-tRNA suppressor as a positive control and would allow for the production of near-WT levels of T4 Mre11 for all suppressor strains.

It was noted that all previously used *E. coli* strains that harbored the amber suppressors were *rpsL* mutants (to prevent cell culture contamination). *RpsL* encodes the ribosomal protein S12. Mutations in *rpsL* have been shown to confer resistance to streptomycin. Importantly, these same mutations have also been shown to increase the accuracy of translational proofreading and thus, reduce the efficiency of suppression (EGGERTSSON and SOLL 1988). We proposed that using a WT *rpsL* strain would increase the efficiency of suppression of the histidine-tRNA suppressor.

The histidine-tRNA suppressor was transformed into KL16-99 cells (*rpsL*$^{+}$). After repeating the phage growth and titering of both K10 WT phage and *47*^{amHis10} phage, it was observed that the new *E. coli* strain dramatically increased the histidine-tRNA suppressor efficiency. Instead of a 5x growth difference between K10 WT phage and *47*^{amHis10} phage, the growth difference between the phage was greatly reduced (The K10 WT average phage titer was 4.90 E10 phage/mL whereas the *47*^{amHis10} average phage

titer was 3.50 E10 phage/mL). We therefore used KL16-99 for our host strain with the plasmid-borne amber suppressors and were able to use the histidine-tRNA amber suppressor as a positive control.

To test the importance of the histidine residue in motif I in T4 DSB processing and RDR, we used the plasmid RDR assay shown in Figure 2-1. Plasmid model systems provide useful windows for studying the details of phage T4 DSB processing/repair and the RDR that is induced during the DSB repair reactions (GEORGE and KREUZER 1996; GEORGE *et al.* 2001; KREUZER *et al.* 1995; STOHR and KREUZER 2002). These systems utilize phage derivatives carrying *denA* and *denB* mutations to prevent phage-induced plasmid DNA breakdown. Plasmid pTD101 carries a 787-bp duplication with an I-*Tev*I site located in between the direct repeats. This plasmid is very similar to the previously used plasmid pTD001, except that pTD101 is on a pACYC184 backbone while pTD001 is on a pBR322 backbone (see (TOMSO and KREUZER 2000) for derivation of pTD001). After infection by T4, induction of I-*Tev*I endonuclease leads to a DSB, and subsequent repair occurs predominantly by an RDR mechanism that generates rolling circle products with only one copy of the repeat per plasmid segment (Figure 2-1A) (GEORGE *et al.* 2001; TOMSO and KREUZER 2000). Control infections with gene *47*$^{+}$ phage were conducted to test whether any of the suppressors interfere with T4 RDR for some trivial reason (i.e., generating a dominant-negative replication protein due to read-through).

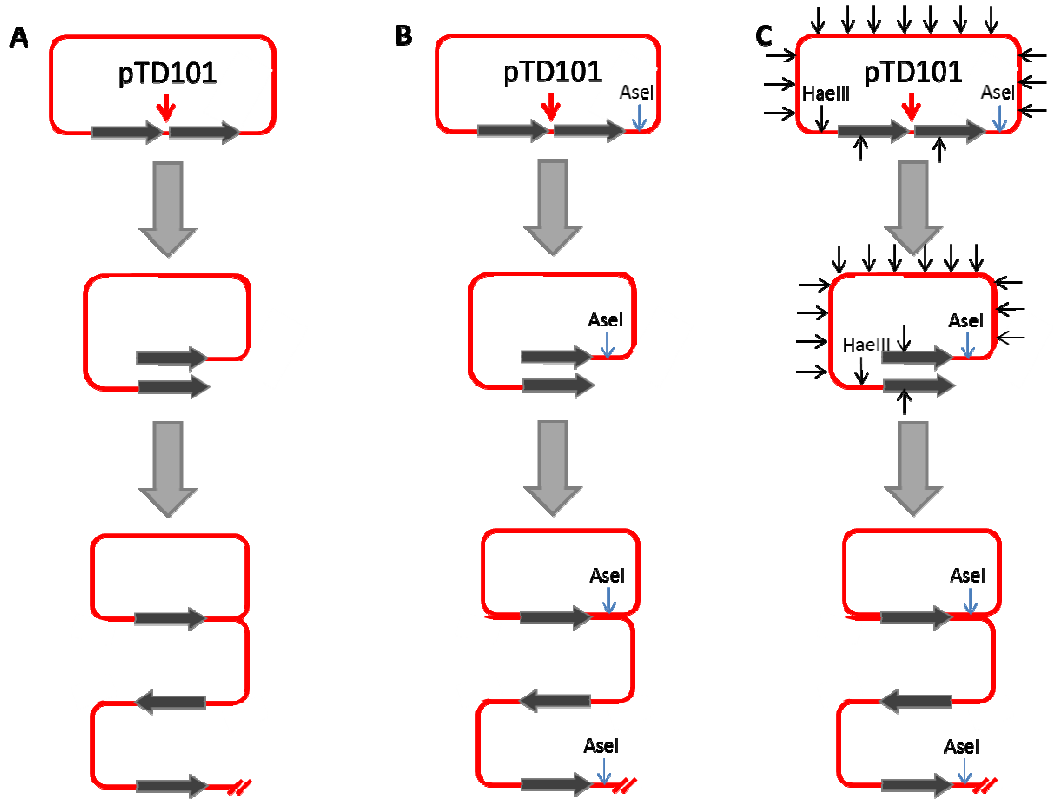

Figure 2-1: Impact of the T4 MR complex on RDR of plasmid pTD101.

(A) Diagram of plasmid pTD101, which contains direct repeats (thick black arrows) flanking an I-*Tev*I recognition site (red arrow). I-*Tev*I cleavage induces rolling circle replication as shown. (B) Same 2-1A Diagram but with AseI restriction sites indicated. AseI is able to digest both phage-replicated and unreplicated DNA. (C) Same 2-1A Diagram but with AseI + HaeIII restriction sites indicated (for simplicity, we only show 16 of the 32 HaeIII cut sites). HaeIII is able to digest unreplicated DNA but is unable to digest phage replicated DNA.

Seven of the tested suppressors are plasmid borne, and results with these strains are shown in Figures 2-2 and 2-3 (the suppressor plasmids are in a pBR322 backbone, which is compatible with the pACYC184-based pTD101 plasmid). It is important to note that in Figure 2-2, total DNA from the infections was digested with AseI whereas in Figure 2-3, total DNA from the infections (same samples from Figure 2-2) was digested with AseI + HaeIII. The AseI digestion allowed for analysis of both phage-replicated and unreplicated (full-length and I-*Tev*I-cleaved) DNA (Figure 2-1B) whereas the AseI + HaeIII digestion allowed for analysis of only phage replicated DNA since the HaeIII enzyme cuts unmodified phage DNA into small pieces that run off the gel (Figure 2-1C). The 47^{+} infection generated robust levels of plasmid pTD101 RDR product in the His, Cys, Pro, Glu, Arg and Phe suppressor strains (with some delay in the Glu suppressor strain). However, infections of the Gly suppressor-containing strain consistently generated somewhat reduced levels of plasmid RDR product. The $47^{amHis10}$ phage, in contrast, generated plasmid RDR product only in the strain with the cognate His suppressor (Figures 2-2 and 2-3). Furthermore, the I-*Tev*I-cleaved plasmid bands were stabilized in each of the suppressor containing strains (except His suppressor) after infection by the $47^{amHis10}$ phage. We conclude that double-strand end processing is inhibited and RDR is completely blocked by these six substitutions at the His10 codon of the T4 Mre11.

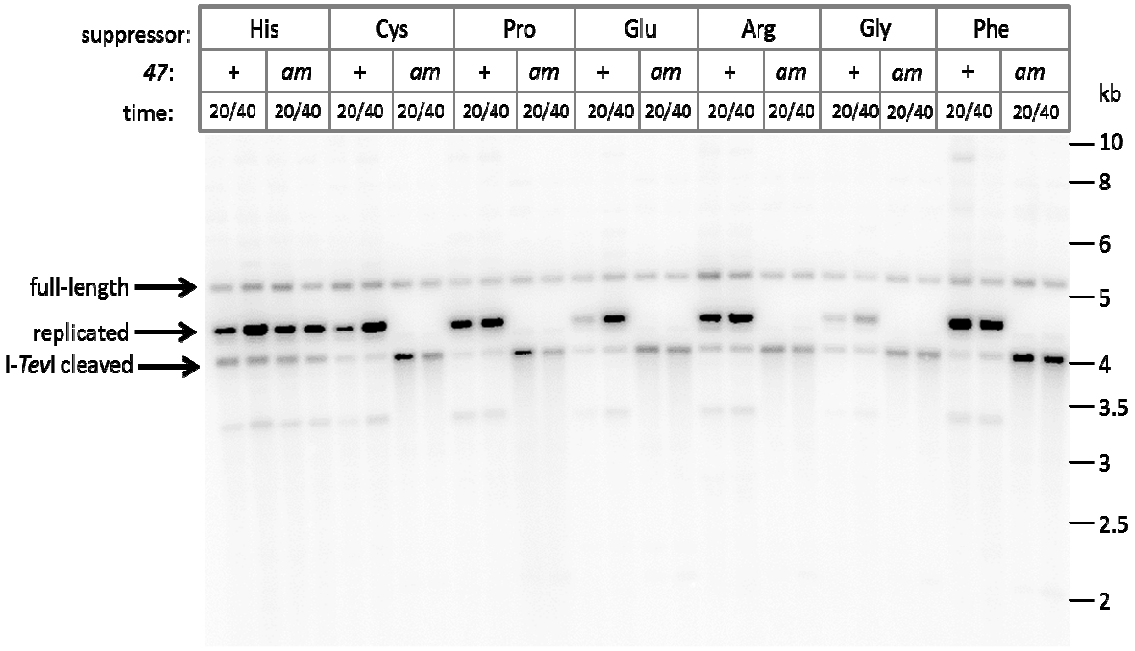

Figure 2-2: Plasmid RDR induced by T4 *47*^{amHis10} phage upon infection of cells with different plasmid-borne suppressors.

E. coli KL16-99 cells that contained pTD101 and the indicated plasmid-borne suppressor were infected with either *47*$^{+}$ or *47*^{amHis10} phage and samples were harvested after 20 and 40 min. Total DNA from the infections was digested with AseI and analyzed by Southern blot with a pACYC184-derived probe. The AseI digestion allowed for analysis of both phage-replicated and unreplicated (full-length and I-*Tev*I-cleaved) DNA. The band labeled "full length" represents unreplicated plasmid containing both tandem repeats, while the band labeled "replicated" represents phage-replicated plasmid containing only one of the two tandem repeats. The shorter band created by cleavage of the full length plasmid band at the I-*Tev*I recognition site is indicated.

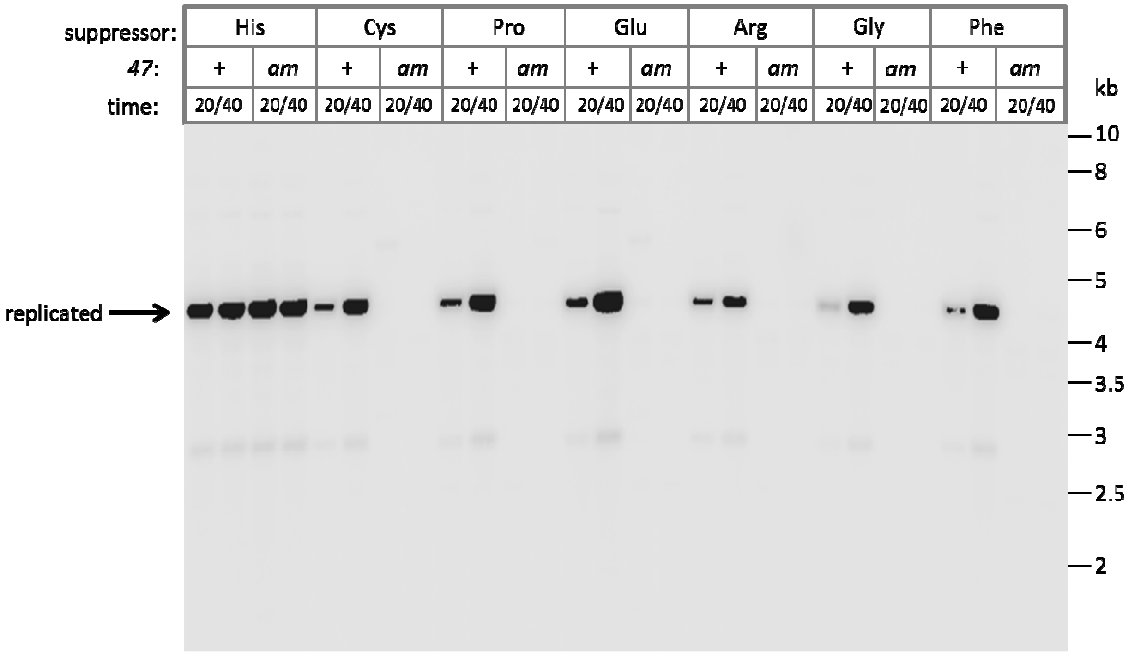

Figure 2-3: Plasmid RDR induced by T4 *47*^{amHis10} phage upon infection of cells with different plasmid-borne suppressors.

E. coli KL16-99 cells that contained pTD101 and the indicated plasmid-borne suppressor were infected with either *47*$^{+}$ or *47*^{amHis10} phage and samples were harvested after 20 and 40 min. Total DNA from the infections was digested with AseI + HaeIII and analyzed by Southern blot with a pACYC184-derived probe. The AseI + HaeIII digestion allowed for analysis of phage replicated DNA. The HaeIII enzyme cuts unmodified phage DNA into small pieces that run off the gel. The band labeled "replicated" represents phage-replicated plasmid containing only one of the two tandem repeats.

Five additional suppressors are located in the *E. coli* chromosome in a distinct genetic background. Since the efficiency of suppression can vary between genetic backgrounds, we introduced the His suppressor (on its pBR322-based plasmid) into the suppressor-free version of this genetic background as a positive control (Figures 2-4 and 2-5). Again, it is important to note that in Figure 2-4, total DNA from the infections was digested with AseI whereas in Figure 2-5, total DNA from the infections (same samples from Figure 2-4) was digested with AseI + HaeIII. The AseI digestion allowed for analysis of both phage-replicated and unreplicated (full-length and I-*Tev*I-cleaved) DNA (Figure 2-1B) whereas the AseI + HaeIII digestion allowed for analysis of only phage replicated DNA since the HaeIII enzyme cuts unmodified phage DNA into small pieces that run off the gel (Figure 2-1C). The 47^{+} phage generated ample amounts of replicated pTD101 deletion product in either the suppressor-free or His suppressor-containing host (Figures 2-4 and 2-5). Without any suppressor, the $47^{amHis10}$ phage generated no plasmid RDR product but robust amounts of stabilized I-*Tev*I-cleaved plasmid DNA, while the presence of the His suppressor effectively suppressed these defects (Figures 2-4 and 2-5). We conclude that this is a suitable genetic background to assess the effect of substitutions at the His-10 residue of the T4 Mre11.

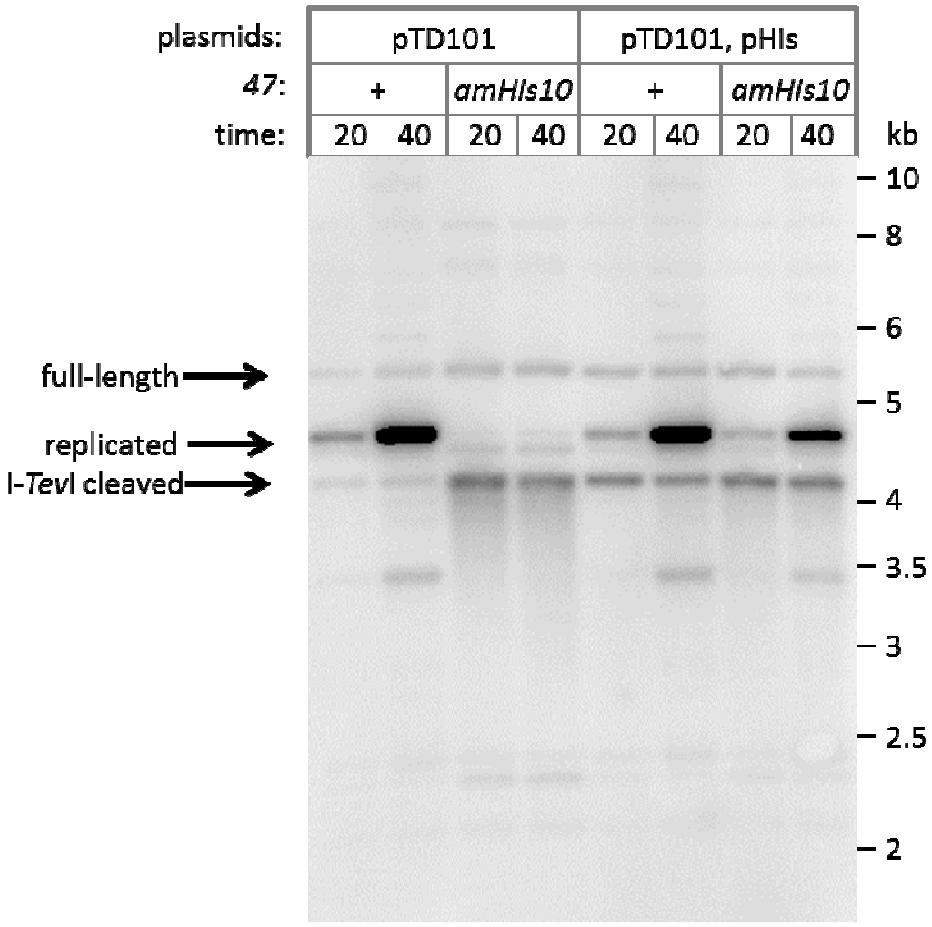

Figure 2-4: Plasmid RDR induced by T4 *47*^{amHis10} phage upon infection of cells with or without the plasmid-borne histidine suppressor.

E. coli CSH108 cells that contained pTD101, with or without the plasmid-borne His suppressor, were infected with either *47*$^{+}$ or *47*^{amHis10} phage and samples were harvested after 20 or 40 min. Total DNA from the infections was digested with AseI and analyzed by Southern blot with a pACYC184-derived probe.

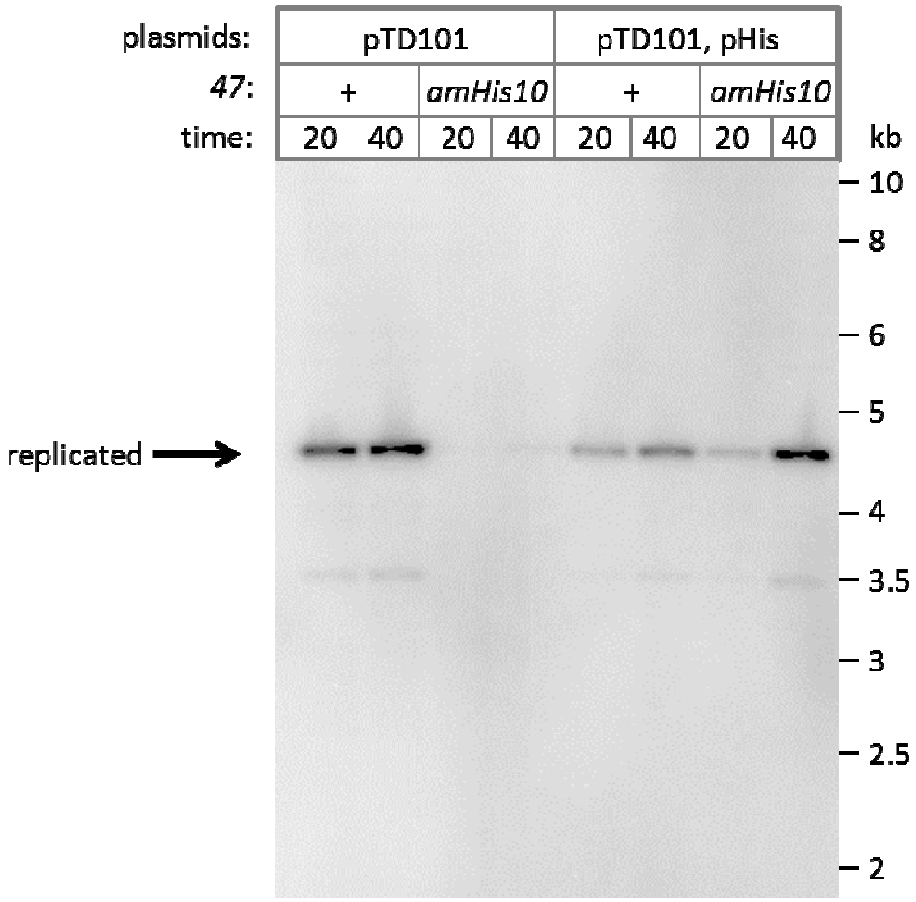

Figure 2-5: Plasmid RDR induced by T4 *47*^{amHis10} phage upon infection of cells with or without the plasmid-borne histidine suppressor.

E. coli CSH108 cells that contained pTD101, with or without the plasmid-borne His suppressor, were infected with either *47*$^{+}$ or *47*^{amHis10} phage and samples were harvested after 20 or 40 min. Total DNA from the infections was digested with AseI + HaeIII and analyzed by Southern blot with a pACYC184-derived probe.

Turning to results with the five additional suppressors, the *47*$^{+}$ phage produced plasmid RDR product with little or no stabilization of the broken ends (Figures 2-6 and 2-7, see previous discussion about AseI vs. AseI + HaeIII digest, respectively). Somewhat reduced levels of RDR product was seen in the Gln and Leu suppressor strains. In contrast, the *47*^{amHis10} phage produced no plasmid RDR product but did show robust amounts of stabilized I-*Tev*I-cleaved plasmid DNA in each of the strains (Figures 2-6 and 2-7).

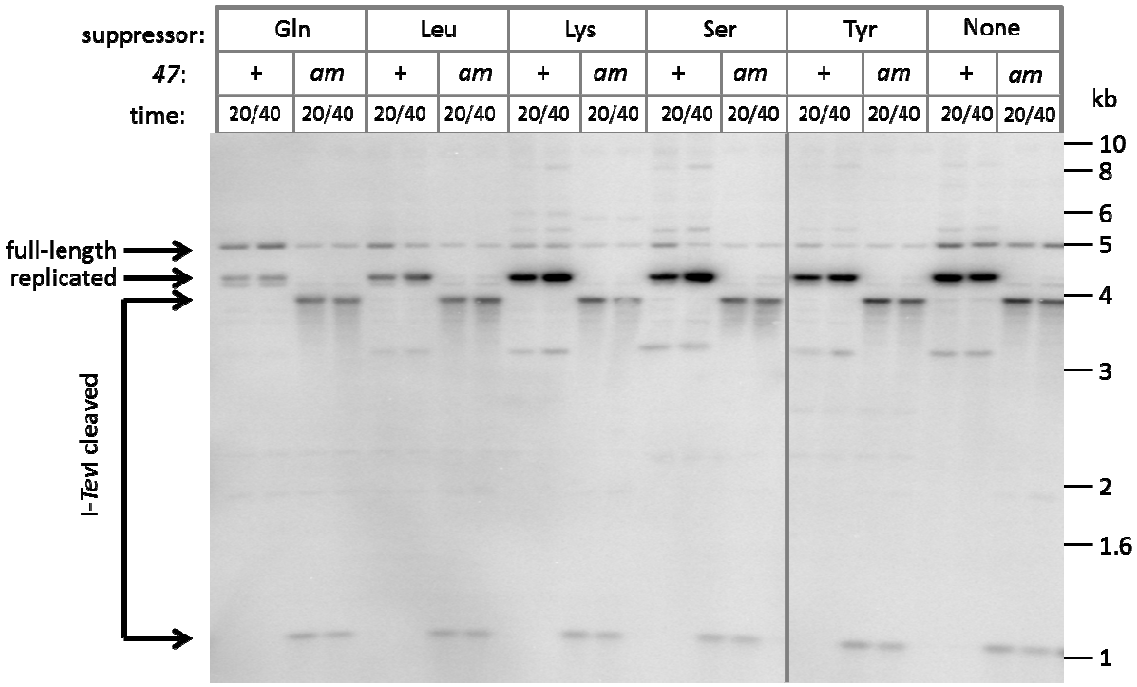

Figure 2-6: Plasmid RDR induced by T4 *47*^{amHis10} phage upon infection of cells with different chromosome-borne suppressors.

E. coli CSH108 cells that contained pTD101 and the indicated chromosomal-borne suppressor were infected with either *47*$^{+}$ or *47*^{amHis10} phage and samples were harvested after 20 or 40 min. Total DNA from the infections was digested with AseI and analyzed by Southern blot with a pACYC184-derived probe.

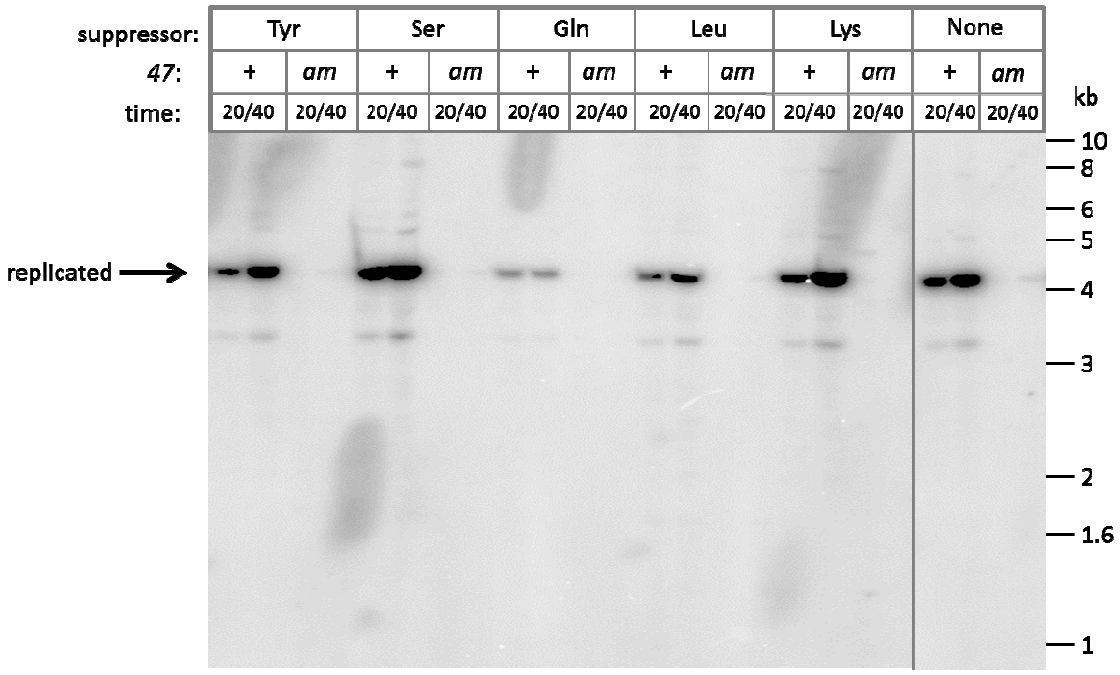

Figure 2-7. Plasmid RDR induced by T4 *47*^{amHis10} phage upon infection of cells with different chromosome-borne suppressors.

E. coli CSH108 cells that contained pTD101 and the indicated chromosomal-borne suppressor were infected with either *47*$^{+}$ or *47*^{amHis10} phage and samples were harvested after 20 or 40 min. Total DNA from the infections was digested with AseI + HaeIII and analyzed by Southern blot with a pACYC184-derived probe.

We conclude that a wide range of substitutions at the His-10 codon of T4 Mre11 abolishes the *in vivo* end processing and RDR activities of the T4 MR complex. These strong defects in end processing and RDR could be due to very poor suppression and/or production of unstable protein, which would trivialize the overall significance of these results. We therefore analyzed the level of soluble T4 Mre11 in parallel infections by performing Western blots. Roughly equal amounts of total protein from 20-minute infections of suppressor strains were compared. Considering the chromosomal suppressors, the tyrosine, serine, glutamine and leucine suppressors all resulted in at least as much T4 Mre11 as the positive control histidine suppressor, while the lysine suppressor resulted in very little protein (Figure 2-8). Considering the plasmid-based suppressors, the proline, glutamic acid and glycine suppressors resulted in more T4 Mre11 than the histidine suppressor, while the arginine, phenylalanine and cysteine suppressors resulted in less. Since the histidine suppressor appeared to be fully functional *in vivo* at its relative level of expression, we conclude that at least seven of the amino acid substitutions had sufficient levels of MR complex to sustain biological function but yet did not do so (while four others had lower levels of T4 Mre11 which might possibly have contributed to their lack of function). In any case, we conclude that at least seven substitutions of the His-10 codon block biological function even when expressed at levels sufficient for function with the wild-type T4 Mre11. These results highlight the importance of the nuclease motif in T4 Mre11.

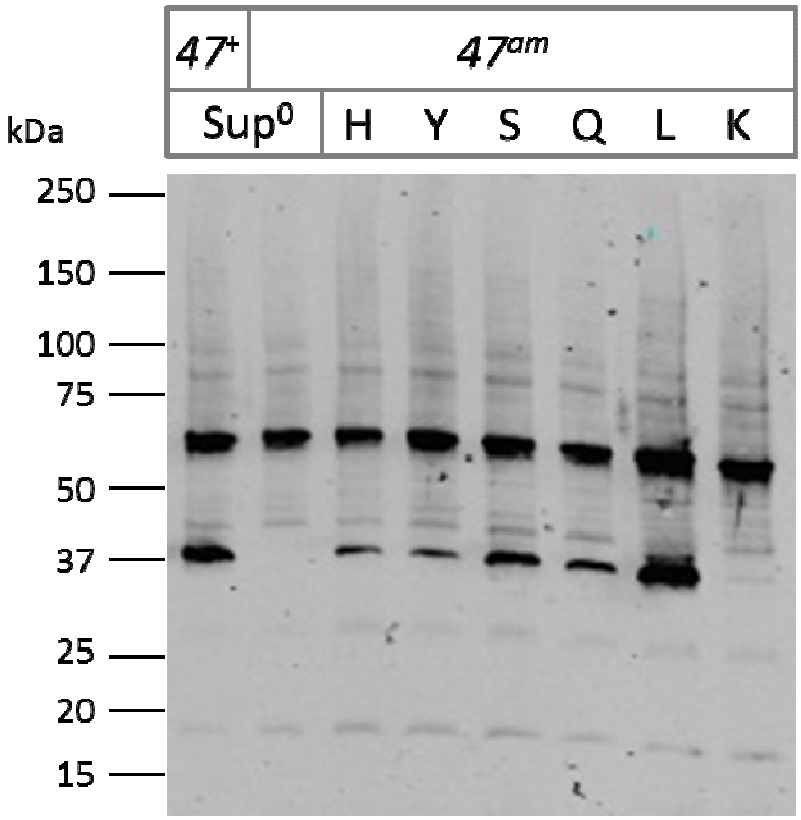

Figure 2-8: Western blot analysis of infections by T4 *47*^{amHis10} phage in cells with chromosomal-borne suppressors.

E. coli CSH108 cells that contained pTD101 with no suppressor (first two lanes) or the plasmid-borne His suppressor (third lane) or chromosomal-borne suppressors (last 5 lanes) were infected with either *47*$^{+}$ (first lane) or *47*^{amHis10} (all other lanes) phage for 20 min. Roughly equal amounts of total protein from the infections were analyzed by Western blot with a gp46/47 anti-rabbit primary antibody. Gp47 (39.2 kDa) is the faster migrating band, while the slower migrating band present in every lane is an unidentified cross-reacting host protein (also present in uninfected cells).

The effect of the H10S mutation on the nuclease activity of T4 Mre11

To confirm that mutation of the conserved motif I (DXH) of T4 Mre11 abolishes its nuclease activity, the Nelson lab generated the H10S point mutant in the pTYB1-gp47 expression plasmid, expressed the protein in *E. coli* BL21 (DE3) cells and purified it to homogeneity. The mutant protein exhibited similar levels of expression and purified in an identical manner as the wild-type protein (data not shown). As expected, the H10S mutant was completely defective in nuclease activity using two established nuclease assays (performed by the Nelson lab). The first assay tests the ability of the MR complex to perform multiple nucleotide excisions on a uniformly ^{32}P-labeled 1680-bp linear dsDNA and is dependent on hydrolysis of ATP by Rad50 (HERDENDORF *et al.* 2011). As shown in Figure 2-9A, the wild-type MR complex removes approximately ~45% of the nucleotides during a rapid phase followed by a second, much slower phase. As described in Herdendorf *et al.* (2011), the data can be fit to a single-exponential plus linear equation and control experiments have assigned these phases as dsDNA exo and ssDNA exo/endo nuclease activities, respectively. The MR-H10S complex has no measurable activity during the time course of the reaction, consistent with the expected loss of nuclease activity due to the removal of this important metal ligating residue (HOPFNER *et al.* 2001; MOREAU *et al.* 1999). The second nuclease assay is performed under steady-state conditions and relies on the removal of the fluorescent nucleotide analog, 2-aminopurine from the 3' end of a 50 bp dsDNA substrate (ALBRECHT *et al.*

2012). In this assay the Mre11 is activated by the presence of the Rad50 but ATP hydrolysis is not required. As seen in Figure 2-9B, the MR-H10S complex is also completely defective in ATP-independent nuclease activity.

To determine if H10S-Mre11 binds to both Rad50 and dsDNA, the Nelson lab performed ATP hydrolysis assays (HERDENDORF *et al.* 2011). This assay is performed in the absence of $MnCl_2$ so that the nuclease activity of the wild-type T4 Mre11 is absent. As shown in Figure 2-9C, the Rad50 alone has relatively little ATP hydrolysis activity and the addition of either the T4 Mre11 subunit or dsDNA alone has little effect. However, addition of either the wild-type or H10S-Mre11 together with DNA causes an approximately 20-fold activation in ATP hydrolysis activity of the Rad50. This indicates that the H10S-Mre11 retains its ability to bind to the Rad50 and that the H10S-MR complex binds to dsDNA in a normal fashion. Together these results indicate that the H10S-Mre11 subunit is specifically defective in its nuclease activity but fully functional in complex assembly and DNA binding.

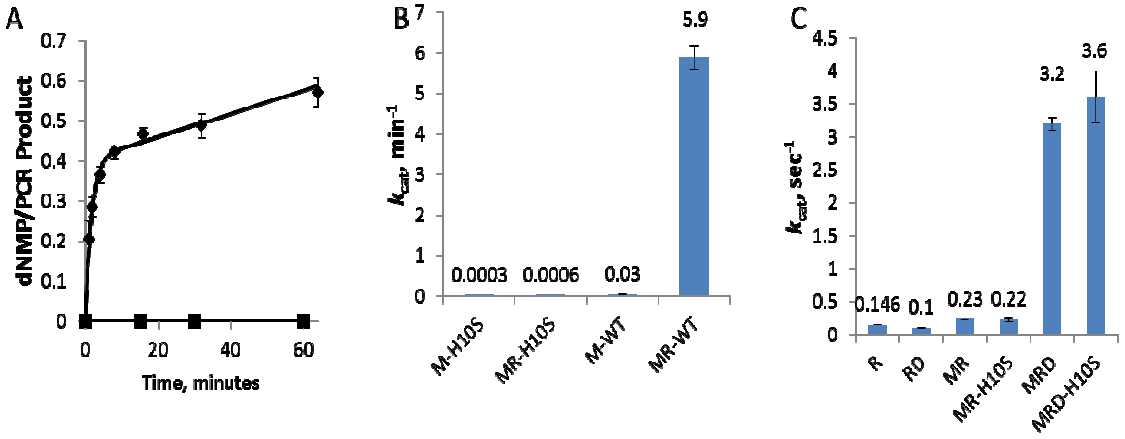

Figure 2-9: Biochemical characterization of the T4 Mre11-H10S mutant conducted by the Nelson lab.

(A) Nuclease activity of the MR complex in the presence of ATP using a uniformly ^{32}P-labeled 1680-bp dsDNA substrate. The wild-type and H10S activity is represented by diamonds and squares, respectively. The solid lines are fits to the data as described in "Results". (B) Steady-state exonuclease activity of the T4 Mre11 subunit (M) and the T4 MR complex (MR) for wild-type (WT) and the H10S mutant. The value shown above the bar represents the apparent-k_{cat}. (C) Steady-state ATP hydrolysis activity of the Rad50 subunit (R) and the MR complex (MR). Assays performed in the presence of 50-bp linear dsDNA are indicated by the inclusion of the letter D. In all cases the data for the wild-type proteins come from Herdendorf *et al.* (2011).

ATPase-deficient substitutions of the T4 Rad50 subunit (gp46)

Studies in other systems have demonstrated the importance of Rad50 and the conserved motifs in the Rad50 nucleotide binding domain, including the highly conserved Signature motif (S•G/A•G•E/Q•K/R) (see Introduction). We are particularly interested in the possible importance of the T4 Rad50 (gp46) ATPase activity, since the T4 MR complex is so important in double-strand end processing. In collaboration with Dr. Scott Nelson, we took advantage of a collection of plasmids that each expressed a different T4 Rad50 ATPase mutation to introduce different gp46 substitutions, with the pET28-gp46WT plasmid serving as a positive control. It should be noted that for all described pET28 experiments (unless otherwise indicated), the expression of T4 Rad50 protein was due to leaky expression. The pET28 expression plasmid contains the *lac* operator and a T7 promoter. The T7 promoter is specific to the T7 RNA polymerase (absent in our pET28 infections).

To confirm that the pET28-gp46WT plasmid complemented the 46^{am} knockout as a positive control, we used the same plasmid RDR assay shown in Figure 2-1. We introduced pET28 and pET28-gp46WT plasmid into the *E. coli* KL16-99 + pTD101 background and compared infections between K10 (46^{+}) and K10 46^{am} (46^{-}) phage. The 46^{+} phage generated ample amounts of replicated pTD101 deletion product in either the pET28 or pET28-gp46WT containing host (Figure 2-10). Without the pET28-gp46WT plasmid (only pET28), the 46^{am} phage generated no plasmid RDR product, while the

presence of the pET28-gp46WT plasmid suppressed these defects (Figure 2-10). We conclude that the pET28-gp46WT plasmid complements the *46*^{am} phage and is thus a suitable positive control to assess the effect of different T4 Rad50 substitutions.

We then took advantage of a collection of different pET28-gp46 ATPase-deficient mutant plasmids that each carry a different T4 Rad50 NBD conserved motif mutation to introduce different T4 Rad50 substitutions, with the pET28-gp46WT plasmid serving as positive control. The ATPase-deficient substitutions were made in the conserved Signature motif, D-loop, coiled-coil domain, H-loop, and Walker B motif (see Table 2-1 for the list of specific mutations and their observed/proposed biochemical effects). The Signature motif is known to complete the dimeric ATP binding site. The conserved serine (S471) interacts with the gamma phosphate of ATP. Mutations of this residue alter the binding of ATP to the ATPase active site (HERDENDORF and NELSON 2011). The conserved glutamate (E474) forms hydrogen bonds with the backbone amide of S471. Mutations of this residue effect the positioning of S471 and as a result, the binding of ATP. Finally, mutations of the conserved lysine (K475) act to destabilize the Signature motif (HERDENDORF and NELSON 2011). This residue has additionally been proposed to be involved in controlling the position of the coiled-coil domain, which in turn interacts with Mre11 (WILLIAMS *et al.* 2011).

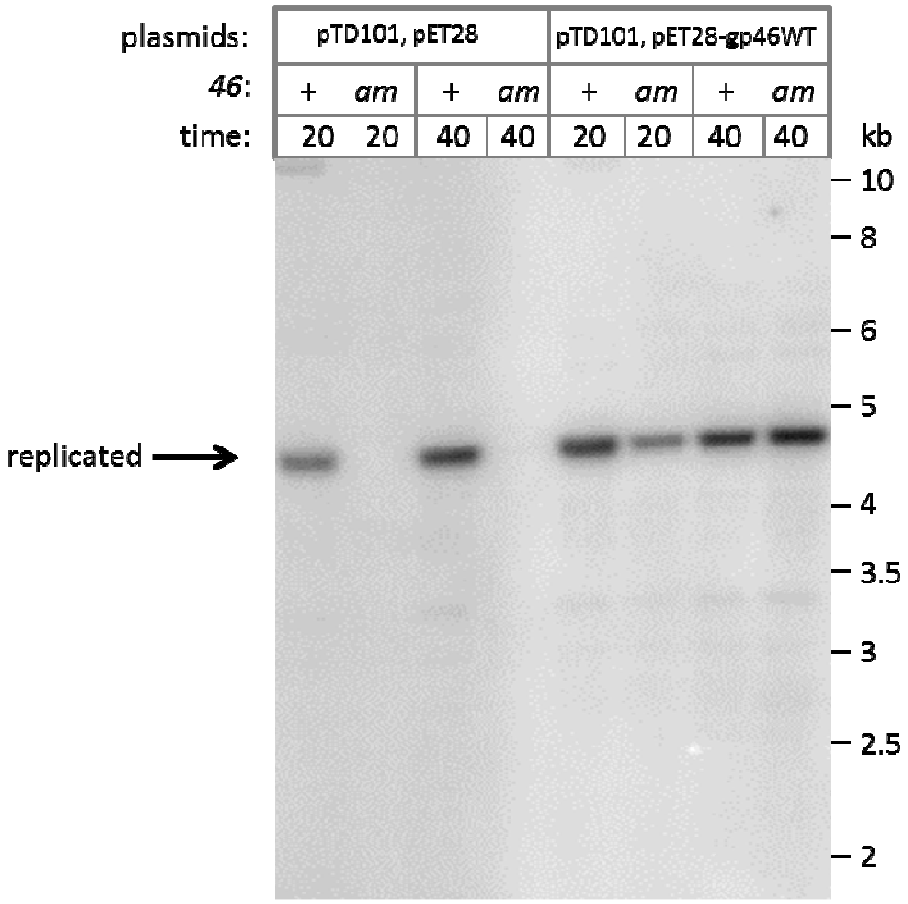

Figure 2-10: Plasmid RDR induced by T4 *46*^{am} phage upon infection of cells with pET28 or pET28-gp46WT plasmid.

E. coli KL16-99 cells that contained pTD101 and pET28 or pET28-gp46WT, were infected with either *46*$^{+}$ or *46*^{am} phage and samples were harvested after 20 or 40 min. Total DNA from the infections was digested with AseI + HaeIII and analyzed by Southern blot with a pACYC184-derived probe.

Table 2-1: T4 Rad50 mutations and their observed/proposed biochemical effects.

Rad50 Mutation	Location	Biochemical Effect	Citation
S471A	Signature motif	Greatly reduced ATP hydrolysis and ATP binding to active site	Herdendorf and Nelson, 2011
S471M	Signature motif	Greatly reduced ATP hydrolysis and ATP binding to active site	Herdendorf and Nelson, 2011
E472G	Signature motif	Reduced ATP hydrolysis and altered ATP position	Herdendorf and Nelson, 2011
E474Q	Signature motif	Greatly reduced ATP hydrolysis and ATP binding to active site	Herdendorf and Nelson, 2011
K475M	Signature motif	Greatly reduced ATP hydrolysis and destabilized Signature motif	Herdendorf and Nelson, 2011
D512A	D-loop	Greatly reduced ATP hydrolysis and disrupted Walker A interaction for catalysis	De la Rosa and Nelson, 2011
46-cc	Just the coiled-coil domain	Possibly tethers full-length gp46 to prevent gp46-gp46 tethering	Unpublished
46-2CS	Coiled-coil domain	Mutated zinc-hook motif that prevents tethering	Unpublished
H536A	H-loop	Greatly reduced ATP hydrolysis and no Rad50 cooperativity	Unpublished
E505Q	Walker B motif	Greatly reduced ATP hydrolysis	Unpublished
E505Q/H536A	Walker B motif/H-loop	Greatly reduced ATP hydrolysis and no Rad50 cooperativity	Unpublished

The conserved T4 Rad50 D-loop interacts with the Signature motif and is proposed to form the nucleotide binding domain active site in *trans* by interacting with the Walker A motif; the nucleotide binding domain active site is formed when the Walker A, Walker B, H-loop, and Q-loop motifs from one monomer interact with the D-loop and Signature motifs of the adjacent monomer (DE LA ROSA and NELSON 2011). Specifically, the conserved D-loop aspartate (D512) is proposed to stabilize a conserved Walker A asparagine in a favorable position for hydrolysis. As a result, mutations of the D-loop aspartate greatly reduce ATP hydrolysis.

As discussed above, each Rad50 subunit adopts a long coiled coil structure and can dimerize with a second Rad50 subunit through their so-called zinc-hooks. This Rad50 dimer serves as a flexible tether connecting Mre11 proteins on each end (HOPFNER *et al.* 2002). Dr. Scott Nelson proposed that a mutated gp46 that only contained the coiled-coil domain (amino acids 152-410) would tether to full-length gp46 and as a result, disrupt gp46-gp46 tethers. Also discussed above, the zinc-hook is a conserved CXXC motif at the apex of the coiled-coil domain that forms a zinc tetrathiolate center upon dimerization. Dr. Scott Nelson proposed that a gp46-2CS mutation (CXXC to SXXS) would disrupt the zinc tetrathiolate center and as a result, disrupt tethering.

Results with the T4 Rad50 ATPase-deficient mutants (Table 2-1) are shown in Figures 2-11-2-14. The 46^{+} infection generated robust levels of plasmid pTD101 RDR product for all mutants. The 46^{am} phage, in contrast, generated plasmid RDR product

only in the presence of the gp46WT plasmid (Figures 2-11-2-14). Furthermore, the I-*Tev*I-cleaved plasmid bands were stabilized in each of the ATPase-deficient plasmids (except for gp46WT) after infection by the 46^{am} phage (Figures 2-11 and 2-12). We conclude that double-strand end processing is inhibited and RDR is completely blocked by these ATPase-deficient substitutions of T4 Rad50. Although we were unable to analyze the levels of soluble T4 Rad50 mutant protein with Western Blots, the Nelson lab observed that the mutant proteins all exhibited similar levels of expression and purified in an identical manner as the wild-type protein (personal communication; (DE LA ROSA and NELSON 2011; HERDENDORF and NELSON 2011)).

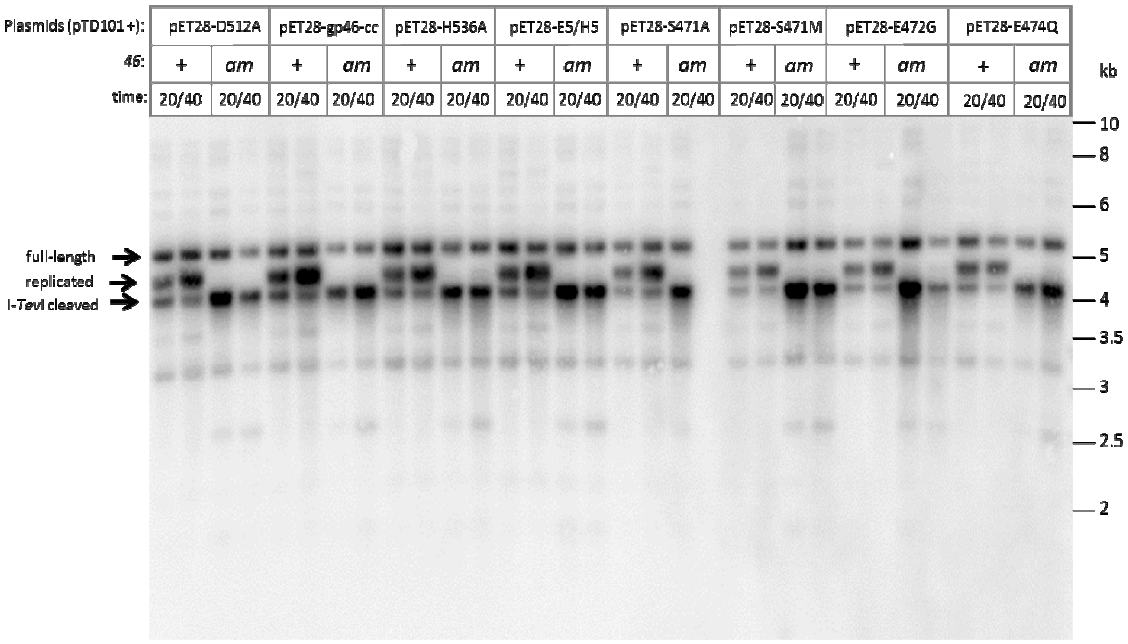

Figure 2-11: Plasmid RDR induced by T4 *46^{am}* phage upon infection of cells with different T4 Rad50 ATPase-deficient expressing plasmids.

E. coli KL16-99 cells that contained pTD101 and the indicated T4 Rad50 ATPase-deficient mutant plasmids were infected with either *46^{+}* or *46^{am}* phage and samples were harvested after 20 and 40 min. Total DNA from the infections was digested with AseI and analyzed by Southern blot with a pACYC184-derived probe. Note that the pET28-S471A *46^{am}* 40' lane of the gel is blank due to improper loading of the sample.

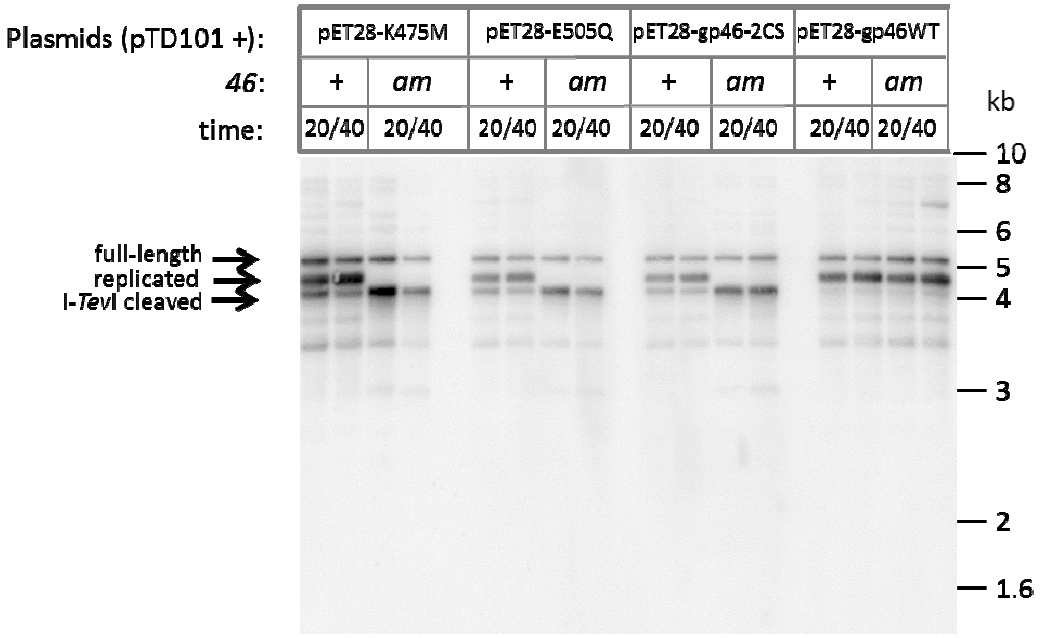

Figure 2-12: Plasmid RDR induced by T4 *46*^{am} phage upon infection of cells with different T4 Rad50 ATPase-deficient expressing plasmids.

E. coli KL16-99 cells that contained pTD101 and the indicated T4 Rad50 ATPase-deficient mutant plasmids were infected with either *46*$^{+}$ or *46*^{am} phage and samples were harvested after 20 and 40 min. Total DNA from the infections was digested with AseI and analyzed by Southern blot with a pACYC184-derived probe. Figures 2-11 and 2-12 are from the same gel (top half and bottom half, respectively).

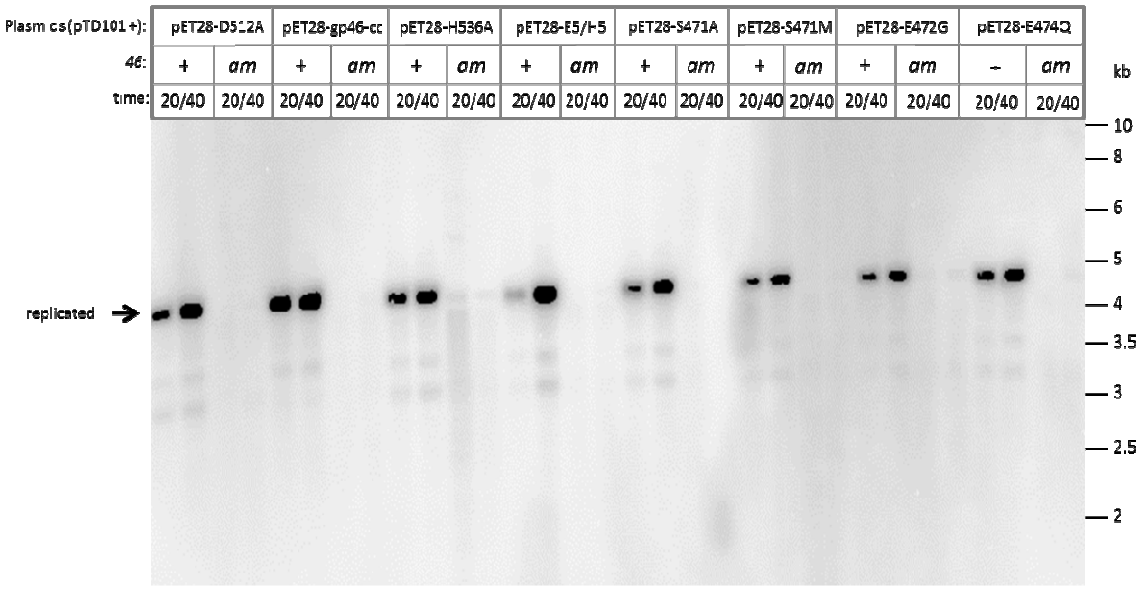

Figure 2-13: Plasmid RDR induced by T4 *46^{am}* phage upon infection of cells with different T4 Rad50 ATPase-deficient expressing plasmids.

E. coli KL16-99 cells that contained pTD101 and the indicated T4 Rad50 ATPase-deficient mutant plasmids were infected with either *46^{+}* or *46^{am}* phage and samples were harvested after 20 and 40 min. Total DNA from the infections was digested with AseI + HaeIII and analyzed by Southern blot with a pACYC184-derived probe.

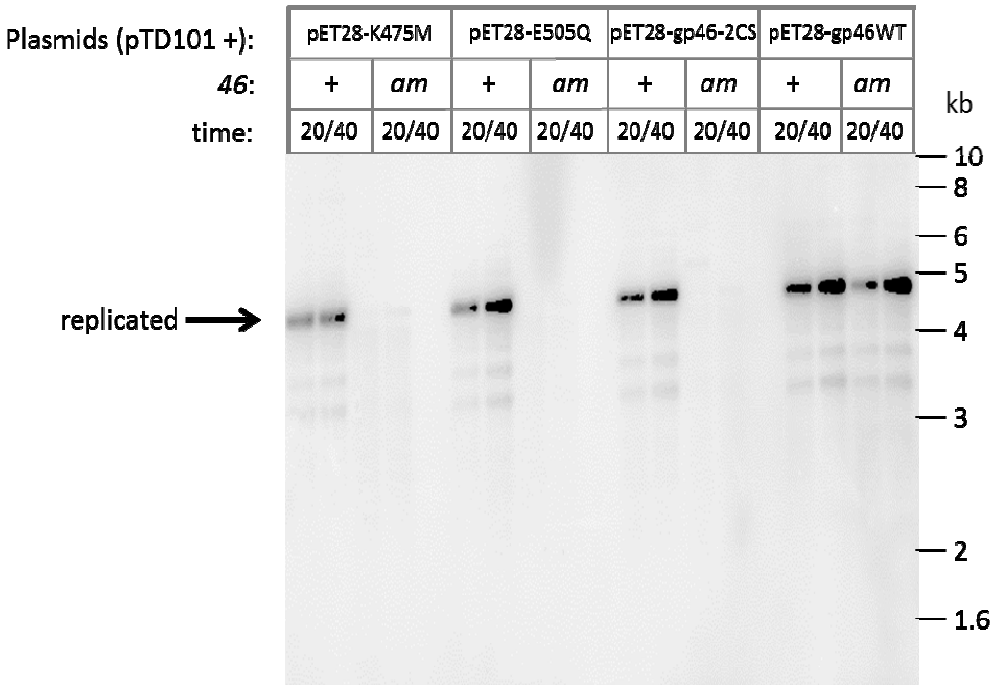

Figure 2-14: Plasmid RDR induced by T4 *46*^{am} phage upon infection of cells with different T4 Rad50 ATPase-deficient expressing plasmids.

E. coli KL16-99 cells that contained pTD101 and the indicated T4 Rad50 ATPase-deficient mutant plasmids were infected with either *46*$^{+}$ or *46*^{am} phage and samples were harvested after 20 and 40 min. Total DNA from the infections was digested with AseI + HaeIII and analyzed by Southern blot with a pACYC184-derived probe. Figures 2-13 and 2-14 are from the same gel (top half and bottom half, respectively).

For all previously described pET28 plasmid experiments, the expression of T4 Rad50 protein was due to leaky expression. We were interested in testing the T4 Rad50 mutants for the possibility of a dominant-negative effect, i.e. whether some of the T4 Rad50 mutants could out-compete the WT T4 Rad50 for T4 Mre11 binding (reviewed in (LUBIN *et al.* 2013)). Therefore, we introduced the λDE3 prophage into the *E. coli* KL16-99 + pTD101 + pET28 background. We tested different levels of IPTG to control transcription of the T7 RNA polymerase, and as a result, vary the transcription/expression of the T4 Rad50 protein that is cloned into the pET28 plasmid. Specifically, we tested the effect on RDR of different levels of three T4 Rad50 WT/mutant proteins (E505Q, gp46-cc, and gp46WT) in the presence of WT T4 Rad50 (K10 infection) to see if we could determine any dominant-negative effects.

Results with pET28-gp46WT, -gp46-cc, and –E505Q are shown in Figure 2-15. We were particularly interested in testing the gp46-cc construct since gp46-cc is proposed to prevent the tethering of WT T4 MR complexes to each other (discussed above). Additionally, we were interested in testing the E505Q mutation as the Nelson lab uses this mutation as the model ATPase-deficient mutant. The 46^{+} infection generated robust levels of plasmid pTD101 RDR product for gp46WT, gp46-cc, and E505Q at no and low levels of IPTG. At higher levels of IPTG, plasmid pTD101 RDR is reduced, even in the presence of WT gp46 (pET28-gp46WT) (see below for further discussion). Additionally, the I-*Tev*I-cleaved plasmid bands are stabilized at higher levels

of IPTG (data not shown). We conclude that double-strand end processing is inhibited and RDR is completely blocked by higher levels of E505Q mutant/WT T4 Rad50 expression (dominant over-expression effect). Also, some RDR inhibition is detected even with the gp46-cc construct, suggesting disruption of the coiled-coil.

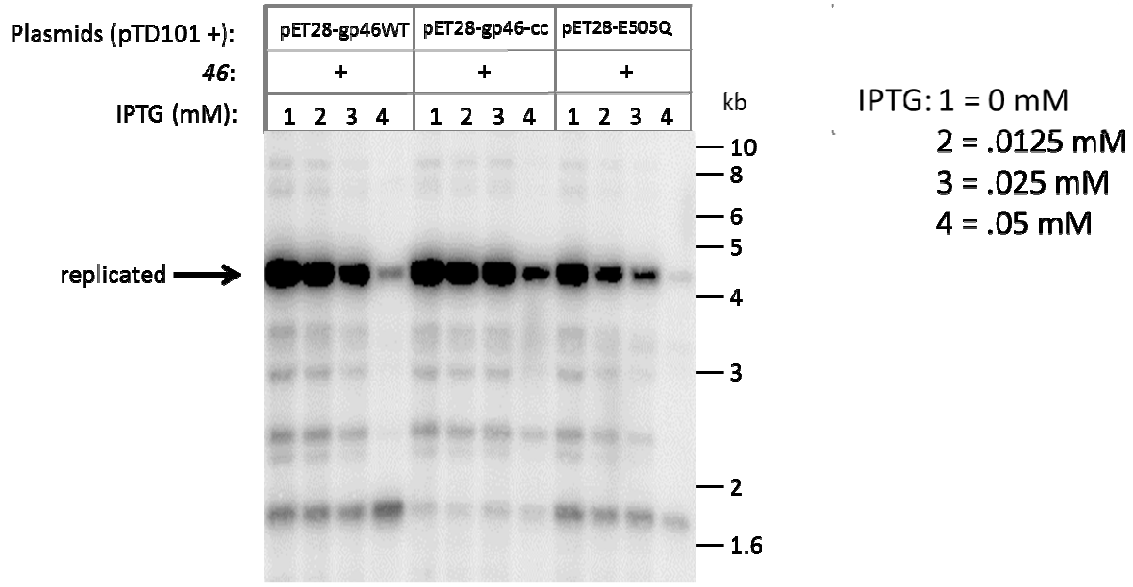

Figure 2-15: Plasmid RDR induced by T4 *46*$^{+}$ phage upon infection of cells with different levels of induced T4 Rad50 WT/ATPase-deficient protein.

E. coli KL16-99λ cells that contained pTD101 and the indicated T4 Rad50 WT/ATPase-deficient mutant plasmids were induced with varying levels of IPTG and infected with *46*$^{+}$ phage. Samples were harvested after 40 min. Total DNA from the infections was digested with AseI + HaeIII and analyzed by Southern blot with a pACYC184-derived probe. Additional unidentified bands are likely due to star cutting.

2.4 Discussion

The Mre11/Rad50 complex is a key factor in DSB repair and damage signaling that is conserved widely in evolution. We have investigated the detailed roles of the T4 MR complex by generating phage with substitutions in a conserved nuclease/phosphoesterase motif in T4 Mre11 and by generating phage with ATPase-deficient substitutions in conserved motifs that form the nucleotide binding domain in T4 Rad50.

We have approached the role of the Mre11 nuclease active site in T4 DNA metabolism. We found that at least eight different substitutions at the conserved His-10 residue abolish T4 growth, end processing, and RDR, demonstrating that this active site is critically important. Furthermore, we showed that a His10 to Ser substitution abolishes the *in vitro* nuclease activity of the MR complex, while having no effect on DNA binding by the MR complex or stimulation of the Rad50 ATPase activity (Figure 2-9). These *in vitro* results can be directly compared with the complete defects in end processing and RDR *in vivo* when the $47^{amHis10}$ mutant infected a serine-suppressing host (Figure 2-6).

As described above (see Introduction), the eukaryotic and *P. furiosus* MR complexes have 3' to 5' exonuclease activity as well as endonuclease activity, and the endonuclease activity on the 5' strand is important for activating 5' to 3' exonucleases

for strand resection. The activities of the T4 MR complex are very similar, although it is not yet clear whether it too activates other exonucleases for 5' to 3' resection (see (HERDENDORF *et al.* 2011)). As described above, UvsY and gp32 activate a Mg^{++}-dependent endonuclease activity in the T4 MR protein that may be involved in end resection (HERDENDORF *et al.* 2011). Our finding of a strict dependence of DSB end processing and repair on the T4 Mre11 nuclease active site demonstrates the key nature of the nuclease activity of the T4 complex, but does not resolve the question of which enzyme catalyzes the extensive 5' end resection in the DSB repair reaction (see Chapter 4 for further discussion).

While the role of the Mre11 nuclease motif in yeast and mammalian systems is complex and species-specific (STRACKER and PETRINI 2011), recent evidence in yeast and mammalian systems suggests that the nuclease motif of Mre11 is critical for many of its DNA repair functions. Mutations in the nuclease motif of the *S. pombe* Mre11 homolog caused hypersensitivity to DNA damaging agents comparable to that of Mre11-deleted mutants (WILLIAMS *et al.* 2008). Similarly, mice either lacking Mre11 entirely or harboring a nuclease-deficient mutant Mre11 showed early embryonic lethality, and their cells were equally hypersensitive to ionizing radiation (BUIS *et al.* 2008). Intriguingly, while the murine cells with nuclease-deficient Mre11 were defective in the activation of the ATR kinase, activation of the ATM kinase after DNA damage was not

significantly impacted (BUIS *et al.* 2008). Thus, the nuclease motif of Mre11 is critical for some but not all of its functions.

In summary, we found that the nuclease motif in T4 Mre11 is critically important for the plasmid model of RDR and for phage growth, with at least 7 substitutions providing no complementing activity. One of these mutations was shown directly to abolish nuclease activity *in vitro* while preserving the ability of the mutant protein to interact with Rad50 and DNA. Future studies can now focus on the precise role of the nuclease motif, in either activating nucleolytic processing by MR itself or by licensing some other nuclease for this key step in DSB repair.

We have also approached the role of the Rad50 nucleotide binding domain (ATPase active site) in T4 DNA metabolism. The NBD is formed by six conserved motifs: the Walker A, Walker B, D-loop, H-loop, Q-loop, and Signature motifs. The Walker A, Walker B, H-loop, and Q-loop motifs from one monomer interact with the D-loop and Signature motifs of the adjacent monomer to form the active site. Specifically, we found that 11 different ATPase-deficient substitutions of important residues in the conserved motifs (Signature motif, D-loop, H-loop, Walker B, and coiled-coil domain) that help to form the ATPase active site abolish end processing and RDR, demonstrating that the ATPase active site is critically important.

For example, one of the Signature motif mutations that we examined, K475M, has been shown to reduce ATPase activity *in vitro* by destabilizing the Signature motif

(HERDENDORF and NELSON 2011). This residue is additionally involved in influencing the position of the coiled-coil domain, which in turn effects the interaction with Mre11 (WILLIAMS *et al.* 2011). The additional T4 Rad50 ATPase-deficient mutants each had negative effects on ATP binding, MR complex tethering, and/or NBD conserved motif interactions. Our findings that the mutations abolished end processing and RDR suggests that ATP hydrolysis is critical for the MR nuclease activity.

Furthermore, we tested two of the ATPase-deficient mutants (coiled-coil domain and Walker B) as well as WT T4 Rad50 for a dominant-negative effect. We were interested in discovering whether over-expression of mutant T4 Rad50 proteins or WT Rad50 protein could out-compete the binding of T4 Mre11 by WT T4 Rad50. We were able to observe a dominant over-expression effect for both WT and E505Q mutant Rad50 at higher levels of expression (greatly reduced resection/RDR). This result suggests that over-expression of E505Q mutant or WT Rad50 disrupts the formation of the MR complex heterotetramer. Another possibility is that the two Rad50 proteins bind to the unidentified nuclease partner(s) or some other protein involved in RDR (i.e. UvsX or UvsY).

In summary, we found that the nucleotide binding domain in T4 Rad50 is critically important for the plasmid model of RDR, with 11 substitutions providing no complementing activity. Our finding of a strict dependence of DSB end processing and repair on the T4 Rad50 ATPase active site demonstrates the key nature of the nuclease

activity of the T4 complex, but does not resolve the question of which enzyme catalyzes the extensive 5' end resection in the DSB repair reaction. Future studies can now focus on the precise role of the ATPase active site, in either activating nucleolytic processing by MR itself or by licensing some other nuclease for this key step in DSB repair (see Chapter 4 for further discussion). Additionally, future studies can focus on determining whether any of the other ATPase-deficient mutations can cause dominant-negative effects.

3. An Investigation of the Proposed Regulation of Bacteriophage T4 Endonuclease VII Expression and Its Role in Replication Fork Processing

3.1 Introduction

Bacteriophage T4 late replication is dependent on recombination. This recombination (RDR) is strikingly similar to homologous recombination used by higher organisms. As shown in Table 1-1, the T4 proteins involved in RDR are homologous and/or functionally similar to higher organism proteins. One of the key proteins involved in RDR is Endonuclease VII. We were interested in investigating the proposed regulation of expression of Endonuclease VII, which is encoded by gene *49* (gp49). We were also interested in investigating EndoVII's role in replication fork processing.

T4 EndoVII acts as a Holliday junction resolvase and was the first enzyme characterized to do so (MIZUUCHI *et al.* 1982). T4 EndoVII shares functional similarities to proteins across multiple organisms. For instance, T4 EndoVII is functionally analogous to *E. coli* RuvC, *Saccharomyces cerevisiae* Yen1, and human GEN1 (RASS *et al.* 2010; TAY and WU 2010). The basic structure of T4 EndoVII was elucidated (RAAIJMAKERS *et al.* 1999). EndoVII is active as a dimer and exhibits a novel HJ resolvase folding pattern that is represented by domain swapping. The N-terminal domain of one monomer interacts with the C-terminal domain of the other monomer. Unlike other HJ resolvases, such as RuvC, EndoVII can bind and act on a wide variety of structures in addition to HJs, such as Y-junctions (JENSCH and KEMPER 1986).

Although T4 EndoVII can act on a wide variety of structures, one of its accepted major roles is the resolution of the highly-branched DNA that is a result of T4 replication (KEMPER and BROWN 1976; KEMPER and JANZ 1976). This resolution of the highly-branched DNA allows packaging of the phage DNA into the phage head at late times of infection. As discussed in Chapter 1 Introduction, it has been proposed that T4 EndoVII is expressed at both early and late times of infection. We were interested in characterizing the proposed regulation of EndoVII expression and its biological consequences.

The regulation of EndoVII expression is of great interest as the protein is active at late times of infection but has been proposed to be translated at both early and late times of infection from two different transcripts (BARTH *et al.* 1988). This early and late translation was proposed to be regulated by the presence of a hairpin loop (see Figure 1-7) based on the gene *49* sequence as well as plasmid-protein expression. Barth *et al.* cloned gene *49* into different plasmid expression vectors and monitored the production of EndoVII protein using polyacrylamide gels and autoradiograms. Using this technique, the authors proposed that at early times of infection, an early, inactive 12 kDa EndoVII protein is expressed, while at late times of infection (hairpin loop does not exist), a late, active 18 kDa EndoVII protein is expressed. The authors proposed that a possible function of the short form of the protein could be the binding of HJs to prevent early, unwanted cleavage. Although this hairpin loop regulation has been seen with other late

T4 proteins, such as T4 lysozyme (McPheeters *et al.* 1986), the results from Barth *et al.* seemed ambiguous. For instance, the gel that the authors described as having the 12 and 18 kDa protein bands also contained multiple other bands of different sizes that were not discussed.

To study the regulation of EndoVII expression, Long and Kreuzer constructed a gene *49* hairpin mutation (49^{HP-}) (CC→AA) using the T4 I/S system ((Long and Kreuzer 2008; Selick *et al.* 1988) see Figure 1-7). This mutation should disrupt the hairpin loop and as a result, allow for abnormal early expression of active EndoVII. The hairpin loop mutation was used in this study as a valuable resource by which to monitor the regulation of EndoVII expression.

In addition to studying the proposed regulation of EndoVII expression, we were also interested in studying the involvement of EndoVII in replication fork processing. Specifically, EndoVII has been shown to cleave stalled replication forks *in vitro* (Hong and Kreuzer 2003). The authors used purified EndoVII and T4 DNA that contained drug-induced blocked replication forks. EndoVII was able to cleave the blocked replication forks. Additionally, the authors were able to show that blocked replication forks accumulate at a higher level *in vivo* in the absence of EndoVII (see Figure 1-7). This suggests that EndoVII can cleave stalled replication forks *in vivo* (simple fork cleavage model). The cleavage of stalled replication forks should produce double-stranded DNA ends that can be repaired using RDR.

Long and Kreuzer tested the involvement of EndoVII in replication fork processing using the gene *49* hairpin mutation. Using gradient plates, Long and Kreuzer were able to show that the gene *49* hairpin mutation was hypersensitive (compared to wild-type gene *49*) to two inhibitors that are known to block or stall replication forks: *m*-AMSA and hydroxyurea (HU) (see Figure 3-1) (LONG and KREUZER 2008). HU is a drug that inhibits ribonucleotide reductase, which catalyzes the production of deoxyribonucleotides from ribonucleotides (ELLEDGE *et al.* 1992; NOGUCHI *et al.* 2003; WARNER and HOBBS 1969). Consequently, HU reduces the available nucleotide pools for DNA replication and causes an increase in the accumulation of stalled replication forks. Since EndoVII is thought to cleave stalled replication forks, then in the presence of HU (more stalled forks), the gene *49* hairpin mutation (abnormal early expression) was hypothesized to produce an increased amount of broken replication forks that overwhelm the phage infection and lead to blocked phage production (HU sensitivity). Thus, the results were interpreted to support the theory that EndoVII is involved in cleaving HU-stalled replication forks to create a DSB that is funneled into RDR for repair (simple fork cleavage model). The hairpin loop mutation was used in this study to query the involvement of EndoVII in replication fork processing.

In this study, we used the gene *49* hairpin mutation to address the proposed regulation of EndoVII expression. We generated a FLAG-tagged wild-type and hairpin mutant gene *49* to monitor the production of EndoVII protein using Western Blots. In the presence of wild-type gene *49* we observed only the full-length EndoVII protein. In

the presence of the gene *49* hairpin mutation we observed no EndoVII protein. We conclude that EndoVII is not regulated to express different length proteins at different times of infection. We also conclude that the gene *49* hairpin mutation does not allow for abnormal early expression of active EndoVII.

We also used the gene *49* hairpin mutation to investigate EndoVII's role in replication fork processing. We generated phage strains to monitor EndoVII's effect on recombination using a plasmid x phage recombination assay. Taken with the above conclusions and other results discussed below, we propose that the gene *49* hairpin mutation disrupts the late promoter and reduces the amount of active EndoVII available (as opposed to abnormal early expression). In turn, this would affect the phage's ability to package its DNA due to unresolved recombination junctions and its ability to survive.

Finally, we investigated the finding that the original 49^{HP-} strain was HU hypersensitive. We crossed K10 49^{+} and K10 49^{HP-} phage stocks and collected thirty progeny. Our HU plating results were inconclusive but we did notice a growth defect with the no drug control. We were able to isolate 49^{+} large and small pickates as well as 49^{HP-} large and small pickates. We grew up phage stocks of the four different isolates and tested their growth at different temperatures. We observed that the small strains were temperature sensitive compared to the large strains and proposed the presence of a temperature sensitive mutation in the small strains.

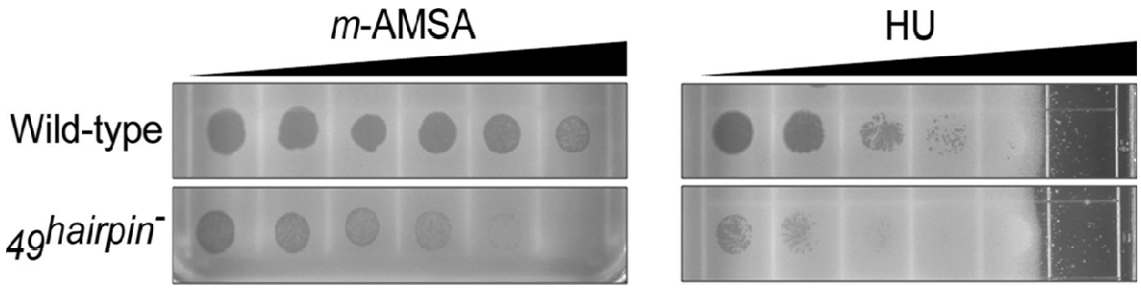

Figure 3-1: *49*$^{HP-}$ is hypersensitive to *m*-AMSA and HU.

49^{+} and *49*$^{HP-}$ phage of equal PFU were plated on *E. coli* MCS1 (*supD*) lawns on gradient plates of increasing concentrations of *m*-AMSA and HU. *49*$^{HP-}$ is hypersensitive to both *m*-AMSA and HU compared to *49*$^{+}$.

(LONG and KREUZER 2008).

We observed that the 49^{HP-} large strain is HU resistant not HU hypersensitive like the original 49^{HP-} strain. We also observed that the original 49^{HP-} strain has the same temperature sensitive phenotype like the 49^{WT} and 49^{HP-} small stocks. Taken together, these results suggested that the temperature sensitive mutation, not the hairpin mutation, causes HU hypersensitivity. Using Illumina MiSeq next generation whole genome sequencing through the Duke Institute for Genome Sciences and Policy, we were able to conclude that the temperature sensitivity was due to a mutation in T4 DNA polymerase (gp43). By comparing $49^{HP-}43^{+}$ *to* $49^{+}43^{TS}$ strains, we were also able to conclude that the gene *43* temperature sensitive mutation caused HU hypersensitivity.

3.2 Materials and Methods

Materials. Restriction enzymes, PCR primers, and T4 DNA ligase were purchased from New England Biolabs (Beverly, MA), Apex Taq RED Master Mix from Genesee Scientific (San Diego, CA), QuikChange™ Site Directed Mutagenesis Kit from Stratagene (La Jolla, CA), 4-20% Mini-PROTEAN TGX gels and Precision Plus Dual Color Standards from BIO-RAD (Hercules, CA), O'GeneRuler DNA Ladder Mix from Thermo Fisher Scientific (Waltham, MA), Rabbit anti-FLAG® antibody from Sigma-Aldrich (St. Louis, MO), Goat anti-Rabbit IR Dye 800CW from LI-COR Biosciences (Lincoln, NE), and Nytran Nylon Transfer Membrane from GE Healthcare (Waukesha, WI). Luria Broth (LB) was formulated as follows: Bacto-Tryptone (10 g/L), Yeast Extract (5 g/L), and NaCl (10 g/L). T4 plates were formulated as follows: Bacto-Tryptone (13 g/L), NaCl (8 g/L), Na Citrate-

$2H_20$ (2 g/L), Glucose (dextrose) (1.3 g/L), and Bactoagar (10 g/L). T4 top agar was formulated as follows: Bacto-Tryptone (13 g/L), NaCl (8 g/L), Na Citrate-$2H_20$ (2 g/L), Glucose (dextrose) (3 g/L), and Bactoagar (6.5 g/L). Terrific Broth (TB) was formulated as follows: Bacto-Tryptone (12 g), Yeast Extract (24 g), and Glycerol (4 mL) were added to 900 mL of water and autoclaved; this mixture was combined with a sterile 100 mL solution made up of 0.17M KH_2PO_4 and 0.72M K_2HPO_4.

Strains. Escherichia coli strains CR63 (*supD*), BE-BS (non-suppressing), MCS1 (*supD*), AB1, and MH1 (*araD*139 Δ*lacX*74 *galU*$^-$ *galK*$^-$ *hsr*$^-$ *hsm*$^+$ *rpsL* non-suppressing) were described previously (EDGAR *et al.* 1964; KREUZER *et al.* 1988; SELICK *et al.* 1988). The pBSfs209 plasmid (*supF*) was moved into strain MH1 for analysis of T4 recombination.

The bacteriophage T4 strains used for plasmid x phage recombination and other experiments are derivatives of strain K10, which carries the following mutations: *am*B262 (gene *38*), *am*S29 (gene *51*), *nd*28 (*denA*), and *rIIPT8* (*denB-rII*$^{\Delta}$) (SELICK *et al.* 1988).

The T4 K10 *49*$^{HP-}$ mutant was previously constructed using the T4 insertion/substitution system and contains a GG→TT mutation at T4 coordinates 46880-46881 (LONG and KREUZER 2008; SELICK *et al.* 1988). The T4 K10 *uvsY* mutant was also previously constructed using the T4 insertion/substitution system (KREUZER *et al.* 1988; SELICK *et al.* 1988). This *uvsY* mutation is a 120 base pair deletion of the *uvsY* promoter

region and prevents expression of the UvsY protein. Additional T4 strains were constructed by genetic crosses and confirmed using PCR/DNA sequencing.

Plasmids. Plasmid pBSfs209 (*supF*) was previously developed and contains a region of homology with the T4 genome that allows for homologous recombination and integration into the T4 chromosome (SELICK *et al.* 1988). If homologous recombination occurs, the *supF* suppressor on the plasmid acts to suppress the T4 phage amber mutations and thus allows normal phage growth. One can measure phage recombination by plating on a suppressing strain (CR63) which allows for growth of all phage and a non-suppressing strain (BE-BS) which only allows growth of phage that have undergone recombination. Plasmid pBSPLO +/- (*supF*) was also previously developed and contains a useful polylinker for cloning (SELICK *et al.* 1988).

Construction of FLAG-tagged gene 49. To construct the T4 strains with FLAG-tagged gene *49*, we amplified the T4 gene *49* C-terminal region (T4 coordinates 46008-46634) with added XbaI and NdeI linkers and subcloned into the pBSPLO +/- expression plasmids' polylinker. We generated a FLAG-tagged C-terminal domain gene *49* using the Stratagene QuikChange™ site-directed mutagenesis kit and transformed into *E. coli* MH1. The sequence of the forward mutagenic primer was as follows: 5'-gcagcttagaaagagtttaaaa**gactacaaagacgatgacgacaag**tgacaattgaaaaagaaattg-3', where the FLAG-tag is shown in bold (HOPP *et al.* 1988). The second mutagenic primer was the reverse complement of the forward. The MH1 strain carrying the FLAG-tagged gene *49*

fragment was infected with either K10 49^{WT} or K10 49^{HP-} phage and plated on BE-BS for integrants. These integrants were grown in CR63 to allow for segregation. Finally, plaques were PCR/sequenced for the FLAG-tag insertion into the T4 chromosome. Correct strains (FLAG-tagged wild-type gene *49* and gene *49* hairpin mutation) were grown as high titer lysate stocks.

Growth and titering of T4 phage stocks. T4 phage stocks that are used throughout this study are all high titer lysates. The growth and titering procedures are described in Chapter 2 Materials and Methods.

Analysis of plasmid x phage recombination in T4-infected cells. The indicated bacterial strains were pre-grown in LB containing appropriate antibiotic(s) with shaking at 37°C to an OD_{560} of 0.5, and the indicated phage strain was then added at a MOI of 3. The infected cultures were incubated at 37°C for 4 min without shaking to allow phage adsorption and then 1 hr with vigorous shaking. Each culture was chilled on ice for 15 min and about 500 µl of chloroform was added to each culture. The cultures were lysed overnight at 4°C. The next day, the culture (not chloroform) was spun at 8500 rpm for 20 min. The supernatant was stored in a glass phage vial at 4°C with a small amount of chloroform.

Next, serial dilutions of each culture were titered on both CR63 (*supD*) and BE-BS (non-suppressing). The T4 plates were incubated at 37°C overnight to produce phage plaques. The next day, the phage plaques were counted (plaque forming units) and

multiplied by the serial dilution/100 to calculate the phage titer/µl. To calculate the % recombination frequency, the BE-BS titer was divided by the CR63 titer and multiplied by 100. The same procedure was used for the dominance tests except varying MOIs of phage (co-infections) were added to each bacterial strain.

Analysis of T4 gene 49 expression levels after infection with K10 49^{WT}-FLAG or K10 49^{HP-}-FLAG. The same growth and infection steps described just above for analysis of plasmid x phage recombination were used to produce CR63 cells infected with the indicated T4 phage for 0, 10, 20, and 40 min. The infected cells were collected by centrifugation in a microfuge and the pellets were resuspended by vortexing in 500 µl of a wash buffer (100 mM NaCl, 50 mM Tris-HCl pH 8, 1 mM EDTA). The cells were recollected by centrifugation and the supernatant was removed. The pellets were resuspended by vortexing in 25 µl of H_20 and then 25 µl of 2X SDS Loading Buffer (2.7 M glycerol, 0.1 M Tris pH 6.8, 2% SDS, 0.29 M 2-mercaptoethanol, bromophenol blue at 10 mg/L) was added. Samples were boiled for 5 min and debris was removed by centrifugation in a microfuge for 10 min, with the cleared supernatant ready for gel electrophoresis.

The samples were analyzed by Western blotting using a rabbit anti-FLAG® primary antibody. Samples were run on 4-20% Mini-PROTEAN TGX gels and then transferred to a nitrocellulose membrane using an iBlot (Invitrogen). The membrane was blocked with 5% non-fat milk buffer for 1 hour at room temperature. Next, 0.1%

Tween 20 and a 6400-fold dilution of the primary antibody were added into the blocking buffer and incubated overnight at 4°C with shaking. The following day, the membrane was rinsed once with TBS-T (0.14M NaCl, 0.02 M Tris HCl (pH 7.6), 0.1% Tween 20) followed by three 10-min washes with TBS-T at room temperature. The membrane was next incubated with goat anti-rabbit IR Dye 800CW secondary antibody (1:20,000) in 5% non-fat milk buffer for 1 h at room temperature with shaking. The membrane was rinsed with TBS-T once followed by three 10-min washes with TBS-T at room temperature. Western blots were scanned using an Odyssey Infrared Imager (LI-COR Biosciences) and analyzed with the Odyssey Infrared Imaging System Application Software (LI-COR Biosciences, Version 3.0).

Growth of T4 phage pickates. The referred to phage pickates were grown from single phage plaques (after phage stocks were streaked on bacterial lawns or phage stocks were titered). Each phage pickate was grown in LB at 37°C for 2 hr without shaking. The pickates were chilled and stored with 50 µL chloroform.

Analysis of T4 phage sensitivity to HU and m-AMSA on gradient plates. T4 phage sensitivity to HU and *m*-AMSA was analyzed as described by Long and Kreuzer (2008). 25 mL of T4 agar with HU (0, 1.125, or 2.25 mg/mL) or *m*-AMSA (0 or 75 µg/mL) was poured into square petri dishes with one side elevated by a pencil under the dish (less HU side). Once the plate was solidified, the plate was leveled and another 25 mL of T4 top agar (no HU or *m*-AMSA) was added to the square petri dish. These square dishes were

allowed to solidify overnight at room temperature. Also, calculated phage dilutions (based on phage titer) to give specified plaque-forming units (PFU) were titered on T4 plates with MCS1 and incubated at 37°C overnight. The next day, the MCS1 plates were counted for plaques and the phage dilutions were adjusted accordingly so that 3 µL of dilution would give the specified phage PFU.

E. coli MCS1 was grown in pre-warmed LB to an OD_{560} of 0.5. Next, 500 µL of MCS1 was added to 5 mL of T4 top agar (no HU) and poured on top of the HU square gradient plates to form a lawn of bacteria. Once the bacterial lawns were solidified, aliquots of specified T4 PFUs were spotted across the gradient plates and incubated overnight at the indicated temperatures.

Preparation and analysis of T4 phage DNA for Illumina MiSeq whole genome sequencing. The indicated phage strains (high titer lysates) were spun at 14,000 rpm for 90 min. Each pellet was resuspended in 50 µL 1X TE (10 mM Tris-HCl pH 8 and 1 mM EDTA pH 8). Total DNA was purified using phenol extraction and dialysis as described previously (STOHR and KREUZER 2001). About 2 µg of DNA for each sample was sent to the Duke Institute for Genome Sciences and Policy for sequencing. The samples were analyzed by aligning their sequences to the WT T4 genome, T4T (HM137666.1) (PETROV *et al.* 2010), using Geneious R6 Computer Software (Biomaters Ltd., Version 6.1.6). The T4T genome sequence was developed using highly accurate next generation sequencing. It is important to note that the T4T sequence contains many changes in comparison to

the original WT T4 genome sequence (NC_000866) (MILLER *et al.* 2003). Many of the SNPs (single nucleotide polymorphisms) in the T4T sequence compared to the original WT T4 sequence were likely due to sequencing errors in the original T4 sequence, not actual SNPs.

The sequenced phage samples were compared to T4T for the presence of variants/SNPs using the same Geneious computer software (see Tables 3-1 and 3-2). The variants/SNPs that were found were selected for as having a minimum variant frequency of 95%. However, most found variants had frequencies of greater than 99%. The variants also had a coverage ranging from 900-1500. Interestingly, our K10 strain had 31 SNPs when compared to the T4T sequence that were maintained in the sequenced pickates (K10 background) (see Table 3-1). Additionally, our K10 strain contained a deletion from bases 165,764 to 423 that was also maintained in the sequenced pickates.

Table 3-1: K10 SNPs/variants compared to T4T.

Location	Amino Acid Change	CDS Position	Change	Codon Change	Coverage	Polymorphism Type	Protein Effect	Variant Frequency	gene
163,815	A -> T	79	C -> T	GCC -> ACC	912	SNP (transition)	Substitution	95.00%	*motA.1*
161,731	R -> K	89	C -> T	AGA -> AAA	1,240	SNP (transition)	Substitution	100.00%	*arn.1*
159,946	W -> Stop	284	G -> A	TGG -> TAG	1,105	SNP (transition)	Truncation	100.00%	*38*
151,972	P -> L	1,151	C -> T	CCA -> CTA	1,285	SNP (transition)	Substitution	100.00%	*34*
148,028	G -> D	527	C -> T	GGT -> GAT	1,332	SNP (transition)	Substitution	100.00%	*segG*
147,113	A -> T	754	C -> T	GCT -> ACT	1,192	SNP (transition)	Substitution	99.70%	*32*
138,157		981	C -> T	CAG -> CAA	1,307	SNP (transition)	None	100.00%	*nrdB*
137,658	W -> Stop	310	G -> A	TGG -> TAG	1,303	SNP (transition)	Truncation	99.80%	*denA*
136,641		840	G -> A	GAC -> GAT	1,394	SNP (transition)	None	99.90%	*rnlA*
134,883	G -> D	41	C -> T	GGT -> GAT	1,273	SNP (transition)	Substitution	99.80%	*pseT*
134,238	R -> H	686	C -> T	CGT -> CAT	1,377	SNP (transition)	Substitution	99.90%	*pseT*
130,922		129	C -> T	CTG -> CTA	1,265	SNP (transition)	None	99.90%	*rIII*
130,653			G -> A		1,040	SNP (transition)		99.90%	*intergenic*
126,847	P -> S	379	G -> A	CCA -> TCA	1,156	SNP (transition)	Substitution	99.90%	*30*
124,335		1,185	G -> A	ACC -> ACT	1,459	SNP (transition)	None	100.00%	*alt*
123,377		91	G -> A		1,435	SNP (transition)	None	99.90%	*alt.-1*
122,685	M -> I	921	G -> A	ATG -> ATA	1,081	SNP (transition)	Substitution	99.90%	*54*
116,692	E -> Stop	202	C -> T	CAG -> TAG	1,254	SNP (transition)	Truncation	99.90%	*51*
113,443		756	C -> T	TGC -> TGT	1,388	SNP (transition)	None	99.90%	*uvsW*
113,024	E -> K	337	G -> A	GAA -> AAA	1,195	SNP (transition)	Substitution	99.90%	*uvsW*
110,431	S -> R	898	T -> G	AGT -> CGT	960	SNP (transversion)	Substitution	100.00%	*hoc*
107,807		507	C -> A	GCC -> GCA	1,434	SNP (transversion)	None	99.90%	*24*
88,907	V -> I	844	G -> A	GTT -> ATT	1,524	SNP (transition)	Substitution	99.90%	*10*
81,995		936	G -> A	GGG -> GGA	1,306	SNP (transition)	None	100.00%	*6*
74,101	M -> I	288	C -> T	ATG -> ATA	1,158	SNP (transition)	Substitution	99.70%	*57B*
56,175		258	A -> G	CTT -> CTC	1,318	SNP (transition)	None	99.90%	*nrdC.11*
24,419	S -> P	1,023	T -> C	TCA -> CCA	1,468	SNP (transition)	Extension	99.80%	*b-gt*
15,683	D -> G	584	T -> C	GAC -> GGC	1,083	SNP (transition)	Substitution	100.00%	*segF*
7,421		216	G -> A	TAC -> TAT	1,250	SNP (transition)	None	100.00%	*motB.1*
848	E -> K	1,342	C -> T	GAA -> AAA	1,221	SNP (transition)	Substitution	100.00%	*rIIA*
722	T -> A	1,468	T -> C	ACT -> GCT	1,381	SNP (transition)	Substitution	99.90%	*rIIA*
165,764-423						Deletion			

3.3 Results

EndoVII's role in replication fork processing – Simple fork cleavage model

EndoVII was previously shown to cleave stalled replication forks *in vitro* (HONG and KREUZER 2003). We hypothesized a simple fork cleavage model where EndoVII could cleave stalled replication forks to generate DSBs that would be repaired with RDR but could overwhelm the system if present at a very high level. Thus, in the presence of the gene *49* hairpin mutation (abnormal early expression) we predicted that there would be hyper-recombination due to an increase in fork cleavage and DSBs. An increased amount of DSBs would lead to an increased amount of RDR (recombination) for repair.

The T4 I/S plasmid model system provides a useful window for studying the details of phage T4 homologous recombination (SELICK *et al.* 1988). This system utilizes phage derivatives carrying *denA* and *denB* mutations to prevent phage-induced plasmid DNA breakdown. The T4 phage strains also contain amber mutations in the essential genes *38* and *51* which are required for phage particle assembly. The I/S plasmid pBSfs209 carries the *supF* suppressor as well as a 209 base pair region of homology with the T4 genome. This plasmid is useful for measuring plasmid x phage recombination. After infection by T4, the plasmid can integrate into the phage chromosome by homologous recombination. If homologous recombination occurs, the *supF* suppressor on the plasmid acts to suppress the T4 phage amber mutations and thus allows normal phage growth. One can determine the recombination frequency by plating on a

suppressing strain (CR63) which allows for growth of all phage and a non-suppressing strain (BE-BS) which only allows growth of phage that have undergone recombination.

Using the above plasmid x phage recombination assay, we investigated the effect of T4 EndoVII on recombination. We indeed observed significant ($p < 0.05$) hyper-recombination (greater than 10X) with the gene *49* hairpin mutation when compared to WT gene *49* (see Figure 3-2). This result supported our simple fork cleavage model.

Based on our results above that supported the simple fork cleavage model, we predicted that the gene *49* hairpin mutation should be a dominant mutation. WT gene *49* is actively expressed at late times of infection, as opposed to the abnormal early expression of the gene *49* hairpin mutation. In the presence of the gene *49* hairpin mutation there should be hyper-recombination, even in the presence of varying levels of WT gene *49*, due to an increase in fork cleavage and DSBs that induce RDR.

We tested plasmid x phage recombination using co-infections of varying levels of WT gene *49* and the gene *49* hairpin mutation. If the gene *49* hairpin mutant was dominant, we expected to see hyper-recombination for all co-infections, even with lower levels of the gene *49* hairpin mutation and higher levels of WT gene *49*. However, we observed WT levels for all co-infections, even in infections with 80% gene *49* hairpin mutant. We conclude that the gene *49* hairpin mutation is a recessive mutation. This argued against abnormal early expression of EndoVII in the hairpin mutant and challenged the validity the simple fork cleavage model.

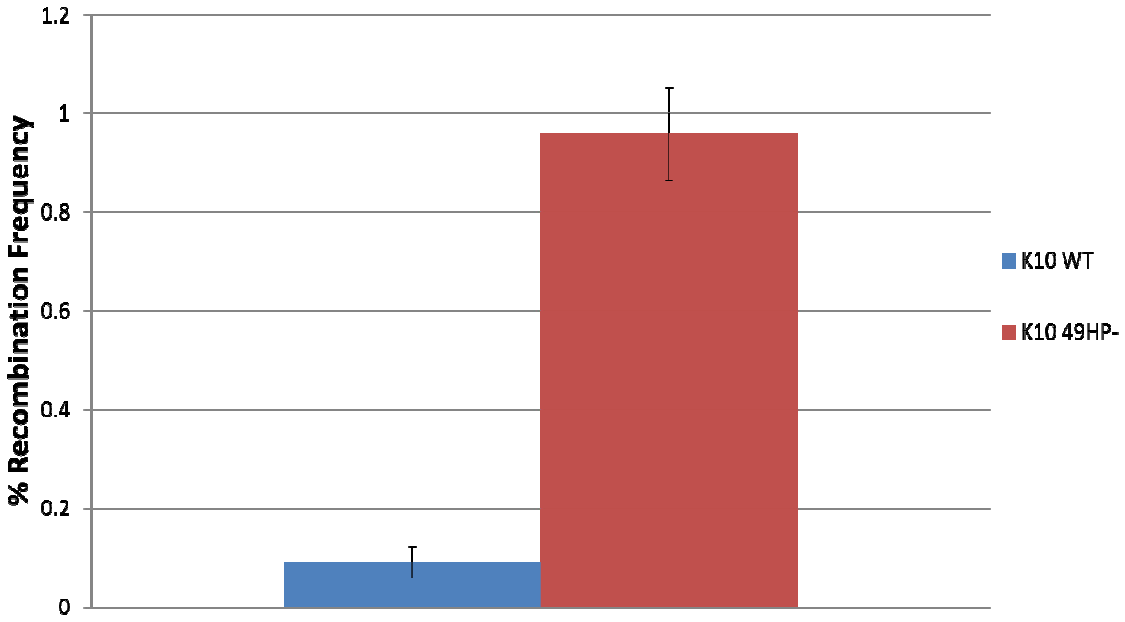

Figure 3-2: The gene *49* hairpin mutation caused plasmid x phage hyper-recombination.

E. coli MH1 cells that contained pBSfs209 were infected with either 49^{+} or 49^{HP-} phage. The resultant phage lysates were titered on CR63 (*supD*) and BE-BS (non-suppressing) to calculate the % recombination frequency. Error bars are standard deviations based on triplicate lysates.

We repeated and confirmed the HU gradient plate results shown in Figure 3-1 (LONG and KREUZER 2008) that the gene *49* hairpin mutation was hypersensitive to HU. These HU plate results appeared to support the theory that EndoVII is involved in cleaving stalled replication forks to create a DSB that is funneled into RDR for repair. To further investigate the HU gradient plates results (that supported the simple fork cleavage model), we constructed an EndoVII hairpin/UvsY double mutant ($49^{HP-}/uvsY^{\Delta}$). The $uvsY^{\Delta}$ is a 120 base pair deletion of the *uvsY* promoter region and prevents expression of the UvsY protein (KREUZER *et al.* 1988). As stated above, UvsY is an accessory protein that assists in the loading of UvsX onto ssDNA that is coated with gp32 (BLEUIT *et al.* 2001). If our simple fork cleavage model was correct, we expected that inactivation of the HR mediator protein UvsY would cause even more broken forks to accumulate that cannot be repaired. Thus, we expected that the double mutant should be even more hypersensitive to HU or possibly even display synthetic lethality. However, unlike our predictions, the $49^{HP-}/uvsY^{\Delta}$ double mutant strain was observed to be HU resistant (Figure 3-3), again suggesting that the simple fork cleavage model was incorrect. Taken with the above result that the EndoVII hairpin mutant is a recessive mutation, we concluded that the proposed abnormal early expression of EndoVII by the EndoVII hairpin mutation was incorrect, and moved on to a different model (opposed to the simple fork cleavage model).

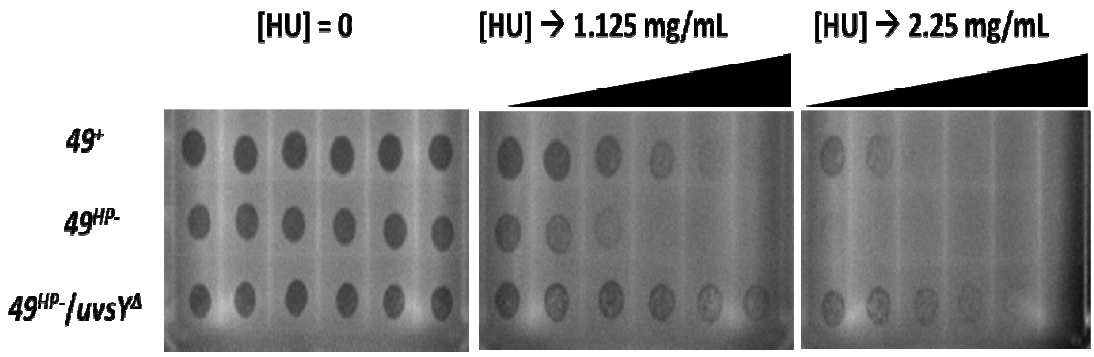

Figure 3-3: *49^{HP-}/uvsY$^{\Delta}$* is resistant to HU.

49^{+}, *49^{HP-}*, and *49^{HP-}/uvsY$^{\Delta}$* phage of equal PFU were plated on *E. coli* MCS1 (*supD*) lawns on gradient plates of increasing concentrations of HU = 0, 1.125, and 2.25 mg/mL. *49^{HP-}/uvsY$^{\Delta}$* is resistant to HU compared to *49^{+}* and *49^{HP-}*.

Proposed regulation of EndoVII expression – Reduced EndoVII model

Looking back at the original *49*$^{HP-}$ mutation (LONG and KREUZER 2008), one can see that the gene *49* hairpin mutation is adjacent to the late promoter consensus sequence ((BARTH *et al.* 1988) see Figure 3-4). As reviewed by Shamoo *et al.*, this consensus sequence is critical for late transcription (SHAMOO *et al.* 1995a). We came up with a new model to explain our results, after disproving the first model. Specifically, we propose that our gene *49* hairpin mutation reduces the late transcript level by disrupting the late promoter, resulting in insufficient EndoVII for packaging the highly-branched DNA into the phage head (reduced EndoVII model).

The reduced EndoVII model can be used to explain the previously described hyper-recombination result for the gene *49* hairpin mutation in the plasmid x phage assay (see Figure 3-5a and b). Specifically, we propose that WT levels of EndoVII allows for resolution of the plasmid x phage recombination event into rolling circle replication. Rolling circle replication would result in a product with multiple tandem copies of the plasmid. This product can undergo phage packaging but is not viable and thus, is not selected by the assay as an integrant (see Figure 3-5 a and b). Hence, in the presence of WT gene *49*, there should be more rolling circle products and fewer integrants (reduced recombination). We also propose that reduced levels of EndoVII disrupt resolution of the plasmid x phage recombination event into rolling circle replication. In the absence of EndoVII, DNA synthesis can proceed through the HJ to give a simple integrant (MOSIG

et al. 1984). Thus, in the presence of the gene *49* hairpin mutation, there should be fewer rolling circle products and more integrants (hyper-recombination) since there is a reduced amount of EndoVII available.

To directly test the reduced EndoVII model, we constructed C-terminal domain FLAG-tagged WT gene *49* (K10) and gene *49* hairpin mutant (K10 49^{HP-}) phage strains using the T4 I/S system (SELICK *et al.* 1988). We monitored the expression of EndoVII protein with Western blots using an anti-FLAG antibody. We introduced the FLAG-tag into the CTD of gene *49* because the HJ resolvases, Yen1 and GEN1 (functionally similar to EndoVII) were shown to be active with a CTD FLAG-tag (IP *et al.* 2008). Additionally, the gene *49* CTD coding sequence is downstream of the hairpin region, so it should not disrupt the previously proposed hairpin loop regulation of EndoVII expression.

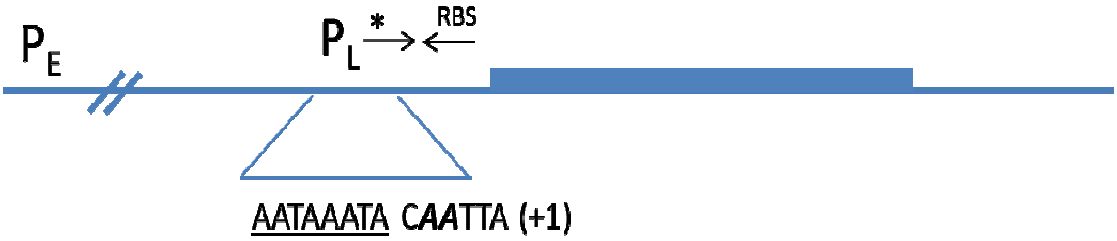

Figure 3-4: The gene *49* hairpin mutation is adjacent to the late promoter consensus sequence.

49^{HP-} (*, **AA**) is adjacent to the EndoVII late promoter consensus sequence (P_L, AATAAATA). Also represented are EndoVII's early promoter (P_E), ribosome binding site (RBS), and coding sequence (blue box).

Adapted from Barth *et al.* 1988.

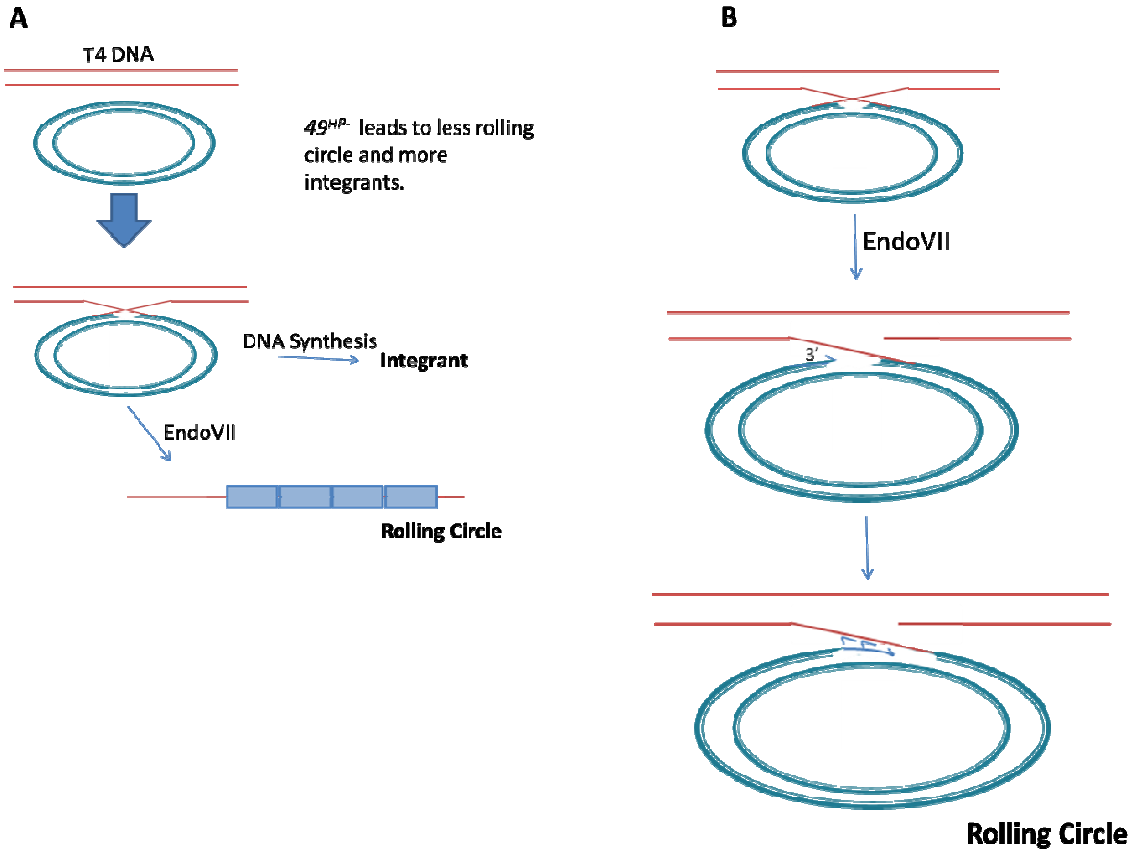

Figure 3-5: Proposed model of EndoVII's effect on the plasmid x phage recombination assay.

(A) The plasmid x phage recombination assay allows one to monitor for integration of plasmid pBSfs209 (blue circles) into the T4 chromosome. We predict that WT levels of EndoVII allows for resolution of the recombination event into rolling circle replication (not selected as an integrant). In the presence of the gene *49* hairpin mutation (reduced EndoVII model), there should be fewer rolling circle products and more integrants due to DNA synthesis through the HJ. (B) Proposed rolling circle replication model.

For *49*$^{+}$, we observed the expression of the full-length, active 18 kDa EndoVII protein but saw no evidence for the short, inactive 12 kDa EndoVII protein (see Figure 3-6). This argues against the theory that EndoVII is expressed from early and late transcripts at different times of infection (BARTH *et al.* 1988). For the gene *49* hairpin mutation, we were unable to observe any expression of full-length, active EndoVII or short, inactive EndoVII (see Figure 3-6). This argues against the abnormal early expression of EndoVII theory for the hairpin mutant and supports our reduced EndoVII model (gene *49* hairpin mutation disrupts the late promoter and reduces EndoVII expression). We further investigated the reduced EndoVII model below.

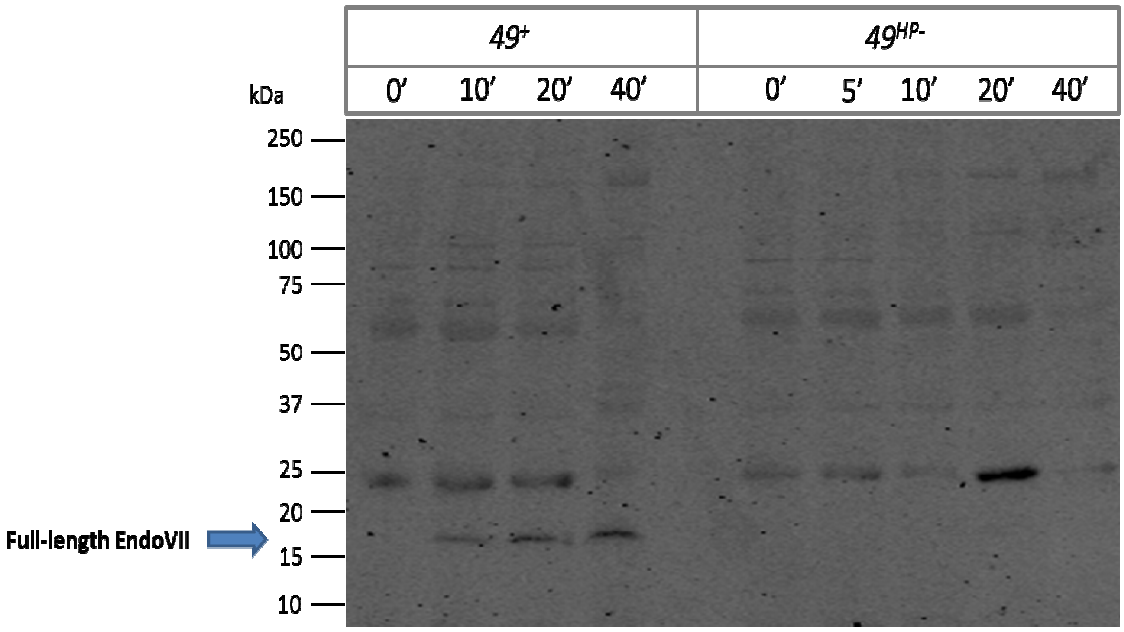

Figure 3-6: Western blot analysis of infections by T4 K10 *49*$^{+}$ and *49*$^{HP-}$ phage in *E. coli* CR63 (*supD*) cells for 0, 5, 10, 20, and 40 min.

Total protein from the infections was analyzed by Western blot with an anti-FLAG primary antibody. Full-length, active EndoVII (18 kDa) is the faster migrating band, while the slower migrating bands present in every lane are unidentified cross-reacting host proteins (also present in uninfected cells).

EndoVII's role in replication fork processing – The discovery of an uncharacterized temperature sensitive mutation

We constructed pairs of *49*$^{+}$ and *49*$^{HP-}$ strains for genetic testing. We wanted to test how these strains responded to HU. Our reduced EndoVII model predicts stimulated recombination due to the increase in stalled forks in the presence of HU, which leads to more branched structures that require EndoVII resolution for packing into the phage head. Hence, our reduced EndoVII model predicts that the gene *49* hairpin mutation would have particular difficulty dealing with the increased number of recombination branches induced by HU due to insufficient levels of EndoVII. However, we saw no difference in HU sensitivity for the *49*$^{HP-}$ strains compared to the *49*$^{+}$ strains. This result seems to be in direct conflict with our original findings that the gene *49* hairpin mutant phage was HU hypersensitive (see Figures 3-1 and 3-3) compared to the WT gene *49* phage. The only explanation that made sense is that the original *49* hairpin mutant phage carried some other mutation that causes the HU phenotype, and we had lost that other mutation during the genetic crosses to make these new strains.

To examine whether the *49* hairpin mutation, or some secondary mutation in the original *49* hairpin mutant strain caused HU hypersensitivity, we crossed K10 (*49*$^{+}$) to an amplified K10 *49*$^{HP-}$ strain (grown from the original K10 *49*$^{HP-}$ stock strain) and screened thirty pickates (progeny). The K10 and the amplified K10 *49*$^{HP-}$ strains are referred to as the parental strains below. Based on our reduced EndoVII model (discussed above), we expected that all *49*$^{+}$ pickates should be HU resistant, whereas all

49^{HP-} pickates should be HU hypersensitive. We were unable to reliably interpret the pickates' HU sensitivity due to size differences and plaque number between the pickates. However, we were able to clearly observe both small (S) and large (L) plaque pickates. We hypothesized that the growth defect was due to the gene *49* hairpin mutation since the K10 (*49*$^{+}$) and K10 *49*$^{HP-}$ strains used for the cross were L and S, respectively. In contrast to our hypothesis, we were able to isolate eight *49*$^{+}$ L, four *49*$^{+}$ S, nine *49*$^{HP-}$ S, and nine *49*$^{HP-}$ L pickates (see Table 3-2), suggesting that an unidentified mutation caused the growth defect instead of the hairpin mutation. We proposed that the reduced growth at 37° might reflect a temperature sensitive mutation at intermediate temperature, so we tested whether the mutation might be a temperature sensitive mutation.

We grew phage stocks of each type of pickate, *49*$^{+}$ L and S, and *49*$^{HP-}$ L and S and tested the strains for temperature sensitivity at 30, 37, and 40°C without HU. Indeed, the S stocks were temperature sensitive at 40°C compared to the L stocks. Separately, we confirmed that all thirteen S pickates were temperature sensitive at 40°C whereas all seventeen L pickates were temperature resistant (see Table 3-2). We also observed that the original K10 *49*$^{HP-}$ strain was temperature sensitive at 40°C compared to K10 *49*$^{+}$, leading us to believe that the original *49*$^{HP-}$ strain had an uncharacterized temperature sensitive (TS) mutation.

We wanted to determine whether the hairpin mutation or the temperature sensitive mutation caused the HU hypersensitivity. Therefore, we tested amplified phage stocks of the 49^{+} L (non-TS) and S (TS) and the 49^{HP-} L (non-TS) and S (TS) strains for HU sensitivity using the same HU gradient plate method described above. We observed that with increasing amounts of HU, the 49^{+} and 49^{HP-} non-TS strains were HU resistant whereas the 49^{+} and 49^{HP-} TS strains were HU hypersensitive (see Figure 3-7). Since the TS mutation is present in both 49^{+} and 49^{HP-} TS strains, this suggested that the temperature sensitive mutation caused the HU hypersensitivity, not the hairpin mutation. As a result, we were interested in characterizing the previously unknown TS mutation that was discovered in the original 49^{HP-} strain.

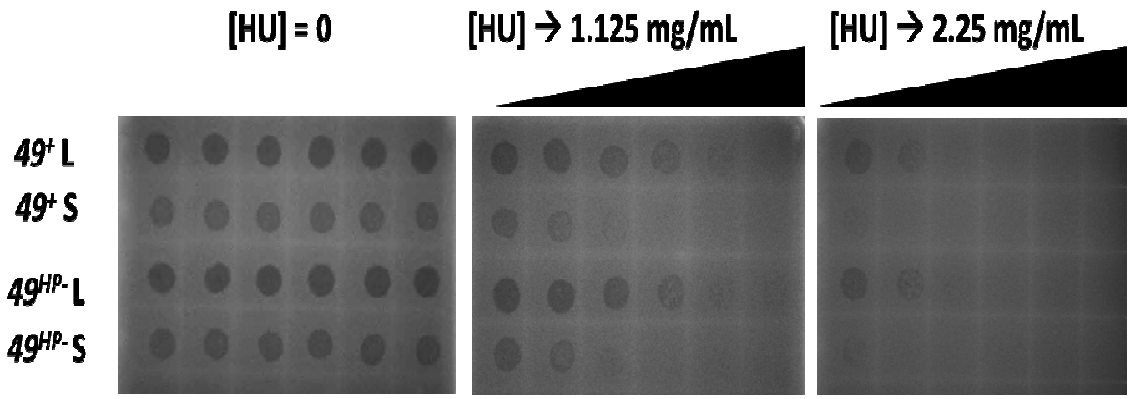

Figure 3-7: The *49*$^{+}$ and *49*$^{HP-}$ L strains (non-TS) are resistant to HU whereas the *49*$^{+}$ and *49*$^{HP-}$ S strains (TS) are HU hypersensitive.

49^{+} L and S and *49*$^{HP-}$ L and S phage of equal PFU were plated on *E. coli* MCS1 (*supD*) lawns on gradient plates of increasing concentrations of HU = 0, 1.125, and 2.25 mg/mL. Both L strains were HU resistant whereas both S strains were HU hypersensitive.

To determine the temperature sensitive mutation, we sent purified phage DNA from K10 (49^{+}), 49^{HP-} L (non-TS, **pickate #5**), and 49^{HP-} S (TS, **pickate #2**) lysates to the Duke Institute for Genome Sciences and Policy for Illumina MiSeq next generation whole genome sequencing (see Tables 3-1 and 3-2). We hoped to observe a single mutation difference between the 49^{HP-} L (non-TS) and S (TS) strains. However, surprisingly, we found three mutations in the 49^{HP-} S strain that were not present in the L strain: *dda* (DNA helicase, C→T mutation at position 10,694), gene *43* (DNA polymerase, G→A mutation at position 29,389), and gene *6* (Baseplate wedge subunit, A→G mutation at position 82,819). These three mutations all changed the reading frame and were candidates for the temperature sensitive mutation. We also found two mutations in the 49^{HP-} L strain that were not present in the S strain: *mobA* (Homing endonuclease, T→C mutation at position 3346) and *rpbA* (RNA polymerase binding protein, T→C mutation at position 32,792). All mutations (except *mobA*) mutated the encoded amino acid in addition to the base pair change.

Table 4-2: Temperature sensitivity (TS) and PCR/DNA sequencing results from the parental strains, K10 and Amplified K10 *49*$^{HP-}$, and the 30 pickates (progeny).

Strain/ # Pickate	*49*	Size	TS @ 40°C	*dda*	gene *43*	gene *6*	*mobA*	*rpbA*
K10	WT	L	-	WT	WT	WT	WT	WT
Amplified *49*$^{HP-}$	HP-	S	+	-	-	WT	WT	WT
1	WT	L	-	WT	WT	WT	WT	WT
3	WT	L	-	WT	WT	WT	WT	WT
5 (HP- L)	HP-	L	-	WT	WT	WT	-	-
7	HP-	L	-	WT	WT	WT	WT	WT
9	HP-	L	-	-	WT	WT	WT	WT
11	WT	L	-	-	WT	WT	WT	WT
13	HP-	L	-	WT	WT	WT	WT	WT
14	HP-	L	-	-	WT	WT	WT	WT
15	WT	L	-	-	WT	WT	WT	WT
17	HP-	L	-	WT	WT	WT	WT	WT
19	WT	L	-	WT	WT	WT	WT	WT
21	WT	L	-	-	WT	WT	WT	WT
23	HP-	L	-	-	WT	WT	WT	WT
24	WT	L	-	-	WT	WT	WT	WT
25	WT	L	-	-	WT	WT	WT	WT
27	HP-	L	-	WT	WT	WT	WT	WT
29	HP-	L	-	WT	WT	WT	WT	WT
2 (HP- S)	HP-	S	+	-	-	-	WT	WT
4	HP-	S	+	-	-	WT	WT	WT
6	HP-	S	+	-	-	WT	WT	WT
8	HP-	S	+	-	-	WT	WT	WT
10	WT	S	+	WT	-	WT	WT	WT
12	HP-	S	+	WT	-	WT	WT	WT
16	HP-	S	+	-	-	WT	WT	WT
18	WT	S	+	-	-	WT	WT	WT
20	WT	S	+	WT	-	WT	WT	WT
22	HP-	S	+	WT	-	WT	WT	WT
26	WT	S	+	WT	-	WT	WT	WT
28	HP-	S	+	WT	-	WT	WT	WT
30	HP-	S	+	WT	-	WT	WT	WT

Since we had three candidates for the temperature sensitive mutation, we screened all thirty pickates for *dda*, gene *43*, and gene *6* mutations using PCR/DNA sequencing (Table 3-2). We hypothesized that all S pickates would have the temperature sensitive mutation. We observed that all of the S pickates had the gene *43* mutation whereas there was a mixture of S pickates that either did/did not have the *dda* and/or the gene *6* mutation. Importantly, all seventeen L pickates had the wild-type gene *43* sequence. We also PCR/DNA sequenced the K10 and amplified K10 49^{HP-} parental strains and found that they differed in only the 49^{HP-}, *dda*, and gene *43* mutation. Therefore, we conclude that the temperature sensitive mutation is the gene *43* (DNA polymerase) mutation.

We also hypothesize that either the 49^{HP-} or gene *43* mutation (likely the gene *43* mutation) cause a high mutator phenotype due to the fact that both K10 49^{HP-} strains L and S that were whole genome sequenced contained unrelated spontaneous mutations that were not from either parent strain (gene *6*, *mobA,* and *rpbA* mutations). The proposal of a high mutator phenotype is further strengthened since the mutation frequency for WT T4 is estimated to be .15 per genome after 38 replication cycles compared to the mutation frequency of 2 and 1 observed for the whole genome sequenced 49^{HP-} L and S strains, respectively (both sequenced lysates were grown from single phage particles through 38 replication cycles)(DRAKE *et al.* 1998). The estimated WT T4 mutation frequency for 38 replication cycles is based on the estimated mutation rate of 0.0040 mutations per genome per replication observed by Drake *et al.* The

authors monitored the mutation frequency of a single T4 gene and then extrapolated the data to the whole genome to estimate a mutation rate. Additionally, multiple T4 gene *43* mutations have been shown to cause a mutator phenotype (reviewed by (REHA-KRANTZ 1994)). We are in the process of characterizing whether the gene *49* hairpin or the gene *43* mutation causes the mutator phenotype (see Discussion section).

Looking back at the HU gradient results above that show both 49^{+} S and 49^{HP-} S strains (TS) are HU hypersensitive (see Figure 3-7), we also conclude that the gene *43* mutation and not the 49^{HP-} causes HU hypersensitivity. T4 gene *43* mutations have not previously been shown to cause HU hypersensitivity. We also observed that the gene *43* mutation and not the 49^{HP-} caused *m*-AMSA sensitivity (see Figure 3-8). T4 gene *43* mutations have not previously been shown to cause *m*-AMSA sensitivity. We are in the process of characterizing further the gene *43* mutation's implication on replication fork processing (see Discussion section).

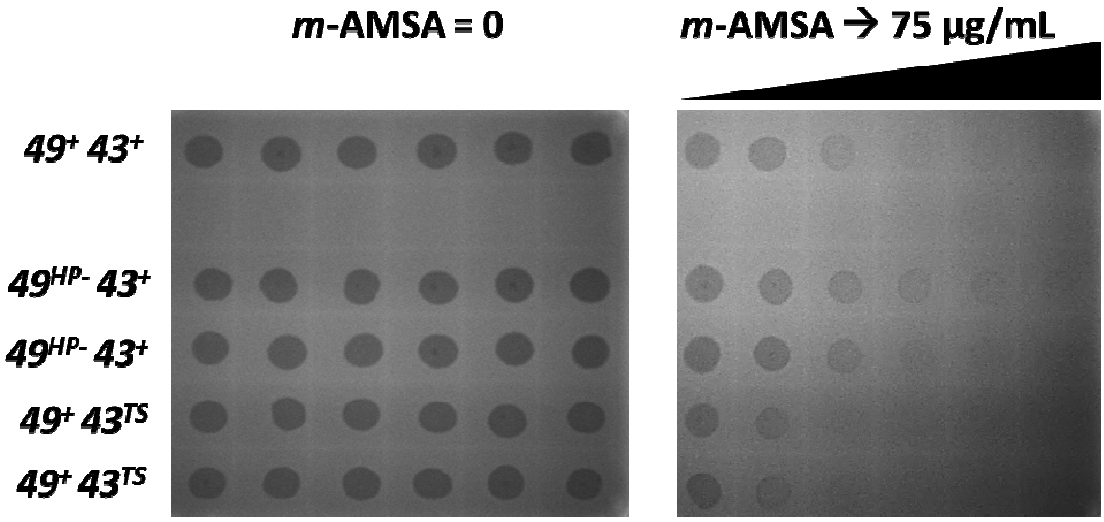

Figure 3-8: 43^{TS} caused *m*-AMSA sensitivity.

$49^{+}43^{+}$, $49^{HP-}43^{+}$, and $49^{+}43^{TS}$ phage of equal PFU were plated on *E. coli* MCS1 (*supD*) lawns on gradient plates of increasing concentrations of *m*-AMSA = 0 and 75 µg/mL. The duplicated strains shown were grown from different pickates. The $49^{+}43^{+}$ and $49^{HP-}43^{+}$ strains were *m*-AMSA resistant whereas the $49^{+}43^{TS}$ strains were *m*-AMSA sensitive.

3.4 Discussion

T4 EndoVII is an essential HJ resolvase that is conserved widely in evolution. We have investigated and characterized the proposed regulation of T4 EndoVII expression as well as its role in replication fork processing by using the gene *49* hairpin mutation. Since EndoVII was shown to cleave stalled replication forks *in* vitro, we proposed a simple fork cleavage model where EndoVII could cleave stalled replication forks to generate DSBs that would be repaired with RDR. Thus, in the presence of the gene *49* hairpin mutation (proposed abnormal early expression) we predicted hyper-recombination. Using a plasmid x phage recombination assay we observed hyper-recombination for the hairpin mutant compared to WT gene *49* that seemed to support our simple fork cleavage model.

We characterized the proposed regulation of T4 EndoVII expression by generating a FLAG-tagged WT gene *49* and gene *49* hairpin mutant to monitor the production of EndoVII protein using Western Blots. In the presence of WT gene *49* we observed only the full-length EndoVII protein. In the presence of the gene *49* hairpin mutation we observed no EndoVII protein. We conclude that EndoVII is not regulated to express different length proteins at different times of infection. We also conclude that the gene *49* hairpin mutation does not allow for early expression of active EndoVII. Instead, we propose that the hairpin mutation disrupts the late promoter and reduces the amount of active EndoVII available (reduced EndoVII model as opposed to abnormal

early expression). In turn, this would affect the phage's ability to package its DNA due to unresolved recombination junctions and its ability to survive (opposed to the simple fork cleavage model).

Interestingly, using whole genome sequencing, we determined that the original K10 49^{HP-} strain had an additional mutation in T4 DNA polymerase (gene *43*) that caused temperature sensitivity. Looking back at our plasmid x phage assay, we would like to determine whether the 49^{HP-} or gene *43* mutation causes hyper-recombination. If the gene *43* mutation causes hyper-recombination, this result would implicate gene *43* in replication fork processing. A DNA polymerase mutation could lead to an increased amount of stalled replication forks that become cleaved to create a DSB that is funneled into RDR for repair (elevated recombination).

We also discovered that the gene *43* mutation, not the gene *49* hairpin mutation, caused HU hypersensitivity and *m*-AMSA sensitivity. We are interested in testing HU sensitivity of 43^{TS} vs. $43^{TS}/uvsY^{\Delta}$. Since we observed that the K10 $49^{HP-}/uvsY^{\Delta}$ was HU resistant, it is plausible that $43^{TS}/uvsY^{\Delta}$ would be HU resistant. The K10 $49^{HP-}/uvsY^{\Delta}$ strain was created from an equal cross between K10 49^{HP-} (which we now know contains the 43^{TS} mutation) and K10 $uvsY^{\Delta}$. Thus, the K10 $49^{HP-}/uvsY^{\Delta}$ strain may have had the 43^{TS} mutation present. It would be extremely interesting if the added UvsY knockout repressed the 43^{TS} HU sensitivity since similar results have been shown with a UvsW knockout (CUNNINGHAM and BERGER 1977). The authors observed that $uvsW^{-}$ was HU hypersensitive whereas a $uvsW^{-}/uvsY^{-}$ double mutant was HU resistant. A result

with *43*^{TS}/*uvsY*$^{\Delta}$ being HU resistant would suggest that gene *43* and UvsW influence the same pathway to process stalled replication forks in different ways and would lead to additional future studies. In the context of just the HU sensitivity results (reduced nucleotide pools), the gene *43* mutation likely causes sensitivity due to polymerase difficulty in extending. However, in the context of both *m*-AMSA and HU sensitivity results, the gene *43* mutation likely causes sensitivity due to an altered response to fork blockage/stalling (see Chapter 4 for further discussion).

Finally, from our whole genome sequencing, we observed spontaneous mutations indicating the presence of a high mutator. We are in the process of characterizing whether the gene *49* hairpin or the gene *43* mutant causes the mutator phenotype. Similar T4 gene *43* mutations have been characterized with a mutator phenotype (reviewed by (REHA-KRANTZ 1994)). Like many of the previously characterized gene *43* mutator mutations, our gene *43* mutation is located in the N-terminal region of gene *43* which encodes for the DNA polymerase's 3'-5' editing exonuclease activity (proofreading). Thus, it is possible that our gene *43* mutation causes the mutator phenotype. However, this would not explain how the gene *49* hairpin mutant strain acquired the gene *43* mutation. Hence, if the hairpin mutation causes the high mutator phenotype, the presence of the gene *43* mutation would be easier to explain.

To determine whether the gene *43* or gene *49* hairpin mutation causes a mutator phenotype, we will grow and sequence multiple strains through multiple growth cycles that only contain either mutation to start with. Specifically, we will

employ whole genome sequencing to sequence both the starting strains (either *43*^{TS} or *49*$^{HP-}$) and the resultant strains after six days of subsequent growth (over one hundred doublings). For either the gene *43* or gene *49* hairpin mutation, we expect to observe additional spontaneous mutations that occur within the strains after multiple growth cycles. This will allow us to determine which mutation causes a mutator phenotype. If the high mutator phenotype is caused by the gene *43* mutation, this would confirm that the mutation indeed disrupts DNA polymerase's proofreading ability. If the high mutator phenotype is caused by the gene *49* hairpin mutation, this would indicate EndoVII's possible involvement in DNA repair and would lead to additional future studies.

4. Concluding Remarks

One of the most harmful forms of DNA damage experienced by the cell is the double-strand DNA break (DSB). If DSBs are not properly repaired, they can lead to genome instability and cell death. We were interested in studying proteins involved in homologous recombination. Homologous recombination is one of the pathways employed to repair DSBs and is described as an error-free pathway. To study homologous recombination, we used the bacteriophage T4 model system, which uses recombination-dependent replication (RDR) to replicate its DNA at late times of infection. This RDR system is very similar to homologous recombination used by higher organisms. Additionally, the T4 RDR proteins are homologous and/or functionally similar to higher organism proteins involved in homologous recombination.

The first step of homologous recombination is the production of a 3' ssDNA overhang and is referred to as DSB resection (5' strand is resected). It has been suggested that the 5' resection activity to create 3' ssDNA is contained in the eukaryotic MR complex (SHIN *et al.* 2004). This 5' resection activity remained controversial as *in vitro* studies of the eukaryotic MR complex showed an opposing 3' to 5' exonuclease activity (KROGH *et al.* 2005; LEWIS *et al.* 2004; LLORENTE and SYMINGTON 2004; TRUJILLO *et al.* 1998). However, more recent studies in *S. cerevisiae* have clarified the role of the MR complex. Specifically, the MR complex, along with Xrs2 and Sae2 clips 50-100 nucleotides from the 5' end of a DSB (MIMITOU and SYMINGTON 2008). Next, ExoI and RPA

or Sgs1/Top3/RmiI, Dna2, and RPA bind to the processed DSB and proceed with a more extensive resection of the DSB (NIU *et al.* 2010; ZHU *et al.* 2008).

We investigated the T4 MR complex (gp46/47) which is homologous to the eukaryotic MR complex. We observed that both the nuclease activity of gp47 and the ATPase activity of gp46 are critically important for DSB resection and repair. However, our results did not resolve the question of which enzyme catalyzes the extensive 5' end resection in the DSB repair reaction (i.e. whether gp46/47 licenses another exonuclease(s) as seen in the eukaryotic system).

Future studies can now focus on determining if a T4 partner exonuclease(s) helps with the 5' end resection of a DSB. A possible candidate for the extensive 5' end resection is T4 RNaseH. The basic structure of T4 RNaseH was elucidated (MUESER *et al.* 1996). T4 RNaseH is composed of 155 amino acids and contains a central groove that closely resembles many DNA-metabolizing enzymes and DNA-binding proteins. T4 RNaseH contains sequence similarity to the N-terminal 5' to 3' exonuclease domain of DNA polymerase I which hydrolyzes both DNA-DNA and RNA-DNA duplexes (HOLLINGSWORTH and NOSSAL 1991; MUESER *et al.* 1996). T4 RNaseH is a nuclease with both 5'-3' exonuclease activity on RNA-DNA and DNA-DNA duplexes as well as endonuclease activity on the junction of single- and double-stranded DNA of fork structures (BHAGWAT *et al.* 1997; HOLLINGSWORTH and NOSSAL 1991). Interestingly, the presence of T4 gp32 (single-stranded DNA-binding protein) converted T4 RNaseH from a

non-processive to a processive exonuclease (BHAGWAT *et al.* 1997). The presence of T4 gp32 also blocked all T4 RNaseH endonuclease activity. These gp32 results suggest an important role for the gp32 protein in regulating how much adjacent DNA is removed along with the RNA primers during lagging strand DNA synthesis (BHAGWAT *et al.* 1997).

In support of our theory that T4 RNaseH is a possible partner exonuclease that performs the extensive 5' end resection, Shcherbakov *et al.* observed that mutations in gp46 and gp47 were effectively suppressed by the T4 RNaseH das (DNA arrest suppressor) mutation (SHCHERBAKOV *et al.* 2006). These T4 RNaseH das suppressor mutations are phenotypically neutral and their suppressing effect is likely due to the enhanced expression of T4 RNaseH which compensates for the 5' exonuclease deficiency of the gp46 and gp47 mutants (MICKELSON and WIBERG 1981). Our collaborator, Dr. Scott Nelson, also has *in vitro* data to suggest that T4 RNaseH can perform the required 5' to 3' resection of DNA ends in the absence of gp46/47 (personal communication). We would like to use our same DSB plasmid repair assay (see Chapter 2) to examine whether the over-expression of T4 RNaseH can compensate for the loss of gp46/47 *in vivo*. Using the same assay, we would also like to test whether the loss of T4 RNaseH effects gp46/47 end resection of DNA ends and RDR.

It is also known that in eukaryotes, DSBs can be created by Spo11, a topoisomerase-like enzyme that forms covalent complexes to DNA. The MR complex is required to make an endonuclease cut to release DNA from the Spo11-DNA covalent

complexes at a DSB in order to proceed with end resection and DSB repair (reviewed in (PAULL 2010)). We would like to investigate whether the nuclease activity of the T4 MR complex plays a role in cleaving next to tightly bound proteins, such as gp2. Gp2 is an end-protecting protein that is bound to the ends of the infecting T4 chromosome (LIPINSKA *et al.* 1989; OLIVER and GOLDBERG 1977; SILVERSTEIN and GOLDBERG 1976a; SILVERSTEIN and GOLDBERG 1976b). Similar to eukaryotes, the T4 MR complex may be required to generate free DNA ends in the infecting phage DNA by cleavage near bound gp2. Genetic evidence with a mutant that makes lower levels of the T4 MR complex is consistent with this model (ALMOND *et al.* 2013).

We also investigated another key protein in T4 RDR, Endonuclease VII. EndoVII is a HJ resolvase and is functionally similar to Yen1/GEN1 in yeast/humans. Specifically, we were interested in investigating the proposed regulation of EndoVII expression as well as its role in replication fork processing (BARTH *et al.* 1988; HONG and KREUZER 2003; LONG and KREUZER 2008). We used a previously constructed gene *49* hairpin mutation to study these characteristics of the protein as the mutation was proposed to allow for abnormal early expression of EndoVII (LONG and KREUZER 2008).

In addition to the proposed regulation, EndoVII was previously shown to cleave stalled replication forks *in vitro* (HONG and KREUZER 2003). We proposed a simple fork cleavage model whereby EndoVII cleaves stalled replication forks to funnel DSBs into RDR for repair. However, using Western blot hybridization, we found no evidence for

the proposed regulation of EndoVII expression or abnormal early expression of the EndoVII hairpin mutant, which argued against the simple fork cleavage model. As a replacement for the simple fork cleavage model, we proposed a reduced EndoVII model whereby the gene *49* hairpin mutation disrupts the EndoVII late promoter, which in turn, reduces EndoVII expression.

Using whole genome sequencing, we discovered an additional, uncharacterized mutation in the original gene *49* hairpin mutant strain that caused temperature sensitivity. We found that the added mutation was in gene *43* (DNA polymerase). We would like to determine whether the gene *49* hairpin or gene *43* mutation causes the hyper-recombination observed for the plasmid x phage recombination assay. If gene *43* causes hyper-recombination, this result would implicate gene *43* in replication fork processing. For example, a gene *43* mutation could lead to an increased amount of stalled forks that become cleaved into DSBs that are repaired using RDR (increased recombination).

Interestingly, we also discovered that the gene *43* mutation and not the gene *49* hairpin mutation caused HU hypersensitivity. In T4*, uvsW*⁻ was observed to be HU hypersensitive whereas u*vsW*⁻/*uvsY*⁻ conferred HU resistance (CUNNINGHAM and BERGER 1977). This result leads us to believe that knocking out UvsW leads to a toxic recombination intermediate that is not formed without the HR mediator protein, UvsY, which assists in the loading of the strand invasion protein, UvsX. Similar findings have

been shown in *S. cerevisiae*. Mutated *Sgs1* (functionally similar to UvsW) was HU hypersensitive whereas a *Sgs1/Rad51* or *Rad52* double mutant conferred HU resistance (BERNSTEIN *et al.* 2009; FABRE *et al.* 2002). We are interested in determining whether a 43^{TS}/*uvsY*$^{-}$ or *uvsX*$^{-}$ double mutant is HU resistant. Since the 49^{HP-}/$uvsY^{\Delta}$ double mutant was observed to be HU resistant (Figure 3-3), it is plausible that a 43^{TS}/$uvsY^{\Delta}$ double mutant would be HU resistant (see Chapter 3 Discussion). This novel result would implicate gp43 and UvsW in similar pathways to process stalled replication forks in different ways.

Additionally, looking back at David Long's gradient plates (Figure 3-1), he observed that the gene *49* hairpin mutation caused *m*-AMSA sensitivity. As discussed in Chapter 1, *m*-AMSA is an anti-cancer drug that creates a cleavage complex to stall replication forks. Hong and Kreuzer showed that EndoVII can cleave *m*-AMSA induced stalled replication forks *in vitro* and proposed that this increases the toxicity of the drug (HONG and KREUZER 2003). Since we know that the original gene *49* hairpin mutant strain contains a gene *43* mutation that causes HU hypersensitivity, we correctly hypothesized and observed that the gene *43* mutation and not the gene *49* hairpin mutation causes *m*-AMSA sensitivity. This is a novel finding and again implicates gp43 in the processing of stalled replication forks.

As discussed in Chapter 1 Introduction, if the cause of replication fork blockage cannot be quickly resolved, it may be necessary to back up the replication fork (fork

regression) and re-load the replisome in order to bypass the blockage. Based on the results and predictions with *m*-AMSA and HU, we propose a new model for both gp43 and UvsW replication fork processing (Figures 4-1 through 4-4). We hypothesize that the gene *43* mutation causes the replisome to disassociate more easily which would lead to increased recombination and the formation of a toxic recombination intermediate (Figure 4-1). Hence, the gene *43* mutation would cause HU and *m*-AMSA sensitivity whereas a double mutant with *uvsX*⁻ or *uvsY*⁻ (strand invasion proteins) would block toxic recombination and lead to HU and *m*-AMSA resistance (Figure 4-2). Additionally, UvsW has been shown to catalyze replication fork regression for replication fork restart in vivo (LONG and KREUZER 2009). It has been predicted that UvsW acts on the replication fork after the replisome disassembles, promoting regression which allows for recovery of the fork. We hypothesize that the *uvsW*⁻ mutation (blocked fork regression) leads to increased recombination and the formation of a toxic recombination intermediate due to competition between UvsW promoting fork regression versus the toxic recombination pathway (Figure 4-3). Hence, the *uvsW*⁻ mutation would cause HU and *m*-AMSA sensitivity whereas a double mutant with *uvsX*⁻ or *uvsY*⁻ would block toxic recombination and lead to HU and *m*-AMSA resistance (Figure 4-4).

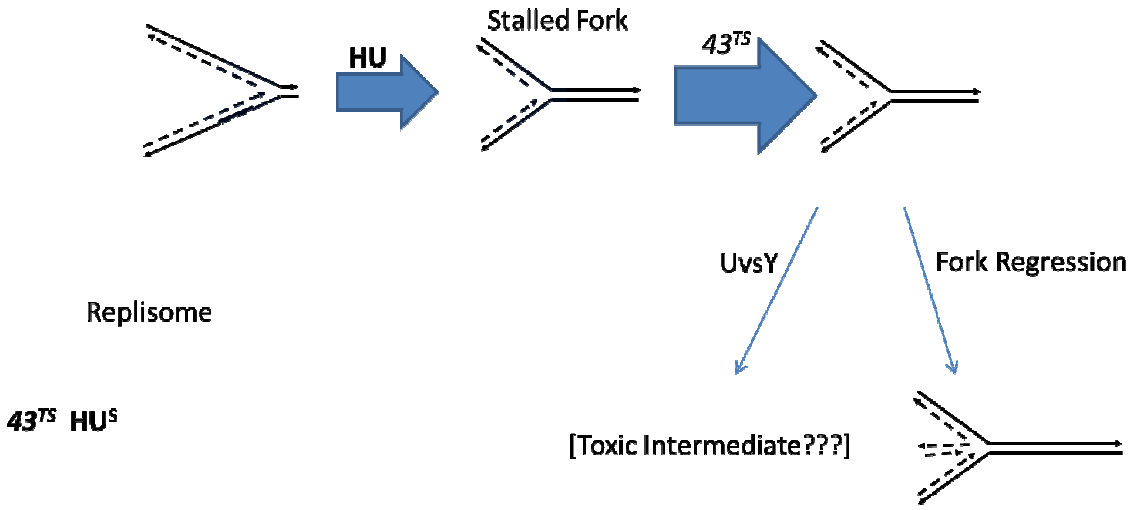

Figure 4-1: Model: *43*^{TS} causes HU^{S}.

The *43*^{TS} mutation caused HU^{S}. In the presence of HU, there are more stalled replication forks. We predict that the *43*^{TS} mutation leads to more replisome disassembly which leads to increased toxic recombination and HU^{S}.

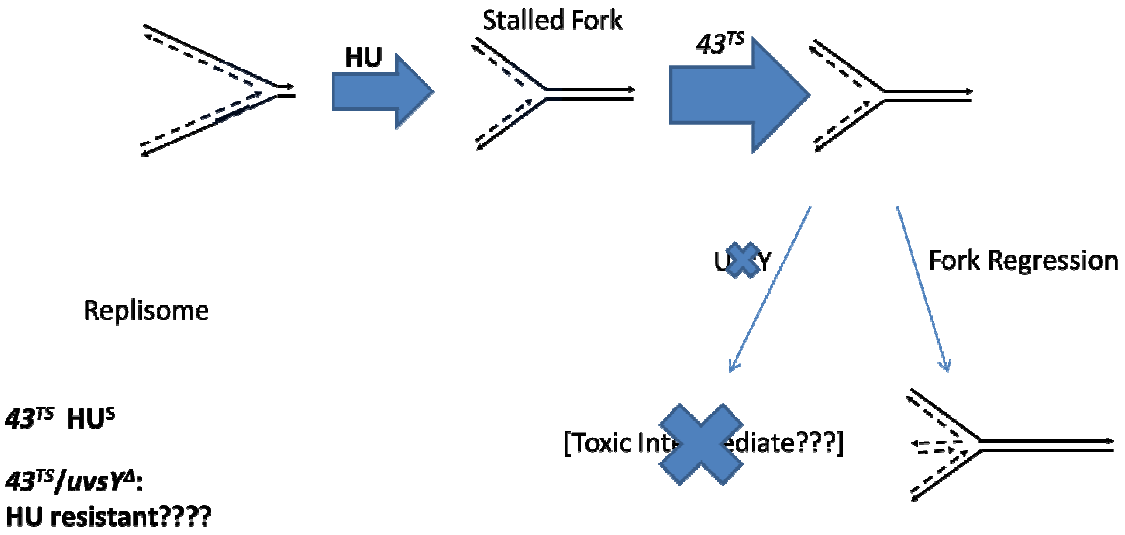

Figure 4-2: Model: *43^{TS}/uvsY$^{\Delta}$* leads to HU^{R}.

We predict that *43^{TS}/uvsY$^{\Delta}$* would lead to HU^{R}. In the presence of HU, there are more stalled replication forks. We predict that the *43^{TS}* mutation leads to more replisome disassembly which leads to increased toxic recombination and HU^{S}. If UvsY is knocked out, we predict the loss of recombination (no toxic recombination intermediate) and HU^{R}.

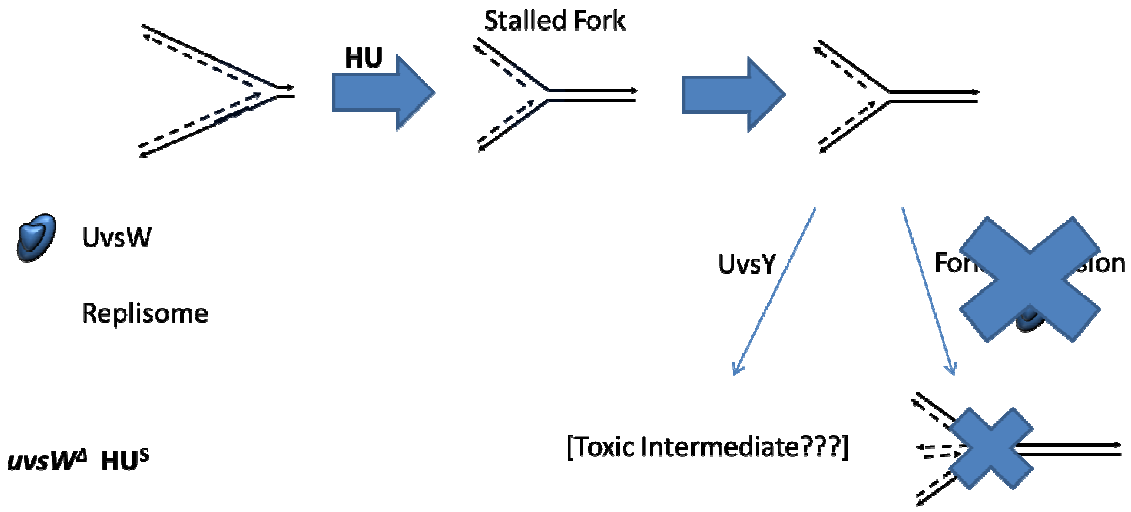

Figure 4-3: Model: *uvsW*$^{\Delta}$ causes HU^{S}.

The *uvsW*$^{\Delta}$ mutation causes HU^{S}. In the presence of HU, there are more stalled replication forks. After replisome disassembly, the replication fork can undergo UvsW-catalyzed fork regression which leads to replication restart. We predict that the *uvsW*$^{\Delta}$ mutation leads to increased toxic recombination and HU^{S}.

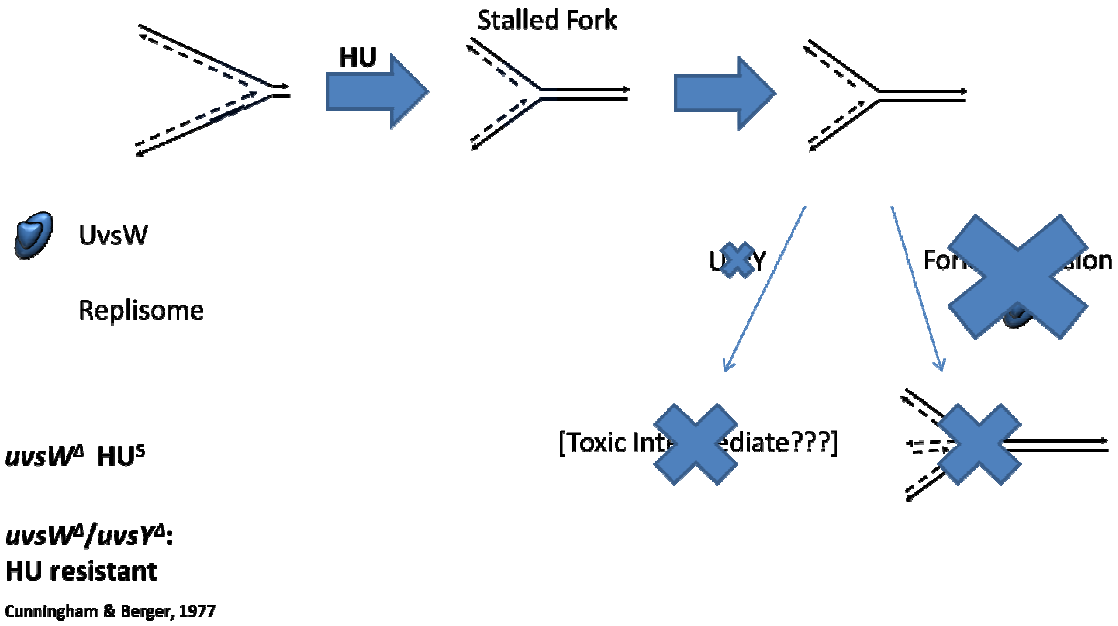

Figure 4-4: Model: *uvsW*$^{\Delta}$/*uvsY*$^{\Delta}$ causes HU^{R}.

The *uvsW*$^{\Delta}$ mutation causes HU^{S} whereas the *uvsW*$^{\Delta}$/*uvsY*$^{\Delta}$ leads to HU^{R}. In the presence of HU, there are more stalled replication forks. After replisome disassembly, the replication fork can undergo UvsW-catalyzed fork regression which leads to replication restart. We predict that the *uvsW*$^{\Delta}$ mutation leads to increased toxic recombination and HU^{S}. If UvsY is knocked out, we predict the loss of recombination (no toxic recombination intermediate) and HU^{R}.

The exact nature of the toxic recombination intermediate remains elusive. In eukaryotes, the toxic recombination intermediate was proposed to be the product of a lagging strand template lesion (MAGNER *et al.* 2007). The authors proposed that translesion synthesis of the lagging strand would lead to a toxic inversion due to incorrect strand switching. Similar to the proposal in eukaryotes, the toxic recombination intermediate was proposed to be the product of incorrect template strand switching in bacteriophage T4 (SCHULTZ and DRAKE 2008). Since the toxic recombination intermediate remains unknown, the characterization of the toxic intermediate will be a focus of future studies.

Finally, using whole genome sequencing, we observed that either the gene *49* hairpin or gene *43* mutation seems to cause a high mutator phenotype. We are currently investigating which mutation leads to an increased mutation rate. If the gene *43* mutation causes the high mutator phenotype, this would confirm that the mutation indeed disrupts DNA polymerase's proofreading ability. We determined that the gene *43* mutation is located in the N-terminal region of DNA polymerase, which encodes for the 3'-5' editing exonuclease activity (proofreading). If the gene *49* hairpin mutation (reduced EndoVII) causes the high mutator phenotype, this would implicate EndoVII in DNA repair. EndoVII is known to bind to a wide variety of structures in addition to HJs, such as Y-junctions (JENSCH and KEMPER 1986). EndoVII was previously proposed to be involved in DNA repair as it was observed to cleave the 3' side of mismatched DNA

bases *in vitro* (BIRKENKAMP and KEMPER 1995; SOLARO *et al.* 1993). The authors proposed that EndoVII can recognize and bind to DNA mismatches since the mismatches alter the DNA shape (introduce a kink). One can imagine that if EndoVII is involved in DNA repair, EndoVII would bind to and create a DSB at the site of the DNA mismatch. This in turn would initiate repair of the mismatch by resection and RDR with another correct DNA template. Thus, if EndoVII is involved in DNA repair, the absence of EndoVII (*49* hairpin mutation) could explain the high mutator phenotype as more mutations would be allowed to persist throughout DNA replication.

References

ALBRECHT, D. W., T. J. HERDENDORF and S. W. NELSON, 2012 Disruption of the bacteriophage T4 Mre11 dimer interface reveals a two-state mechanism for exonuclease activity. J Biol Chem **287:** 31371-31381.

ALBRIGHT, L. M., and E. P. GEIDUSCHEK, 1983 Site-specific cleavage of bacteriophage T4 DNA associated with the absence of gene 46 product function. J Virol **47:** 77-88.

ALMOND, J. R., B. A. STOHR, A. K. PANIGRAHI, D. W. ALBRECHT, S. W. NELSON *et al.*, 2013 Coordination and Processing of DNA Ends During Double-Strand Break Repair: The Role of the Bacteriophage T4 Mre11/Rad50 (MR) Complex. Genetics.

ANDERSON, D. E., K. M. TRUJILLO, P. SUNG and H. P. ERICKSON, 2001 Structure of the Rad50 x Mre11 DNA repair complex from Saccharomyces cerevisiae by electron microscopy. J Biol Chem **276:** 37027-37033.

ANDERSON, D. G., and S. C. KOWALCZYKOWSKI, 1997 The translocating RecBCD enzyme stimulates recombination by directing RecA protein onto ssDNA in a chi-regulated manner. Cell **90:** 77-86.

BARTH, K. A., D. POWELL, M. TRUPIN and G. MOSIG, 1988 Regulation of two nested proteins from gene 49 (recombination endonuclease VII) and of a lambda RexA-like protein of bacteriophage T4. Genetics **120:** 329-343.

BERNSTEIN, K. A., E. SHOR, I. SUNJEVARIC, M. FUMASONI, R. C. BURGESS *et al.*, 2009 Sgs1 function in the repair of DNA replication intermediates is separable from its role in homologous recombinational repair. EMBO J **28:** 915-925.

BHAGWAT, M., L. J. HOBBS and N. G. NOSSAL, 1997 The 5'-exonuclease activity of bacteriophage T4 RNase H is stimulated by the T4 gene 32 single-stranded DNA-binding protein, but its flap endonuclease is inhibited. J Biol Chem **272:** 28523-28530.

BIRKENKAMP, K., and B. KEMPER, 1995 In vitro processing of heteroduplex loops and mismatches by endonuclease VII. DNA Res **2:** 9-14.

BLEUIT, J. S., H. XU, Y. MA, T. WANG, J. LIU *et al.*, 2001 Mediator proteins orchestrate enzyme-ssDNA assembly during T4 recombination-dependent DNA replication and repair. Proc Natl Acad Sci U S A **98:** 8298-8305.

BRAMHILL, D., and A. KORNBERG, 1988 A model for initiation at origins of DNA replication. Cell **54:** 915-918.

BUIS, J., Y. WU, Y. DENG, J. LEDDON, G. WESTFIELD *et al.*, 2008 Mre11 nuclease activity has essential roles in DNA repair and genomic stability distinct from ATM activation. Cell **135:** 85-96.

CARLES-KINCH, K., J. W. GEORGE and K. N. KREUZER, 1997 Bacteriophage T4 UvsW protein is a helicase involved in recombination, repair and the regulation of DNA replication origins. EMBO J **16:** 4142-4151.

CONNELLY, J. C., E. S. DE LEAU and D. R. LEACH, 1999 DNA cleavage and degradation by the SbcCD protein complex from Escherichia coli. Nucleic Acids Res **27:** 1039-1046.

CONNELLY, J. C., L. A. KIRKHAM and D. R. LEACH, 1998 The SbcCD nuclease of Escherichia coli is a structural maintenance of chromosomes (SMC) family protein that cleaves hairpin DNA. Proc Natl Acad Sci U S A **95:** 7969-7974.

CONNELLY, J. C., and D. R. LEACH, 2002 Tethering on the brink: the evolutionarily conserved Mre11-Rad50 complex. Trends Biochem Sci **27:** 410-418.

CROMIE, G. A., and D. R. LEACH, 2001 Recombinational repair of chromosomal DNA double-strand breaks generated by a restriction endonuclease. Mol Microbiol **41:** 873-883.

CUNNINGHAM, R. P., and H. BERGER, 1977 Mutations affecting genetic recombination in bacteriophage T4D. I. Pathway analysis. Virology **80:** 67-82.

DAVIDSON, A. L., E. DASSA, C. ORELLE and J. CHEN, 2008 Structure, function, and evolution of bacterial ATP-binding cassette systems. Microbiol Mol Biol Rev **72:** 317-364, table of contents.

DE JAGER, M., M. L. DRONKERT, M. MODESTI, C. E. BEERENS, R. KANAAR *et al.*, 2001a DNA-binding and strand-annealing activities of human Mre11: implications for its roles in DNA double-strand break repair pathways. Nucleic Acids Res **29:** 1317-1325.

DE JAGER, M., J. VAN NOORT, D. C. VAN GENT, C. DEKKER, R. KANAAR *et al.*, 2001b Human Rad50/Mre11 is a flexible complex that can tether DNA ends. Mol Cell **8:** 1129-1135.

DE LA ROSA, M. B., and S. W. NELSON, 2011 An interaction between the Walker A and D-loop motifs is critical to ATP hydrolysis and cooperativity in bacteriophage T4 Rad50. J Biol Chem **286:** 26258-26266.

DRAKE, J. W., B. CHARLESWORTH, D. CHARLESWORTH and J. F. CROW, 1998 Rates of spontaneous mutation. Genetics **148:** 1667-1686.

EDGAR, B., 2004 The genome of bacteriophage T4: an archeological dig. Genetics **168:** 575-582.

EDGAR, R. S., G. H. DENHARDT and R. H. EPSTEIN, 1964 A Comparative Genetic Study of Conditional Lethal Mutations of Bacteriophage T4d. Genetics **49:** 635-648.

EGGERTSSON, G., and D. SOLL, 1988 Transfer ribonucleic acid-mediated suppression of termination codons in Escherichia coli. Microbiol Rev **52:** 354-374.

ELLEDGE, S. J., Z. ZHOU and J. B. ALLEN, 1992 Ribonucleotide reductase: regulation, regulation, regulation. Trends Biochem Sci **17:** 119-123.

EPSTEIN, R. H., R. S. EDGAR, M. SUSMAN, C. M. STEINBERG, A. BOLLE *et al.*, 1963 Physiological Studies of Conditional Lethal Mutants of Bacteriophage T4d. Cold Spring Harb Symp Quant Biol **28:** 375-&.

FABRE, F., A. CHAN, W. D. HEYER and S. GANGLOFF, 2002 Alternate pathways involving Sgs1/Top3, Mus81/ Mms4, and Srs2 prevent formation of toxic recombination intermediates from single-stranded gaps created by DNA replication. Proc Natl Acad Sci U S A **99:** 16887-16892.

FORMOSA, T., and B. M. ALBERTS, 1986 Purification and characterization of the T4 bacteriophage uvsX protein. J Biol Chem **261:** 6107-6118.

GAJEWSKI, S., M. R. WEBB, V. GALKIN, E. H. EGELMAN, K. N. KREUZER *et al.*, 2011 Crystal structure of the phage T4 recombinase UvsX and its functional interaction with the T4 SF2 helicase UvsW. J Mol Biol **405:** 65-76.

GEORGE, J. W., and K. N. KREUZER, 1996 Repair of double-strand breaks in bacteriophage T4 by a mechanism that involves extensive DNA replication. Genetics **143:** 1507-1520.

GEORGE, J. W., B. A. STOHR, D. J. TOMSO and K. N. KREUZER, 2001 The tight linkage between DNA replication and double-strand break repair in bacteriophage T4. Proc Natl Acad Sci U S A **98:** 8290-8297.

GIBB, E. A., and D. R. EDGELL, 2010 Better late than early: delayed translation of intron-encoded endonuclease I-TevI is required for efficient splicing of its host group I intron. Mol Microbiol **78:** 35-46.

HELLER, R. C., and K. J. MARIANS, 2006 Replisome assembly and the direct restart of stalled replication forks. Nat Rev Mol Cell Biol **7:** 932-943.

HERDENDORF, T. J., D. W. ALBRECHT, S. J. BENKOVIC and S. W. NELSON, 2011 Biochemical characterization of bacteriophage T4 Mre11-Rad50 complex. J Biol Chem **286:** 2382-2392.

HERDENDORF, T. J., and S. W. NELSON, 2011 Functional evaluation of bacteriophage T4 Rad50 signature motif residues. Biochemistry **50:** 6030-6040.

HINTON, D. M., and N. G. NOSSAL, 1986 Cloning of the bacteriophage T4 uvsX gene and purification and characterization of the T4 uvsX recombination protein. J Biol Chem **261:** 5663-5673.

HOLLINGSWORTH, H. C., and N. G. NOSSAL, 1991 Bacteriophage T4 encodes an RNase H which removes RNA primers made by the T4 DNA replication system in vitro. J Biol Chem **266:** 1888-1897.

HONG, G., and K. N. KREUZER, 2000 An antitumor drug-induced topoisomerase cleavage complex blocks a bacteriophage T4 replication fork in vivo. Mol Cell Biol **20:** 594-603.

HONG, G., and K. N. KREUZER, 2003 Endonuclease cleavage of blocked replication forks: An indirect pathway of DNA damage from antitumor drug-topoisomerase complexes. Proc Natl Acad Sci U S A **100:** 5046-5051.

HOPFNER, K. P., L. CRAIG, G. MONCALIAN, R. A. ZINKEL, T. USUI *et al.*, 2002 The Rad50 zinc-hook is a structure joining Mre11 complexes in DNA recombination and repair. Nature **418:** 562-566.

HOPFNER, K. P., A. KARCHER, L. CRAIG, T. T. WOO, J. P. CARNEY *et al.*, 2001 Structural biochemistry and interaction architecture of the DNA double-strand break repair Mre11 nuclease and Rad50-ATPase. Cell **105:** 473-485.

HOPFNER, K. P., and J. A. TAINER, 2003 Rad50/SMC proteins and ABC transporters: unifying concepts from high-resolution structures. Curr Opin Struct Biol **13:** 249-255.

HOPKINS, B. B., and T. T. PAULL, 2008 The P. furiosus mre11/rad50 complex promotes 5' strand resection at a DNA double-strand break. Cell **135:** 250-260.

HOPP, T. P., K. S. PRICKETT, V. L. PRICE, R. T. LIBBY, C. J. MARCH *et al.*, 1988 A Short Polypeptide Marker Sequence Useful for Recombinant Protein Identification and Purification. Bio-Technology **6:** 1204-1210.

IP, S. C., U. RASS, M. G. BLANCO, H. R. FLYNN, J. M. SKEHEL *et al.*, 2008 Identification of Holliday junction resolvases from humans and yeast. Nature **456:** 357-361.

JENSCH, F., and B. KEMPER, 1986 Endonuclease VII resolves Y-junctions in branched DNA in vitro. EMBO J **5:** 181-189.

JONES, P. M., M. L. O'MARA and A. M. GEORGE, 2009 ABC transporters: a riddle wrapped in a mystery inside an enigma. Trends Biochem Sci **34:** 520-531.

KEMPER, B., and D. T. BROWN, 1976 Function of gene 49 of bacteriophage T4. II. Analysis of intracellular development and the structure of very fast-sedimenting DNA. J Virol **18:** 1000-1015.

KEMPER, B., and E. JANZ, 1976 Function of gene 49 of bacteriophage T4. I. Isolation and biochemical characterization of very fast-sedimenting DNA. J Virol **18:** 992-999.

KLEINA, L. G., J. M. MASSON, J. NORMANLY, J. ABELSON and J. H. MILLER, 1990 Construction of Escherichia coli amber suppressor tRNA genes. II. Synthesis of additional tRNA genes and improvement of suppressor efficiency. J Mol Biol **213:** 705-717.

KODADEK, T., D. C. GAN and K. STEMKE-HALE, 1989 The phage T4 uvs Y recombination protein stabilizes presynaptic filaments. J Biol Chem **264:** 16451-16457.

KOWALCZYKOWSKI, S. C., 1991 Biochemical and biological function of Escherichia coli RecA protein: behavior of mutant RecA proteins. Biochimie **73:** 289-304.

KOWALCZYKOWSKI, S. C., 2000 Initiation of genetic recombination and recombination-dependent replication. Trends Biochem Sci **25:** 156-165.

KRAUS, E., W. Y. LEUNG and J. E. HABER, 2001 Break-induced replication: a review and an example in budding yeast. Proc Natl Acad Sci U S A **98:** 8255-8262.

KREUZER, K. N., 2000 Recombination-dependent DNA replication in phage T4. Trends Biochem Sci **25:** 165-173.

KREUZER, K. N., and B. M. ALBERTS, 1985 A defective phage system reveals bacteriophage T4 replication origins that coincide with recombination hot spots. Proc Natl Acad Sci U S A **82:** 3345-3349.

KREUZER, K. N., and B. M. ALBERTS, 1986 Characterization of a defective phage system for the analysis of bacteriophage T4 DNA replication origins. J Mol Biol **188:** 185-198.

KREUZER, K. N., AND J.W. DRAKE, 1994a *Repair of lethal DNA damage*. American Society for Microbiology, Washington, D.C.

KREUZER, K. N., AND S.W. MORRICAL, 1994b *Initiation of DNA replication*. American Society for Microbiology, Washington, D.C.

KREUZER, K. N., H. W. ENGMAN and W. Y. YAP, 1988 Tertiary initiation of replication in bacteriophage T4. Deletion of the overlapping uvsY promoter/replication origin from the phage genome. J Biol Chem **263:** 11348-11357.

KREUZER, K. N., M. SAUNDERS, L. J. WEISLO and H. W. KREUZER, 1995 Recombination-dependent DNA replication stimulated by double-strand breaks in bacteriophage T4. J Bacteriol **177:** 6844-6853.

KREUZER, K. N. A. M., B. , 2005 *Reinitiation of DNA Replication*. ASM Press.

KROGH, B. O., B. LLORENTE, A. LAM and L. S. SYMINGTON, 2005 Mutations in Mre11 phosphoesterase motif I that impair Saccharomyces cerevisiae Mre11-Rad50-Xrs2 complex stability in addition to nuclease activity. Genetics **171:** 1561-1570.

LAMMENS, K., D. J. BEMELEIT, C. MOCKEL, E. CLAUSING, A. SCHELE *et al.*, 2011 The Mre11:Rad50 structure shows an ATP-dependent molecular clamp in DNA double-strand break repair. Cell **145:** 54-66.

LEE, J. H., and T. T. PAULL, 2005 ATM activation by DNA double-strand breaks through the Mre11-Rad50-Nbs1 complex. Science **308:** 551-554.

LEWIS, L. K., F. STORICI, S. VAN KOMEN, S. CALERO, P. SUNG *et al.*, 2004 Role of the nuclease activity of Saccharomyces cerevisiae Mre11 in repair of DNA double-strand breaks in mitotic cells. Genetics **166:** 1701-1713.

LIPINSKA, B., A. S. RAO, B. M. BOLTEN, R. BALAKRISHNAN and E. B. GOLDBERG, 1989 Cloning and identification of bacteriophage T4 gene 2 product gp2 and action of gp2 on infecting DNA in vivo. J Bacteriol **171:** 488-497.

LLORENTE, B., C. E. SMITH and L. S. SYMINGTON, 2008 Break-induced replication: what is it and what is it for? Cell Cycle **7:** 859-864.

LLORENTE, B., and L. S. SYMINGTON, 2004 The Mre11 nuclease is not required for 5' to 3' resection at multiple HO-induced double-strand breaks. Mol Cell Biol **24:** 9682-9694.

LOBACHEV, K., E. VITRIOL, J. STEMPLE, M. A. RESNICK and K. BLOOM, 2004 Chromosome fragmentation after induction of a double-strand break is an active process prevented by the RMX repair complex. Curr Biol **14:** 2107-2112.

LONG, D. T., and K. N. KREUZER, 2008 Regression supports two mechanisms of fork processing in phage T4. Proc Natl Acad Sci U S A **105:** 6852-6857.

LONG, D. T., and K. N. KREUZER, 2009 Fork regression is an active helicase-driven pathway in bacteriophage T4. EMBO Rep **10:** 394-399.

LUBIN, J. W., T. RAO, E. K. MANDELL, D. S. WUTTKE and V. LUNDBLAD, 2013 Dissecting protein function: an efficient protocol for identifying separation-of-function mutations that encode structurally stable proteins. Genetics **193:** 715-725.

LUDER, A., and G. MOSIG, 1982 Two alternative mechanisms for initiation of DNA replication forks in bacteriophage T4: priming by RNA polymerase and by recombination. Proc Natl Acad Sci U S A **79:** 1101-1105.

LUFTIG, R. B., W. B. WOOD and R. OKINAKA, 1971 Bacteriophage T4 head morphogenesis. On the nature of gene 49-defective heads and their role as intermediates. J Mol Biol **57:** 555-573.

MAGNER, D. B., M. D. BLANKSCHIEN, J. A. LEE, J. M. PENNINGTON, J. R. LUPSKI *et al.*, 2007 RecQ promotes toxic recombination in cells lacking recombination intermediate-removal proteins. Mol Cell **26:** 273-286.

MASER, R. S., K. J. MONSEN, B. E. NELMS and J. H. PETRINI, 1997 hMre11 and hRad50 nuclear foci are induced during the normal cellular response to DNA double-strand breaks. Mol Cell Biol **17:** 6087-6096.

MCGLYNN, P., and R. G. LLOYD, 2002 Recombinational repair and restart of damaged replication forks. Nat Rev Mol Cell Biol **3:** 859-870.

MCPHEETERS, D. S., A. CHRISTENSEN, E. T. YOUNG, G. STORMO and L. GOLD, 1986 Translational regulation of expression of the bacteriophage T4 lysozyme gene. Nucleic Acids Res **14:** 5813-5826.

MICKELSON, C., and J. S. WIBERG, 1981 Membrane-associated DNase activity controlled by genes 46 and 47 of bacteriophage T4D and elevated DNase activity associated with the T4 das mutation. J Virol **40:** 65-77.

MILLER, E. S., E. KUTTER, G. MOSIG, F. ARISAKA, T. KUNISAWA *et al.*, 2003 Bacteriophage T4 genome. Microbiol Mol Biol Rev **67:** 86-156, table of contents.

MIMITOU, E. P., and L. S. SYMINGTON, 2008 Sae2, Exo1 and Sgs1 collaborate in DNA double-strand break processing. Nature **455:** 770-774.

MIZUUCHI, K., B. KEMPER, J. HAYS and R. A. WEISBERG, 1982 T4 endonuclease VII cleaves holliday structures. Cell **29:** 357-365.

MOREAU, S., J. R. FERGUSON and L. S. SYMINGTON, 1999 The nuclease activity of Mre11 is required for meiosis but not for mating type switching, end joining, or telomere maintenance. Mol Cell Biol **19:** 556-566.

MORIMATSU, K., and S. C. KOWALCZYKOWSKI, 2003 RecFOR proteins load RecA protein onto gapped DNA to accelerate DNA strand exchange: a universal step of recombinational repair. Mol Cell **11:** 1337-1347.

MORRICAL, S. W., and B. M. ALBERTS, 1990 The UvsY protein of bacteriophage T4 modulates recombination-dependent DNA synthesis in vitro. J Biol Chem **265:** 15096-15103.

MOSIG, G., 1983 *Relationship of T4 DNA replication and recombination*. American Society for Microbiology, Washington, D.C.

MOSIG, G., 1998 Recombination and recombination-dependent DNA replication in bacteriophage T4. Annu Rev Genet **32:** 379-413.

MOSIG, G., and S. BOCK, 1976 Gene 32 protein of bacteriophage T4 moderates the activities of the T4 gene 46/47-controlled nuclease and of the Escherichia coli RecBC nuclease in vivo. J Virol **17:** 756-761.

MOSIG, G., A. LUDER, A. ERNST and N. CANAN, 1991 Bypass of a primase requirement for bacteriophage T4 DNA replication in vivo by a recombination enzyme, endonuclease VII. New Biol **3:** 1195-1205.

MOSIG, G., M. SHAW and G. M. GARCIA, 1984 On the role of DNA replication, endonuclease VII, and rII proteins in processing of recombinational intermediates in phage T4. Cold Spring Harb Symp Quant Biol **49:** 371-382.

MUESER, T. C., N. G. NOSSAL and C. C. HYDE, 1996 Structure of bacteriophage T4 RNase H, a 5' to 3' RNA-DNA and DNA-DNA exonuclease with sequence similarity to the RAD2 family of eukaryotic proteins. Cell **85:** 1101-1112.

NELMS, B. E., R. S. MASER, J. F. MACKAY, M. G. LAGALLY and J. H. PETRINI, 1998 In situ visualization of DNA double-strand break repair in human fibroblasts. Science **280:** 590-592.

NIU, H., W. H. CHUNG, Z. ZHU, Y. KWON, W. ZHAO *et al.*, 2010 Mechanism of the ATP-dependent DNA end-resection machinery from Saccharomyces cerevisiae. Nature **467:** 108-111.

NOGUCHI, E., C. NOGUCHI, L. L. DU and P. RUSSELL, 2003 Swi1 prevents replication fork collapse and controls checkpoint kinase Cds1. Mol Cell Biol **23:** 7861-7874.

NORMANLY, J., L. G. KLEINA, J. M. MASSON, J. ABELSON and J. H. MILLER, 1990 Construction of Escherichia coli amber suppressor tRNA genes. III. Determination of tRNA specificity. J Mol Biol **213:** 719-726.

NORMANLY, J., J. M. MASSON, L. G. KLEINA, J. ABELSON and J. H. MILLER, 1986 Construction of two Escherichia coli amber suppressor genes: tRNAPheCUA and tRNACysCUA. Proc Natl Acad Sci U S A **83:** 6548-6552.

NOSSAL, N. G., K. C. DUDAS and K. N. KREUZER, 2001 Bacteriophage T4 proteins replicate plasmids with a preformed R loop at the T4 ori(uvsY) replication origin in vitro. Mol Cell **7:** 31-41.

OLIVER, D. B., and E. B. GOLDBERG, 1977 Protection of parental T4 DNA from a restriction exonuclease by the product of gene 2. J Mol Biol **116:** 877-881.

PAQUES, F., and J. E. HABER, 1999 Multiple pathways of recombination induced by double-strand breaks in Saccharomyces cerevisiae. Microbiol Mol Biol Rev **63:** 349-404.

PAULL, T. T., 2010 Making the best of the loose ends: Mre11/Rad50 complexes and Sae2 promote DNA double-strand break resection. DNA Repair (Amst) **9:** 1283-1291.

PETERMANN, E., and T. HELLEDAY, 2010 Pathways of mammalian replication fork restart. Nat Rev Mol Cell Biol **11:** 683-687.

PETROV, V. M., S. RATNAYAKA, J. M. NOLAN, E. S. MILLER and J. D. KARAM, 2010 Genomes of the T4-related bacteriophages as windows on microbial genome evolution. Virol J **7:** 292.

RAAIJMAKERS, H., O. VIX, I. TORO, S. GOLZ, B. KEMPER *et al.*, 1999 X-ray structure of T4 endonuclease VII: a DNA junction resolvase with a novel fold and unusual domain-swapped dimer architecture. EMBO J **18:** 1447-1458.

RASS, U., S. A. COMPTON, J. MATOS, M. R. SINGLETON, S. C. IP *et al.*, 2010 Mechanism of Holliday junction resolution by the human GEN1 protein. Genes Dev **24:** 1559-1569.

REHA-KRANTZ, L. J., 1994 *Genetic Dissection of T4 DNA Polymerase Structure-Function Relationships*. American Society for Microbiology, Washington, D.C.

REVEL, H. R., 1983 *Bacteriophage T4*. American Society for Microbiology, Washington, D.C.

ROBINSON, M. J., and N. OSHEROFF, 1990 Stabilization of the topoisomerase II-DNA cleavage complex by antineoplastic drugs: inhibition of enzyme-mediated DNA religation by 4'-(9-acridinylamino)methanesulfon-m-anisidide. Biochemistry **29:** 2511-2515.

SCHULTZ, G. E., JR., and J. W. DRAKE, 2008 Templated mutagenesis in bacteriophage T4 involving imperfect direct or indirect sequence repeats. Genetics **178:** 661-673.

SELICK, H. E., K. N. KREUZER and B. M. ALBERTS, 1988 The bacteriophage T4 insertion/substitution vector system. A method for introducing site-specific mutations into the virus chromosome. J Biol Chem **263:** 11336-11347.

SHAMOO, Y., N. ABDUL-MANAN and K. R. WILLIAMS, 1995a Multiple RNA binding domains (RBDs) just don't add up. Nucleic Acids Res **23:** 725-728.

SHAMOO, Y., A. M. FRIEDMAN, M. R. PARSONS, W. H. KONIGSBERG and T. A. STEITZ, 1995b Crystal structure of a replication fork single-stranded DNA binding protein (T4 gp32) complexed to DNA. Nature **376:** 362-366.

SHARPLES, G. J., and D. R. LEACH, 1995 Structural and functional similarities between the SbcCD proteins of Escherichia coli and the RAD50 and MRE11 (RAD32) recombination and repair proteins of yeast. Mol Microbiol **17:** 1215-1217.

SHCHERBAKOV, V. P., L. PLUGINA, T. SHCHERBAKOVA, S. SIZOVA and E. KUDRYASHOVA, 2006 Double-strand break repair in bacteriophage T4: coordination of DNA ends and effects of mutations in recombinational genes. DNA Repair (Amst) **5:** 773-787.

SHIN, D. S., C. CHAHWAN, J. L. HUFFMAN and J. A. TAINER, 2004 Structure and function of the double-strand break repair machinery. DNA Repair (Amst) **3:** 863-873.

SICKMIER, E. A., K. N. KREUZER and S. W. WHITE, 2004 The crystal structure of the UvsW helicase from bacteriophage T4. Structure **12:** 583-592.

SILVERSTEIN, J. L., and E. B. GOLDBERG, 1976a T4 DNA injection. I. Growth cycle of a gene 2 mutant. Virology **72:** 195-211.

SILVERSTEIN, J. L., and E. B. GOLDBERG, 1976b T4 DNA injection. II. Protection of entering DNA from host exonuclease V. Virology **72:** 212-223.

SOLARO, P. C., K. BIRKENKAMP, P. PFEIFFER and B. KEMPER, 1993 Endonuclease VII of phage T4 triggers mismatch correction in vitro. J Mol Biol **230:** 868-877.

SONODA, E., H. HOCHEGGER, A. SABERI, Y. TANIGUCHI and S. TAKEDA, 2006 Differential usage of non-homologous end-joining and homologous recombination in double strand break repair. DNA Repair (Amst) **5:** 1021-1029.

STAHL, F. W., 1995 The amber mutants of phage T4. Genetics **141:** 439-442.

STEWART, G. S., R. S. MASER, T. STANKOVIC, D. A. BRESSAN, M. I. KAPLAN *et al.*, 1999 The DNA double-strand break repair gene hMRE11 is mutated in individuals with an ataxia-telangiectasia-like disorder. Cell **99:** 577-587.

STOHR, B. A., and K. N. KREUZER, 2001 Repair of topoisomerase-mediated DNA damage in bacteriophage T4. Genetics **158:** 19-28.

STOHR, B. A., and K. N. KREUZER, 2002 Coordination of DNA ends during double-strand-break repair in bacteriophage T4. Genetics **162:** 1019-1030.

STRACKER, T. H., and J. H. PETRINI, 2011 The MRE11 complex: starting from the ends. Nat Rev Mol Cell Biol **12:** 90-103.

SUNG, P., and H. KLEIN, 2006 Mechanism of homologous recombination: mediators and helicases take on regulatory functions. Nat Rev Mol Cell Biol **7:** 739-750.

TAY, Y. D., and L. WU, 2010 Overlapping roles for Yen1 and Mus81 in cellular Holliday junction processing. J Biol Chem **285:** 11427-11432.

TOMSO, D. J., and K. N. KREUZER, 2000 Double-strand break repair in tandem repeats during bacteriophage T4 infection. Genetics **155:** 1493-1504.

TRENZ, K., E. SMITH, S. SMITH and V. COSTANZO, 2006 ATM and ATR promote Mre11 dependent restart of collapsed replication forks and prevent accumulation of DNA breaks. EMBO J **25:** 1764-1774.

TRUJILLO, K. M., and P. SUNG, 2001 DNA structure-specific nuclease activities in the Saccharomyces cerevisiae Rad50*Mre11 complex. J Biol Chem **276:** 35458-35464.

TRUJILLO, K. M., S. S. YUAN, E. Y. LEE and P. SUNG, 1998 Nuclease activities in a complex of human recombination and DNA repair factors Rad50, Mre11, and p95. J Biol Chem **273:** 21447-21450.

WARNER, H. R., and M. D. HOBBS, 1969 Effect of hydroxyurea on replication of bacteriophage T4 in Escherichia coli. J Virol **3:** 331-336.

WEBB, M. R., J. L. PLANK, D. T. LONG, T. S. HSIEH and K. N. KREUZER, 2007 The phage T4 protein UvsW drives Holliday junction branch migration. J Biol Chem **282:** 34401-34411.

WIBERG, J. S., 1966 Mutants of bacteriophage T4 unable to cause breakdown of host DNA. Proc Natl Acad Sci U S A **55:** 614-621.

WILLIAMS, G. J., R. S. WILLIAMS, J. S. WILLIAMS, G. MONCALIAN, A. S. ARVAI *et al.*, 2011 ABC ATPase signature helices in Rad50 link nucleotide state to Mre11 interface for DNA repair. Nat Struct Mol Biol **18:** 423-431.

WILLIAMS, R. S., G. MONCALIAN, J. S. WILLIAMS, Y. YAMADA, O. LIMBO *et al.*, 2008 Mre11 dimers coordinate DNA end bridging and nuclease processing in double-strand-break repair. Cell **135:** 97-109.

YONESAKI, T., and T. MINAGAWA, 1985 T4 phage gene uvsX product catalyzes homologous DNA pairing. EMBO J **4:** 3321-3327.

YONESAKI, T., and T. MINAGAWA, 1989 Synergistic action of three recombination gene products of bacteriophage T4, uvsX, uvsY, and gene 32 proteins. J Biol Chem **264:** 7814-7820.

ZHU, Z., W. H. CHUNG, E. Y. SHIM, S. E. LEE and G. IRA, 2008 Sgs1 helicase and two nucleases Dna2 and Exo1 resect DNA double-strand break ends. Cell **134:** 981-994.

Biography

Joshua Richard Almond

Birth place: **Durham, North Carolina**

Birth date: **December 16, 1985**

Education:

2008-2013 **Ph.D., Biochemistry –** Duke University Medical Center, Department of Biochemistry

Ruth L. Kirschstein National Research Service Award (T32 Grant): NIH Viral Oncology Training Grant

2004-2008 **B.S., Chemistry – Biochemistry –** University of North Carolina at Chapel Hill

Publications:

ALMOND, J. R., B. A. STOHR, A. K. PANIGRAHI, D. W. ALBRECHT, S. W. NELSON *et al.*, 2013 Coordination and Processing of DNA Ends During Double-Strand Break Repair: The Role of the Bacteriophage T4 Mre11/Rad50 (MR) Complex. Genetics.